5-1-1988

Multiphase Flow in Vertical and Inclined Annuli

Rajeev Patel

Recommended Citation

MULTIPHASE FLOW IN VERTICAL AND INCLINED ANNULI

by

Rajeev Patel

B.S., Maharaja Sayajirao University of Baroda, Baroda
India, 1983

A Thesis

Submitted to the Graduate Faculty

of the

University of North Dakota

in partial fulfillment of the requirements

for the degree of

Master of Science

Grand Forks, North Dakota

May, 1988

This thesis submitted by Rajeev Patel in partial fulfillment of the requirements for the Degree of Master of Science from the University of North Dakota has been read by the Faculty Advisory Committee under whom the work has been done, and is hereby approved.

R. Hasan.

Thomas C. Owens

N S Gurwal

This thesis meets the standards for appearance and conforms to the style and format requirements of the Graduate School of the University of North Dakota, and is hereby approved.

A. William Johnson 4/22/88

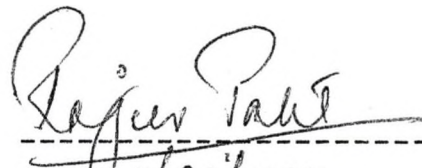
Title <u>Multiphase Flow in Vertical and Inclined Annuli</u>

Department <u>Chemical Engineering</u>

Degree <u>Master of Science</u>

In presenting the thesis in partial fulfillment of the requirements for a graduate degree from the University of North Dakota, I agree that the Library of this University shall make it freely available for inspection. I further agree that permission for extensive copying for scholarly purposes may be granted by the professor who supervised my thesis work or, in his absence, by the Chairman of the Department or the Dean of the Graduate School. It is understood that any copying or publication or other use of this thesis or part thereof for financial gain shall not be allowed without my written permission. It is also understood that due recognition shall be given to me and to the University of North Dakota in any scholarly use which may be made of any material in my thesis.

Signature _____

Date _____4/21/1988_____

iii

CONTENTS

APPENDICES   <u>page</u>

LIST OF FIGURES

LIST OF TABLES

ACKNOWLEDGEMENT

I am very grateful to Dr. A. Rashid Hasan for his help, patience, and perseverance in directing this thesis. Without his able guidance, this thesis would never have reached fruition. Appreciation is also extended to Dr. Thomas C. Owens and Dr. Nanak Grewal for their advice and their willingness to serve as committee members.

My thanks to Joe Miller for his help during the experimental work.

I thank Dr. Thomas C. Owens for granting me financial assistance .

I would like to express my gratitude to my parents whose constant support of me throughout my life as a student has been unfailingly wholehearted.

Finally, and most importantly, I would like to express my extreme gratitude and appreciation to my fiancee, Sudeshna Dass, who helped me through thick and thin and urged and goaded me to finish. This thesis means as much to her as it does to me.

ABSTRACT

The present study was undertaken to experimentally determine the _in situ_ volume fraction of the gas phase when air is bubbled through a stagnant liquid column. The data gathered were used to examine the model proposed by Hasan (1986) for estimating gas void fraction during two-phase flow in vertical and inclined pipes. This model, based on a drift flux approach, relates the _in situ_ velocity of the gas phase to the bubble rise velocity and the mixture velocity.

An experimental set-up consisting of a plexiglass column of 5 inch inside diameter and eighteen feet in height was used to gather data. The column was deviated at 0, 8, 16, 24, and 32 degrees from the vertical. Pipes of 1.87, 2.24, and 3.409 inches were used to create annuli of different dimensions.

Data were gathered for the rise velocities of small and " Taylor" bubbles as well as for void fraction for gas (air) flowing through a stagnant liquid (water) column. These raw data were then converted to superficial gas velocity (V_{sg}) and void fraction (E_g).

Flow patterns during multiphase flow are loosely grouped into bubbly, slug, churn, and annular types. Due to the relatively low air flow rates available from existing air lines, only bubbly and slug flow patterns were observed.

xiii

The void fraction during bubbly and slug flow was given by

$$E_g = \frac{V_{sg}}{CV_{sg} + V_t}$$

The parameter C was found to be unaffected by pipe inclination and annuli dimensions. The value of this parameter remained constant at 2.0 for bubbly flow and at 1.2 for slug flow.

The rise velocity of small bubbles, V_t, was found to be unaffected by either pipe inclination or annuli dimensions. The overall average bubble rise velocity of 0.84 ft/sec. was in very good agreement with the value calculated by using the Harmathy (1960) correlation.

"Taylor" bubble rise velocity data, however, indicated strong influence of both pipe inclination and annulus dimensions. The data gathered were found to agree well with the following "Taylor" bubble rise velocity correlation proposed by Hasan (1986)

$$V_{tT} = [0.35 + 0.1(D_t/D_c)\sin^2\alpha][gD_c(d_1-d_g)/d_1]^2$$
$$[\sqrt{\sin\alpha}(1 + \cos\alpha)^{1.2}]$$

The above expression successfully accounts for both the pipe inclination and the annulus diameters.

The predictions of the proposed model for flow pattern transition and void fraction were compared with data from several other sources. Good agreement between the data and the predictions of the model were noted.

Chapter I

INTRODUCTION

Multiphase flow through pipes is widely encountered in the chemical process industry, in the power industry and in the petroleum industry. In the chemical process industry, especially in heat exchangers and in steam generating equipment, including nuclear power generators, multiphase flow is a frequent occurrence. In heat exchangers and steam generators, the continuously changing proportion of the phases (due to evaporation) results in the rate of heat transfer becoming more important than the rate of momentum transfer. An extreme example is found in the design of refrigerators and air conditioners.

In the petroleum industry, gas or oil production is rarely a single-phase flow phenomenon. Crude production often involves the flow of all three phases - oil, gas and water - posing problems during the production of oil and gas. In recent years there has been a significant change in petroleum production and exploitation. The increase in distance between the production and consumption of petroleum has made economics an important consideration when transporting the two-phase fluids. Transporting a two-phase system has reportedly reduced metal consumption by 40 percent and capital investment by 19 percent as compared

with separating and transmitting the separate phases (Mukherji and Brill 1983).

The economic attractiveness of two-phase transmission has spurred a host of researchers to consider the associated problems. Many gathering lines and long-distance pipelines pass through areas of hilly terrain. This presents no problem in single-phase flow because the potential energy lost in going uphill is recovered in the downhill section. This is not exactly the case for two-phase flow, because the liquid holdup, and thus the entire mixture density, is usually much lower in downhill flow.

The number of directional or inclined wells is increasing as the search for petroleum moves to previously unexplored areas. In offshore drilling, several directional wells are often drilled from the same platform for economic reasons. Deviations of 35 to 45 degrees from the vertical are common. In permafrost areas of Alaska and Canada, the cost of drilling-rig foundations and the difficulty of transportation require that several wells be directionally drilled from one location. Existing vertical-flow correlations frequently fail to adequately predict pressure gradients in these wells.

The analysis of two-phase flow is complicated by such phenomena as slippage between phases, change of flow pattern, and mass transfer between phases. The gas-liquid interface may be smooth or wavy and energy may be transferred between phases. These factors may result in a

much greater pressure loss than can be explained by the reduced area available to flow for each phase. When angle of flow is added to such variables as fluid properties, flow rates, and pipe diameter, the problem is indeed formidable.

The present study will examine the inclined two-phase flow model proposed by Hasan (1986) in light of experimental data.

Chapter II

THEORY

Two-phase flow is a term used to describe the interacting flow of two phases (gas, liquid, or solid) where the interface between the phases is influenced by their motion. In gas liquid flows, this interface takes a variety of forms. There is an almost infinite range of possibilities, but, in general, the surface tension effects tend to create curved interfaces leading to droplets or bubbles. The bigger the occlusion of the discontinuous in the continuous phase, the bigger the departure from a spherical shape. Thus, small droplets tend to be spherical whereas bigger ones are often deformed in the liquid flow. The description of two-phase flow in pipes can be simplified by classifying types of interfacial distribution and naming these flow regimes or flow patterns. For vertical and inclined pipe configurations, four principal flow regimes are recognized: bubbly, slug, churn and annular. These various regimes are defined as follows:

(1) **Bubble flow.** This is a dispersion of bubbles in a continuum of liquid.

(2) **Slug or plug flow.** As the concentration of bubbles in bubble flow increases, bubbles coalesce and, ultimately the bubble diameter approaches that of the tube. Once this occurs, the slug-flow (or plug-flow - the names are used

4

interchangeably for vertical flow) regime is entered, and the characteristic bullet-shaped bubbles are called " Taylor" bubbles.

(3) **Churn-flow.** As the gas flow is increased, the velocity of the " Taylor" bubbles increases and, ultimately, these bubbles breakup. This leads to an unstable regime in which there is, in wide bore tubes, an oscillating upward and downward motion of the liquid in the tube; thus the name " churn" flow is applied. For narrow-bore tubes, the oscillation may not occur and a smoother transition between slug flow and annular flow may be observed.

(4) **Annular Flow.** Liquid flows along the wall of the tube as a film and the gas phase flows through the center in annular flow. Usually some of the liquid phase is entrained as small droplets in the gas core.

The flow regimes that occur and the transition between regimes generally depend on the angle of inclination and variables such as flow rates of both phases and their physical properties. Different inclination angles may lead to different pressure drops in a pipeline with fixed length, pipe diameter, input flow and fluid properties under a constant elevation difference between inlet and outlet.

The most important factor in the analysis of two-phase flow is total pressure drop. The method of analysis for two-phase flow parallels that for single-phase flow. The mechanical energy balance for a single-phase system, flowing through a differential pipe length dz without any heat or

work input may be expressed as

$$(dP/dz) + (1/g_c) [(2fV^2d_1 + (d_1VdV/dz)$$
$$+ gd_1\sin\alpha] = 0 \qquad (1)$$

or

$$(dP/dz) = -(1/g_c) [(2fV^2d_1/D) + (d_1VdV/dz)$$
$$+ gd_1\sin\alpha] \qquad (2)$$

The three terms on the right-hand side of the Equation (2) are the friction loss, the kinetic energy loss, and the potential energy loss. Hence, we may write the total pressure gradient dP/dz in terms of the frictional (F), accelerational (A) or kinetic, and potential (H) or static pressure gradients,

$$(dP/dz) = (dP/dz \ F) + (dP/dz \ A) + (dP/dz \ H) \qquad (3)$$

This equation is also valid for multiphase flow. Two different methods may be adopted to express frictional, accelerational, and potential pressure gradients during multiphase flow. The simpler of the two - the Generalized Approach - tries to develop methods to predict pressure drop and void fraction that would apply to all types of flow geometry and patterns. The generalized approach is further divided into the Homogeneous Flow model and the Separated Flow model. The Homogeneous Flow model assumes that the multiphase mixture behaves essentially as a single-phase fluid, with property values that are some type of average of the constituent phases. The type of average used, i.e., volumetric, weighted etc., reduces the prediction problem to the same level as that for single-phase flow. The

assumption of homogeneity is based on the premise that there exists no slip i.e. all the phases possess the same in situ velocity. This means, in effect, that the in situ void fraction is identical to the input fraction. On the other hand, the Separated Flow model supposes that the phases are segregated and moving with different velocities. In this model, therefore, the slip between the phases and the frictional interaction between them need to be evaluated.

The Flow Pattern approach attempts to prescribe a correlation for each flow regime. Because flow patterns are different for vertical, horizontal and inclined flow, these orientations are treated separately. In addition, varying flow patterns arise from different hydrodynamic conditions, and this approach is believed to lead to more accurate correlations than does the generalised approach. This is why most of the recent research in multiphase flow uses the Flow Pattern approach. One drawback is the need to know the type of flow pattern before one attempts any analysis. Because visual confirmation of the existing flow pattern is virtually impossible in most cases, one needs to employ empirical or semi-empirical correlations or maps to predict the flow pattern. In this thesis, the Flow Pattern approach has been selected to analyze the data.

2.1 THE FLOW PATTERN APPROACH

Several techniques are available to determine the identity of two-phase flow patterns that are present in heated and unheated channels. In transparent channels at

low velocities, it is possible to visually identify the flow patterns. At higher velocities where the flow patterns become indistinct, flash and cine photography can be used to slow the flow down on film and extend the range. However, reflection and refraction at multiple interfaces reduces the accuracy of this method of flow pattern determination. Some investigators have developed various types of probes - electrical, hot wire, pressure, and optical - to study the structure of the flow. The signal from these probes provides indirect information for the deduction of the flow pattern. No satisfactory general method has yet been developed to correctly determine flow pattern for a particular local condition. Part of the reason is the lack of agreement on the description and classification of the flow patterns. Hubbard and Dukler (1968) proposed a method for flow pattern determination based on spectral analysis of wall pressure fluctuations, but their method has not found general acceptance. Another difficulty in correctly predicting flow pattern is that although flow patterns strongly depend on parameters such as phase velocities and volume fractions, other less easily defined variables - such as the method of forming the two-phase flow, the amount of departure from hydrodynamic equilibrium, and the presence of trace contaminants in the system - considerably influence the particular flow pattern. Despite these difficulties, a plethora of methods have been proposed to predict flow pattern during gas-liquid two-phase flow. Some of these

methods could be extended to liquid-liquid systems with lesser accuracy.

2.1.1 **Flow Pattern Maps:** One method to represent flow pattern transitions is to use in flow pattern maps. The different patterns are represented as areas on a graph, the coordinates of which are the superficial phase velocities (V_{sl} or V_{sg}) or generalized parameters containing these velocities. Some of the maps available are those of Hewitt and Roberts (1969) and Govier and Aziz (1972).

2.1.2 **Individual Transition Criteria:** Two-dimensional maps have limitations in representing all flow pattern transitions. An alternative, and more flexible, approach is to study each transition individually and to develop criteria valid for that transition. Because this approach allows physical modelling of individual flow patterns, it is probably the most reliable approach available at present. The individual transition criteria are discussed below.

a) **Bubbly-slug flow transition:** The transition from the condition of small bubbles dispersed throughout the channel to the condition where bubbles become large enough to fill the entire flow cross-section requires either coalescence or agglomeration. Agglomeration is a result of the collisions that take place owing to the zig-zag path followed by the bubbles. Radovcich and Moissis (1962) showed theoretically that at a void fraction of 0.3, the collision frequency becomes so high that a transition to slug flow is to be expected. Griffith and Snyder (1964)

experimentally verified that this transition takes place at a void fraction of 0.25 to 0.3. Hasan, Kabir, and Rahman (1988) also found the transition to occur at a void fraction of about 0.25 even in an annular geometry. Thus $E_g = 0.25$ may be taken as the criterion for the transition from bubbly to slug flow. This criterion may be expressed in terms of the superficial gas velocity, the mixture velocity and the terminal rise velocity, using the expression for bubbly flow (to be derived later), as follows

$$E_g = \frac{V_{sg}}{C_o V_m + V_t} \qquad (4)$$

Since $V_m = V_{sg} + V_{sl}$, we get

$$V_{sg}(1 - E_g C_o) = C_o V_{sl} E_g + V_t E_g \qquad (5)$$

$$V_{sg} = (V_{sl} C_o E_g / (1 - E_g)) + (V_t E_g / (1 - E_g C_o)) \qquad (6)$$

Harmathy (1960) proposed the following correlation for bubble terminal rise velocity, V_t

$$V_t = 1.53 \, [gs \, (d_1 - d_g)^2 / d_1]^{1/4} \qquad (7)$$

Using the Harmathy correlation for V_t, a value of 1.2 for the flow parameter C_o as suggested by Zuber and Findlay (1965a), and $E_g = 0.25$, Equation (6) gives

$$V_{sg} = 0.429 \, V_{sl} + 0.357 \, V_t \qquad (8)$$

$$= 0.429 \, V_{sl} + 0.546 \, [gs \, (d_1 - d_g)^2 / d_1]^{1/4} \qquad (9)$$

For the air-water system at room temperature, V_t is about 0.8 ft/sec. Thus, for a stagnant water column, equation (9) predicts that slug flow will occur whenever the superficial air velocity exceeds 0.29 ft/sec.

Dispersed Bubbly Flow: Equation (9) only applies to transition from bubbly to slug flow at low or moderate flow rates. At high flow rates the turbulence tends to break up the larger agglomerated bubbles, inhibiting the transition to slug flow. In such cases, bubbly flow persists even when the void fraction has exceeded 0.25. This type of bubbly flow, resulting from the break up of large bubbles at high flow rates, is known as dispersed bubbly flow. Taitel, Bornea and Dukler (1980) developed an expression for the onset of dispersed bubbly flow based on the maximum bubble diameter possible under highly turbulent conditions. This expression was later modified by Shoham (1982) as follows

$$V_m^{1.1}(f)^{0.4}(2/D_e)^{0.4}(d_1/d_g)^{0.6}$$

$$[0.4s/(d_1 - d_g)]^{0.5} = 0.725 + 4.15(V_{sg}/V_m)^{0.5} \quad (10)$$

Thus, if the mixture velocity is greater than that given by Equation (10), bubbly flow will persist even when E_g is greater than 0.25. However, Taitel et al. (1980) showed that even for small gas bubbles, the gas void fraction can, at most, be 0.52. At higher void fractions, the transition to slug (or churn) flow must occur.

b) Slug-Churn Flow Transition: In slug flow, " Taylor" bubbles, formed by the agglomeration of smaller bubbles, occupy most of the channel cross-section. These " Taylor" bubbles are axially separated by liquid slugs in which small bubbles are dispersed. The liquid confined between the " Taylor" bubbles and the tube wall flows down the sides of the bubble as a falling film. The interaction

between this falling film and the " Taylor" bubbles inc-
reases with increasing flow rate. The upper limit of slug
flow occurs when the interaction becomes high enough to
break the long bubbles, causing the transition to churn
flow. A semi-theoretical method to predict this critical
interaction (known as "flooding") has been given by Porteous
(1969) which relates the " Taylor" bubble rise velocity V_{tT}
to the total mixture velocity V_m. For moderate tube
diameters and low viscosity liquids, Porteous' (1969)
correlation simplifies to

$$V_m/V_{tT} = 0.3 \sqrt{d_1/d_g} \tag{11}$$

Substituting the Nicklin, Wilkes and Davidson (1962) correl-
ation for V_{tT} i.e.

$$V_{tT} = 0.35 \sqrt{gD(d_1-d_g)/d_1} = 0.35 \sqrt{gD} \tag{12}$$

we get

$$V_m = V_{sg} + V_{sl} = 0.105 \sqrt{gD(d_1-d_g)/d_g} \tag{13}$$

It should is to be noted that although churn flow is
indicated whenever V_m exceeds the value given by Equation
(13), churn flow cannot be attained with high liquid and low
gas flow rates because below a void fraction of 0.25, bubbly
flow must exist (with the exception of small tubes when slug
flow may occur).

c) **Transition to Annular Flow:** At high gas flow
rates, the transition from slug or churn flow to annular
flow takes place. The liquid flows upward along the tube
wall, while the gas flows through the center of the tube.
The liquid film has a wavy interface, and the waves may

break away and be carried by the gas as entrained droplets. The link between flow reversal and the transition to annular flow is best illustrated by considering the relationship between pressure gradient and upward gas flow. Results of this kind have been obtained by Hewitt and Hall-Taylor (1965). The pressure drop in counter-current flow, with the gas going upwards and a falling liquid film on the tube wall, is relatively small and only slightly above the pressure drop for the gas flow alone. However, near the flooding point the pressure drop increases dramatically and, at gas velocities just above the flow-reversal velocity, the pressure drop is typically an order of magnitude greater than its value for counter-current flow at gas velocities just below the flooding point. The reason for this great increase in pressure drop is the formation of a complex pattern of waves on the surface which act as a grossly increased interfacial roughness for the gas flow. Hewitt and Hall-Taylor (1965) showed that there is a minimum in the pressure drop which corresponds to the point at which the wall shear stress is close to zero. The minimum gas flow rate at which this flow reversal takes place may be viewed as the transition to annular flow. Based on this concept, Wallis (1969) proposed the following criterion for the transition to annular flow.

$$V_{sg} = 0.9 \sqrt{gD(d_1-d_g)/d_g} \tag{14}$$

A more rigorous analysis by Jones and Zuber (1978) yields the following

$$V_{sg} = 4(\sqrt{d_g/d_1})(\sqrt{gD(d_1-d_g)}/d_g)$$
$$(V_{s1} \sqrt{d_1/gD(d_1-d_g)} + K) \qquad (15)$$

The value of K depends on the geometry and is 0.35 for circular channels.

2.2   METHOD OF ANALYSIS

In the analysis of vertical multiphase flow, estimating static head is very important. In almost all vertical flow situations, static head is the major contributor to the total head loss, and in some cases (low gas fraction and flow rates), it may account for more than 90 percent of the total gradient. Because the gas void fraction, Eg, figures so prominently in calculating the static head of the fluid column, accurately estimating the void fraction is of paramount importance in vertical two-phase flow. The general correlation, to be derived later, for estimating gas void fraction, E_g, is shown in Equation (16).

$$E_g = V_{sg}/[CV_m + V_t] \qquad (16)$$

Equation (16) introduces the flow parameter C. It is denoted by C_o when applied to bubbly flow and by C_1 when applied to slug flow. C_o (or C_1) is given by Equation (17).

$$C_o = C_1 = (V_m E_g)_{avg}/(V_m)_{avg}(E_g)_{avg} \qquad (17)$$

The subscript avg. refers to the channel cross-sectional average. If the velocity and concentration profiles were flat, C_o would equal unity. In general, however, these profiles are not flat and, hence, C_o does not equal 1. For bubbly flow, the parameter C_o probably lies between 1.2 and 2.0. The classical work of Zuber and Findlay (1965a)

established a value of $C_o = 1.2$ for air-water system in a two inch pipe. Most of the recent work with bubbles rising in stagnant liquid columns in large diameter pipes (¶4 inches), indicate a higher value for C_o. Thus, Mashelkar (1970), Zahradnik (1979) and Haug (1976) have estimated C_o to be 2.0. Hasan, Kabir and Rahman (1988) suggest a value of 1.96 for such systems. For slug flow, since the flow is almost surely turbulent and since the bubbles ride the flat portion of the velocity profile, we expect C_1 to be 1.2. This is indeed found to be the case by Nicklin et al. (1962) and Hasan et al. (1988) and is the accepted value for the parameter. The churn or froth flow regime is rather difficult to analyze and has not been extensively investigated. Govier and Aziz (1972) recommend that Equation (22) be used for churn flow. However, the chaotic nature of the flow would tend to make the mixture velocity and gas concentration profiles flat. This would suggest a value lower than 1.2 for the value of the parameter C_1.

Chapter III

LITERATURE SURVEY

When a gaseous phase flows through a liquid phase in a circular channel, the two phases are seen to be distributed in a variety of flow patterns. Each flow pattern results from different hydrodynamic conditions and, as such, should be treated differently. In bubbly flow the gas flows as discrete bubbles through the continuous liquid phase. Higher flow rates result in coalescence of the bubbles which may eventually fill up the entire flow cross section. This flow is said to be slug flow because of the liquid slugs that are present between these large bubbles. Annular flow, in which the gas phase flows through the core while the liquid phase flows along the wall, is observed only at very high gas flow rates. Pumping oil through a circular channel usually results in only bubbly or slug flow patterns. Theoretical and experimental models for bubbly and slug flow, in vertical and inclined channels, are reviewed here.

The theoretical models have been developed principally by Zuber and Findlay (1965b), Wallis (1969) and Ishii (1975) for the general system where both the liquid and the gaseous phases are flowing. They have pointed out the importance of the relative velocity between the phases, V_{g1}, rather than the absolute insitu velocities, V_g (for gas) and V_1 (for liquid). By definition

$$V_{g1} = V_g - V_1 = [V_{sg}/E_g] - [V_{s1}/(1-E_g)] \qquad (18)$$

or

$$V_{g1}E_g(1-E_g) = V_{sg}(1-E_g) - V_{s1}E_g \qquad (19)$$

where void fraction, E_g, is the fraction of the total volume occupied by the gaseous phase. The superficial velocities, V_{sg} and V_{s1}, are obtained by dividing the volumetric flow rates of each phase by the cross-sectional area. Drift flux, j_{g1}, represents the volumetric flux of a component relative to a surface moving at the average velocity V_m (total volumetric flow rates of gas and liquid divided by the cross-sectional flow area),

$$j_{g1} = E_g(V_g - V_m) \qquad (20)$$

$$= V_{sg} - E_g V_m \qquad (21)$$

$$j_{g1} = V_{sg} - E_g(V_{s1} + V_{sg}) \qquad (22)$$

$$= V_{sg}(1-E_g) - V_{s1}E_g \qquad (23)$$

Combining Equations (21) and (23), the drift flux may be written as

$$j_{g1} = V_{g1}E_g(1-E_g) \qquad (24)$$

which is true at any local point in the flow. The velocity of each phase, however, may vary with radial position in a pipe or annulus, i.e., the velocity profile is, in general, not flat. Under these circumstances, Equation (23) can be rewritten by taking an average of the physical properties

$$V_{sg} = (E_g V_m) + j_{g1} \qquad (25)$$

Therefore

$$V_{sg}/E_g = (E_g V_m)/E_g + j_{g1}/E_g \qquad (26)$$

and since $V_g = (V_{sg}/E_g)$

$$V_g = \frac{\overline{E_g V_m}}{\overline{E_g}\,\overline{V_m}}\, V_m + \frac{\overline{j_{g1}}}{\overline{E_g}} = C_o V_m + \frac{\overline{j_{g1}}}{\overline{E_g}} \tag{27}$$

where $C_o = \overline{E_g V_m}/(\overline{E_g}\,\overline{V_m})$, the ratio of the average of the product of E_g and V_m to the product of the averages of E_g and V_m. C_o may or may not equal unity, depending on the velocity and bubble distribution across the channel. In general, when gas bubbles through a liquid column the velocity profile is such that C_o will never be unity.

3.1   IDEAL BUBBLY FLOW

Ideal bubbly flow occurs when the bubbles do not affect one another and when the bubble concentration is constant across the channel. Wallis (1969) proposed the following empirical equation for the bubble drift flux

$$j_{g1} = V_t (1-E_g)^n E_g \tag{28}$$

where V_t is the terminal rise velocity, which is defined as the velocity of a single bubble of gas through an infinite medium. The exponent n depends on bubble size and flow regime and is experimentally determinable.

For a bubble rising through an infinite stagnant liquid column the buoyancy forces are balanced by the drag forces. Wallis (1961) obtained a theoretical expression for the terminal rise velocity

$$V_t = K\,[gs\,(d_1-d_g)^2/d_1]^{1/4} \tag{29}$$

where s is the surface tension of the liquid, d_1 and d_g are densities of liquid and gas, respectively, and the coefficient K is, in general, a function of system properties. However, K is approximately constant for most

practical purposes when the liquid viscosity is low. Peebles and Garber (1953) extensively studied terminal rise velocity of a single bubble. For most cases when the Reynolds number is greater than 1000, they propose a value of 1.18 for K in Equation (29) which the gives

$$V_t = 1.18 \; [(gs \; (d_1 - d_g)^2 / d_1]^{1/4} \qquad (30)$$

Harmathy (1960) proposed the same equation with a value of 1.53 for K, i.e.,

$$V_t = 1.53 \; [(gs \; (d_1 - d_g)^2 / d_1]^{1/4} \qquad (7)$$

Because Equation (7) has been used by several researchers (Hasan 1986, Hasan and Kabir 1986) to analyze their data, it will be used in this thesis. If n=2, as suggested by Wallis (1961), is used along with Equation (7) for V_t, Equation (28) becomes

$$j_{g1} = 1.53E_g(1-E_g)^2 \; [gs \; (d_1 - d_g)^2 / d_1]^{1/4} \qquad (31)$$

For a stationary liquid column, i.e., $V_m = V_{sg}$, Equation (4) yields

$$j_{g1} = V_{sg}(1-E_g) \qquad (32)$$

Equations (31) and (32) give

$$V_{sg} = 1.53E_g \; (1-E_g) \; [gs \; (d_1 - d_g)^2 / d_1]^{1/4} \qquad (33)$$

For most cases $d_1 \ggg d_g$ and

$$V_{sg} = 1.53E_g \; (1-E_g)(gs/d_1)^{1/4} \qquad (34)$$

Equation (33) relates the void fraction to the superficial gas velocity for ideal bubbly flow for a stagnant liquid column.

There are disagreements over the value of n to be used in Equation (28). Gaylor, Roberts asnd Patt (1953) found a

value of n=2 only for very low Reynolds number Re (usually less than 2). This reinforces the idea that ideal bubbly flow is likely to occur for only small bubble diameter. Miles, Shedlovsky and Ross (1943), working with stable foams, observed n to vary between 1.6 and 1.9. Lockett and Kirkpatrick (1976) found a similar variation in n (between 1.8 and 2.4) even though they took special care to maintain ideal bubbly flow. Zuber and Hench (1962) presented data indicating a value of n = 1.5 for Re greater than 1000. Wallis (1961) obtained significantly different values of n for air bubbling through pure and impure distilled water, tap water and soap solutions. Wallis (1961) also noted similar variation in the values of n with the distance travelled by the bubbles from the point of injection. Lockett and Kirkpatrick (1976) got different values of n depending on the way the bubbles were introduced into the column.

3.2 MODIFICATIONS FOR NON-IDEAL EFFECTS

In practice, some bubble coalescence does occur. The bubbles may be large with a spherical cap and flat at the tail. Thus, the variation in bubble concentration and velocity necessitates modifying simple bubble flow theory. Zuber and Hench (1962) suggested that the result of the entrainment of bubbles in each others' wake is an increase in the velocity and a decrease in the value of the exponent n in Equation (28). They suggested a value of zero for n and proposed using Equation (31) for V_t. This reduces

Equation (31) to the following equation for drift flux
(assuming $d_1 \ggg d_g$)

$$j_{g1} = E_g V_t = 1.53 E_g \ (gs/d_1)^{1/4} \qquad (35)$$

Using the expression for j_{g1} in Equation (27), we get the
following equation.

$$V_g = C_o V_m + V_t = C_o V_m + 1.53 \ (gs/d_1)^{1/4} \qquad (36)$$

Since all equations apply to non-ideal flow, the bar on top
of the variables will be omitted. For a stagnant liquid
column ($V_m = V_{sg}$) Equation (36) reduces to

$$V_g = V_{sg}/E_g = C_o V_m + 1.53 (gs/d_1)^{1/4} \qquad (37)$$

Therefore

$$E_g = \frac{V_{sg}}{C_o V_m + 1.53 (gs/d_1)^{1/4}} \qquad (38)$$

or

$$E_g = \frac{V_{sg}}{C_o V_{sg} + V_t} \qquad (4)$$

The data of Zuber and Findlay (1965b), gathered in a
circular channel, agrees well with Equation (4) when C_o =
1.2.

3.3   SLUG FLOW

At higher gas velocities, the agglomerated bubbles
become large enough to almost fill the entire cross-
sectional area available for flow. These bubbles are
characteristically cylindrical or bullet shaped. The liquid
slugs in between the " Taylor" bubbles may or may not con-
tain smaller gas bubbles entrained in their wake. It is
these liquid slugs that give the name to the flow pattern

and the dynamics of this flow pattern are quite different
from those of bubbly flow. For vertical slug flow, the
terminal rise velocity depends on gravity, surface tension,
as well as forces of inertia and viscous forces. Wallis
(1969) gave the following expression for void fraction in
slug flow

$$E_g = \frac{V_{sg}}{(C_1 V_m + V_{tT})} \tag{39}$$

Suggesting a value of 1.0 for C_1, White and Beardmore (1962)
developed an equation for V_t

$$V_t = K \ (gD \ (d_1 - d_g)/d1)^{1/2} \sim K\sqrt{gD} \tag{40}$$

Hence, Equation (39) becomes

$$E_g = \frac{V_{sg}}{C_1 V_m + K(gd)^{1/2}} \tag{41}$$

The constant K, which varied for different geometries and
was determined experimentally for various channels, is given
by Wallis (1962). For circular channels, K was
experimentally found to have a value of 0.345 by White and
Beardmore (1962) and 0.346 by Dumitrescu (1943). Nicklin et
al. (1962) reported a value of 0.35. For very small
channels (4.07 square inch cross-section), Birkoff and
Carter (1957) obtained a lower value of 0.23. Working
theoretically, Davis and Taylor (1950) and Dumitrescu (1943)
obtained slightly different values for K. Nicklin et al.
(1962) pointed out that variable bubble concentration needs
to be accounted for by using a value of 1.2 for C_1 in
Equation (41). Griffith (1963) showed that in a slug-flow

pattern through an annulus, the outer diameter, and not the equivalent diameter, should be used.

3.4   INCLINED FLOW

Although extensive research in two-phase flow has been conducted in the last 25 years, most of this research has been confined to horizontal or vertical flow.   Several good correlations exist for predicting pressure drop and liquid holdup in horizontal and vertical systems, but these correlations have been largely unsuccessful when applied to flow in inclined pipes.   Pipe inclination adds another complication to already complex two-phase flow phenomena generally observed in vertical pipes.   Available correlations for determining flow pattern and estimating void fraction and pressure gradient in inclined pipes are largely empirical.

The classical study of Beggs and Brill (1973) probably gives the most comprehensive method available at present to predict void fraction and pressure drop in inclined systems. Their correlation is based on a predictive method for the horizontal system with modifications to account for the system inclination.   They divide the observed flow patterns for horizontal systems into four categories: segregated, intermittent, transition, and distributed.   They present a horizontal flow pattern map based on the mixture Froude number, Fr_m (= V_m^2/gD) and the input liquid volume fraction C_1 (= V_{sl}/V_m).   For estimating liquid holdup for a horizontal system, E_{lo} (= in situ liquid fraction = 1 -

E_{go}), they propose the following equation

$$E_{lo} = a \; C_1{}^b / Fr_m{}^c \qquad\qquad (42)$$

The values of the parameters a, b, and c depend on the flow regime. The frictional pressure gradient is calculated using the no-slip density, $d_n = d_1 C_1 + d_g C_g$. The mixture friction factor, f_m, is calculated from the no-slip friction factor f_n (from the no-slip Reynolds number) and a multiplier whose value depends on the liquid input fraction, C_1, and the liquid holdup for the inclined system, E_{lc}.

For inclined systems, Beggs and Brill (1973) use the holdup calculated from Equation (42) and multiply it by a factor, F(c). The value of the multiplier depends upon the pipe inclination c, input liquid fraction C_1, dimensionless liquid velocity number V_{ld}, and the Froude number Fr in the following manner

$$F(c) = 1 + [\{\sin(1.8c) - 0.333\sin^3(1.8c)\}$$
$$\{(1 - C_1)\ln \; d(C_1)^e (V_{ld})^f (Fr)^g\}] \qquad (43)$$

The parameters d, e, f, and g depend on the flow pattern that would exist in an equivalent horizontal system. The predictions from using this method are generally good, as shown by Payne et al. (1979) for inclined systems and by Lawson and Brill (1974) for vertical systems.

However, the use of liquid input fraction in the Beggs and Brill (1973) method to determine the horizontal flow pattern and the correction factor F(c) would be impossible for stagnant liquid columns; and for small values of C_1, the predictions are unreliable. Danesh (1980) points out that

for the flow of gas and condensate oils, consideration of the physical properties indicates a decrease in F(c) with increasing V_{1d} while the Beggs and Brill method for horizontal segregated flow suggests exactly the opposite. Hasan and Kabir (1986) proposed using the density difference, $d_1 - d_g$, instead of the liquid density, d_1, alone to define the dimensionless liquid velocity number.

A number of other workers have proposed methods to predict void fraction and pressure drop in inclined systems. The earliest attempts were probably made by Baker (1957) and Flanigan (1958). Flanigan suggested that the total pressure drop consists of two principal contributions: (1) that due to friction, as in horizontal flow, and (2) that due to the sum of uphill rises multiplied by a liquid head factor, E_H. Baker (1957) followed an almost identical approach, but reported an empirical equation for E_H in terms of the superficial gas velocity. These methods are rather simplistic and only apply to slightly inclined systems. The more recent work of Guzhov, Mamayev and Odishariya (1967), while more sophisticated, is still limited to systems very close to the horizontal. Mukherjee and Brill (1983) recently presented a correlation similar to that of Beggs and Brill (1973).

Methods to predict two-phase flow behavior using the flow pattern approach have also been proposed. These methods are, however, incomplete and address only one flow regime. For example, a number of researchers such as Asheim

(1986) and Aziz, Govier and Fogarasi (1972) have proposed models for inclined flow. Singh and Griffith (1970) proposed a method similar to that used for vertical flow to predict void fraction during slug flow in inclined pipes. They used different pipe sizes with uphill angles of zero to 20 degrees from the horizontal and obtained, for all inclinations,

$$V_g = 0.95V_m + 1.15 \tag{44}$$

In the discussion following their paper, they were unable to explain the fact that the constant 1.15 (ft/sec), which represents the bubble rise velocity in a stagnant liquid, also apparently applied to their horizontal-flow case. In their study, V_g was not measured but calculated.

Bonnecaze, Erskin and Greskovich (1969) developed a model for two-phase slug flow in inclined pipes. In their model, a slug unit consisted of a liquid slug and a gas bubble. The pressure drop was assumed to be caused primarily by the liquid in the slug, for which a two-phase friction factor is obtained. Mattar and Gregory (1974) also presented a method similar to that of Bonnecaze et al. (1969) from data gathered in a similar system. They proposed a relation for liquid volume fraction,

$$E_g = V_{sg}/[1.3V_m + 0.7] \tag{45}$$

Asheim (1986) used a method similar to that of Singh and Griffith (1970) with constant values of C_1 and V_{tT}, without regard to pipe inclinations, flow regimes and pipe dimensions, to predict data gathered from North Sea oil

(1986) and Aziz, Govier and Fogarasi (1972) have proposed models for inclined flow. Singh and Griffith (1970) proposed a method similar to that used for vertical flow to predict void fraction during slug flow in inclined pipes. They used different pipe sizes with uphill angles of zero to 20 degrees from the horizontal and obtained, for all inclinations,

$$V_g = 0.95V_m + 1.15 \qquad\qquad\qquad (44)$$

In the discussion following their paper, they were unable to explain the fact that the constant 1.15 (ft/sec), which represents the bubble rise velocity in a stagnant liquid, also apparently applied to their horizontal-flow case. In their study, V_g was not measured but calculated.

Bonnecaze, Erskin and Greskovich (1971) developed a model for two-phase slug flow in inclined pipes. In their model, a slug unit consisted of a liquid slug and a gas bubble. The pressure drop was assumed to be caused primarily by the liquid in the slug, for which a two-phase friction factor is obtained. Mattar and Gregory (1974) also presented a method similar to that of Bonnecaze et al. (1969) from data gathered in a similar system. They proposed a relation for liquid volume fraction,

$$E_g = V_{sg}/[1.3V_m + 0.7] \qquad\qquad\qquad (45)$$

Asheim (1986) used a method similar to that of Singh and Griffith (1970) with constant values of C_1 and V_{tT}, without regard to pipe inclinations, flow regimes and pipe dimensions, to predict data gathered from North Sea oil

wells.

Vermuelen and Ryan (1971) reported results for air-water slug flow in 1/2-inch diameter pipe for inclinations of -7 degrees, zero degrees and +7 degrees. They presented a semi-empirical model to predict over-all pressure drop. Unfortunately, the slug frequency must be known a priori, which limits the usefulness of their model.

Models that do not account for various flow regimes are likely to be less accurate. In addition, the fact that the bubble rise velocity during intermittent flow depends on pipe inclination appears to be well established. To accurately predict two-phase flow behavior under inclined conditions, it is necessary to recognize the existing flow patterns and to assign values of flow parameter and bubble rise velocity appropriate for each flow regime.

Chapter IV

THE PROPOSED MODEL

The model used in this thesis is based on a flow pattern approach that has successfully predicted vertical multiphase flow data. It is to be noted that for systems that are highly deviated (close to being horizontal), the bubbly flow pattern is sometimes absent. Indeed, Barnea, Shoham, Taitel, and Dukler (1985) maintain that for systems deviated by more than 50 degrees from the vertical, bubbly flow never occurs. However, Weisman and Kang (1981) state that careful observations usually reveal a bubbly flow regime at very low gas flow rates, even for near horizontal systems.

Since the experimental set-up limited the observed flow regimes to bubbly and slug flow, the emphasis of this study will be on these two flow regimes only.

4.1   Bubbly Flow

For circular channels in vertical and inclined flow systems, the in situ velocity of the gaseous phase, V_g, has been expressed as the sum of the bubble rise velocity, V_t, and the mixture velocity at the channel center, $C_o V_m$ (Zuber and Findlay 1965a; Hasan 1986; Hasan and Kabir 1986, 1987) as shown in Equation (37)

$$V_g = C_o V_m + V_t \tag{37}$$

Noting that $V_g = V_{sg}/E_g$, Equation (37) gives

$$E_g = V_{sg} / [C_o V_m + V_t] \tag{4}$$

For circular channels, the terminal rise velocity V_t is given by the Harmathy (1960) correlation. C_o has generally been taken to have a value of 1.2 although its value is 2.0 when the pipe diameter exceeds 100 mm in standing liquid columns.

The proposed model predicts that the pipe inclination and the annulus diameter will not affect the void fraction.

4.1.1 Bubbly-Slug Flow Transition: For circular channels, Griffith and Snyder (1964) and Hasan and Kabir (1987) have experimentally verified the theoretical contention of Radovcich and Moissis (1962) that the transition from bubbly to slug flow occurs at a void fraction of about 0.25. This transition was observed to occur at the same void fraction in annular geometry as well. The effect of pipe inclination on this transition appears to be well represented by the sin $\propto$ factor proposed by Hasan and Kabir (1986) for inclined circular channels. This criterion is expressed in terms of the superficial phase velocities

$$V_{sg} = [C_o V_{sl} + V_t] \sin \propto / (4 - C_o) \tag{46}$$

4.1.2 Dispersed Bubbly Flow: The bubbly-slug flow transition discussed so far applies to low and to moderate flow rates only. Because of the high velocities found in dispersed bubbly flow, annulus dimensions and pipe inclinations are unlikely to affect this transition. Accordingly, Filho (1984) adapted Shoham's model (1982) for

annular channels using the channel equivalent diameter D_e ($= D_o - D_i$), as follows

$$(V_m)^{1.1}(f)^{0.4}(2/D_e)^{0.4}(d_1/d_g)^{0.6}$$

$$[0.4o/(d_1-d_g)]^{0.5} = 0.725 + 4.15(V_{sg}/V_m)^{0.5} \quad (10)$$

Thus, if the mixture velocity is greater than that given by Equation (10), bubbly flow will persist even when E_g is greater than 0.25. However, Taitel et al. (1980) showed that even for small gas bubbles, the gas void fraction cannot exceed 0.52. At higher void fractions, transition to slug (or churn) flow occurs. The data of Filho (1984) shows that although Equation (10) overestimates the superficial liquid velocity at which this transition occurs, overall agreement is reasonable.

Equation (4), with V_t given by the Harmathy (1960) correlation, is proposed for calculating void fraction. Dispersed bubbly flow shall be treated as ordinary bubbly flow. The high fluid velocities involved make it unlikely that the pipe diameters or the inclination angle would have any influence on the flow parameter C_o. Therefore, for dispersed bubbly flow, a value of 1.2 is recommended for C_o in Equation (4).

4.2   Slug Flow

Analysis of slug flow is very similar to that of bubbly flow. Indeed, Equation (4) applies for void fraction in slug flow as well as for bubbly flow, but with different constants. Thus,

$$E_g = V_{sg} / (C_1 V_m + V_{tT}) \quad (39)$$

" Taylor" bubble rise velocity in vertical circular channels, V_{tT}, in slug flow is given by

$$V_{tT} = C_2 \sqrt{gD(d_1 - d_g)/d_1} \sim C_2 \sqrt{gD} \qquad (47)$$

Extensive data and theoretical analyses by a number of researchers indicate that C_2 is influenced by inertial, viscous, and surface forces. However, for many practical systems (if the diameter is not too small) C_2 equals 0.345.

For slug flow in inclined circular channels, Hasan (1986) and Hasan and Kabir (1986) found that C_1 remains constant at 1.2. The variation in terminal rise velocity with pipe inclination was given in the following manner

$$V_{tTo} = V_{tT} \sqrt{\sin \alpha}[1 + \cos \alpha]^{1.2} \qquad (48)$$

As in the case of bubbly flow, void fraction during slug flow in annuli may be represented by Equation (39).

Unlike bubbly flow, the proposed model maintains that both the pipe inclination and the annulus dimensions will affect void fraction during slug flow.

Chapter V

EXPERIMENTAL SET-UP AND PROCEDURE

5.1   EXPERIMENTAL SET-UP

An experimental rig, consisting of a column of 5 inch inside diameter and a height of eighteen feet, made of plexiglass and constructed by Rehana Rahman (1984), was used to gather void fraction data.   Inner tubes, made of opaque polyvinyl chloride, of different internal diameters were inserted into the column. These inner tubes remained empty during experimental runs.   The bottoms of these tubes were threaded on the insides and could be joined to a two-inch extended pipe (threaded on the outside) which was positioned in the center at the base of the column.   Figure 1 illustrates the experimental set-up.

Using a system of bolts and chains, the entire column could be inclined to a maximum deviation of 32 degrees from the vertical.   During experimental runs, the annulus was filled with water to the desired height in the column.   The outer surface of the column was marked at various heights to facilitate measuring single bubble rise velocities and for visual confirmation of liquid height.

Air was allowed to flow into the bottom of the annulus through four equally spaced ports around the bottom of the casing. The air flow through these ports was smoothly controlled by using four metering valves. At pressures in

32
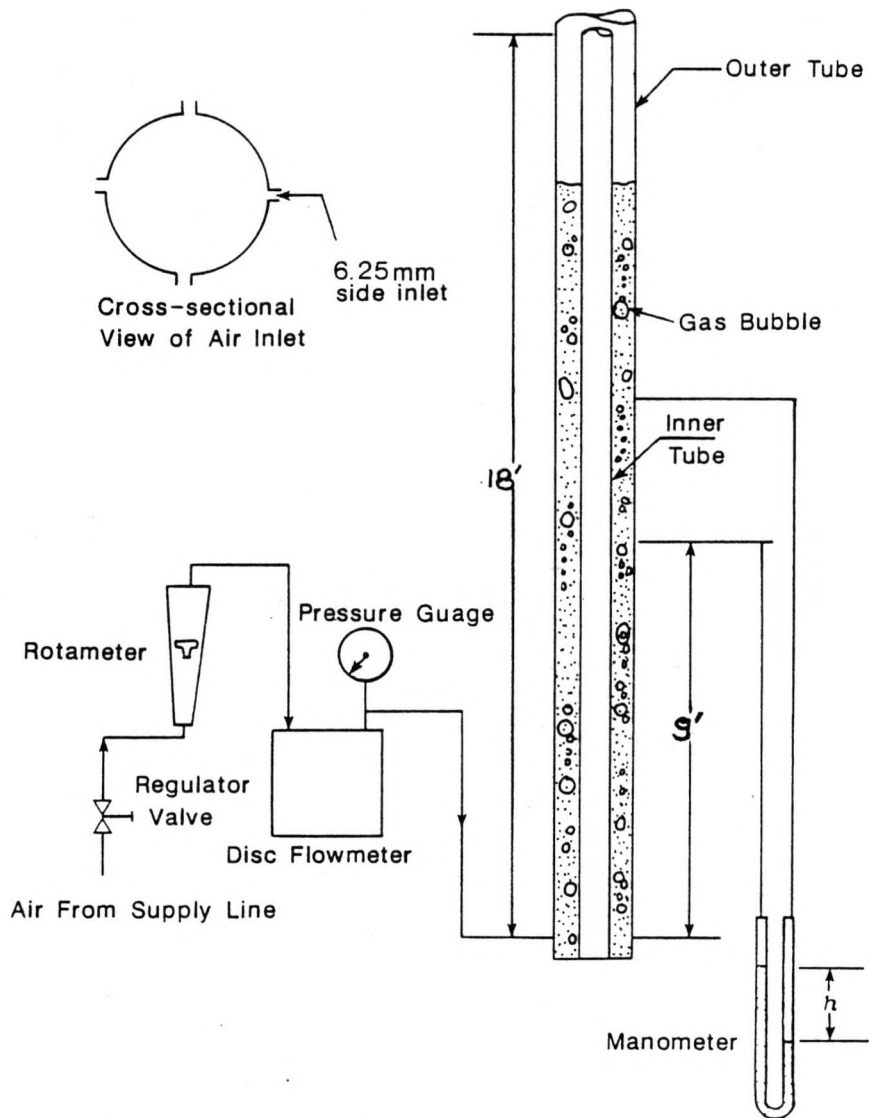
Figure 1: Experimental Set-Up for Measuring Void Fraction.

excess of 30 psig, the air flow regulator was the only means of flow rate control. The pressure at the air flow regulator did not exceed 75 psig due to a relatively low supply pressure.

The air flow rate was measured upstream of the annulus using a disc flowmeter and a stopwatch that measured to 0.01 second. A rotameter was positioned between the disc flowmeter and the outer casing. The rotameter, which was calibrated from 0 to 100, was not very accurate and was used only to ensure that data were gathered over the entire range of flow rates.

Gas void fraction was calculated using differential pressure data gathered using an U-tube manometer. The manometer fluid was a combination of red gage oil and tetrabromoethane, mixed in appropriate proportions to give a specific gravity of 1.62. The manometer was connected to a pair of pressure taps, separated by a known distance, in the column by transparent plastic tubes from which all air bubbles had been removed. A pair of short, flexible tubes connected the plastic tubes to the manometer. These short tubes allowed for the detection of air bubbles. Bleeder valves on the manometer were the main tools to remove air bubbles. The pressure taps were located at a distance of 9 to 13 feet from the bottom of the column.

5.2 EXPERIMENTAL PROCEDURE

The air flow rate was varied from 0.1 to 7.0 cubic feet/minute. The annulus was filled with water to a height

three inches above the topmost pressure tap. Air was fed into the water column using the air ports and sufficient time was allowed for the flow rate to stabilize, as indicated by a steady rotameter float. Experimental runs were made by inclining the column at various angles with inner tubes of different diameters. These experimental runs yielded the following data:

1) differential heights on the manometer

2) the flow rate of air into the column, Q ft^3/min and

3) the pressure at which air was measured, P psia

In addition, bubble rise velocity data for small as well as " Taylor" bubbles were gathered. A single bubble was released and the time it took to travel a pre-determined distance was recorded. To avoid entrance effects, data were gathered between 5 and 15 feet from the entrance. Single bubbles were released by maintaining a very low flow rate through only one air inlet.

Visual observations were also made to try and determine the existing flow patterns. This was possible at low to moderate flow rates where bubbly and slug flow patterns could be discerned. At high flow rates the slug region tended to merge with churn-like flow.

Chapter VI

RESULTS AND DISCUSSION

6.1   EXPERIMENTAL RESULTS

Data gathered using an eighteen feet high column are
presented and analyzed in this chapter.   Single bubble rise
velocity data are examined first followed by the void
fraction data.

6.2   SMALL AND " TAYLOR" BUBBLE RISE VELOCITY

Bubbly flow is the flow regime wherein small bubbles
are uniformly dispersed in the flow medium.   Experimental
values of small bubble rise velocity were gathered by
measuring the time for a bubble to travel a predetermined
distance.   The runs were performed using an open channel and
with inner pipes having diameters of 1.5, 2 and 3 inches
I.D. and a casing of 5 inch I.D.   The data show that the
velocity is unaffected by the pipe inclination and the
annuli dimensions. Average values for the different angles
and annuli dimensions are tabulated in Table 1.   The overall
average of 0.84 ft/sec. is in good agreement with the
Harmathy (1960) correlation.

At higher gas flow rates, the bubbles coalesce into
individual bullet-shaped bubbles called " Taylor" bubbles.
" Taylor" bubble rise velocity was measured by suddenly
opening and closing the gas valve to send a jet of air into
a stationary liquid column.   The " Taylor" bubbles were

grouped according to their size i.e, 1, 2, 3 and 4 inches. The " Taylor" bubble rise velocities are in Table 2. Table 2 contains values of the " Taylor" bubble rise velocity for different angles of inclination and different annuli dimensions.

Table 1

Small Bubble Rise Velocity Data

Deviation from the vertical degrees	Inner Pipe Diameter inches	Terminal bubble Rise Velocity ft./sec.
32	0.000	0.83
	1.870	0.85
	2.240	0.84
	3.409	0.84
24	0.000	0.85
	1.870	0.82
	2.240	0.86
	3.409	0.83
16	0.000	0.84
	1.870	0.86
	2.240	0.82
	3.409	0.85
08	0.000	0.84
	1.870	0.85
	2.240	0.82
	3.409	0.86
00	0.000	0.83
	1.870	0.84
	2.240	0.86
	3.409	0.85
	Overall Average =	0.84

The " Taylor" bubble rise velocity in vertical circular

channels, V_{tT}, in slug flow is given by Nicklin et al. (1962)

$$V_{tT} \sim C_2 \, (gD)^{1/2} \qquad (49)$$

For low pressures and large diameter systems, such as were used in this study, C_2 equals 0.345. Therefore

$$V_{tT} \sim 0.345(gD)^{1/2} \qquad (50)$$

Table 2

" Taylor" Bubble Rise Velocity Data

Deviation from the vertical	Tubing Outside Diameter	Experimental Terminal Rise Velocity	Predicted Terminal Rise Velocity
Degrees	D_t, in.	V_{tT}obs	V_{tT}pred
32	0.000	2.040	1.939
	1.870	2.020	2.090
	2.240	2.120	2.120
	3.409	2.210	2.214
24	0.000	1.790	1.820
	1.870	1.920	1.984
	2.240	1.970	2.017
	3.409	2.080	2.120
16	0.000	1.610	1.668
	1.870	1.790	1.839
	2.240	1.820	1.873
	3.409	1.920	1.979
08	0.000	1.470	1.470
	1.870	1.550	1.626
	2.240	1.640	1.657
	3.409	1.710	1.755
00	0.000	1.270	1.264
	1.870	1.460	1.401
	2.240	1.460	1.428
	3.409	1.530	1.513

The variation in terminal rise velocity with pipe inclination is given by Hasan (1986) and Hasan and Kabir (1986)

$$V_{tTo} = V_{tT} \ (\sqrt{\sin \alpha}) \ [1 + \cos \alpha]^{1.2} \qquad (48)$$

The presence of an inner tube tends to make the nose of the " Taylor" bubble sharper, causing an increase in the rise velocity V_{tT}.

Bubble rise velocity data gathered for the present work agrees with the suggestion by Griffith (1963) that the diameter of the outer tube should be used in Equation (49) to estimate V_{tT} in an annulus. Our " Taylor" bubble rise data for vertical systems show a linear relationship with the diameter ratio D_t/D_c, suggesting the following expression for " Taylor" bubble rise velocity for vertical annular systems

$$V_{tTao} = [0.345 + 0.1(D_t/D_c)][gD_c(d_1 - d_g)/d_1]^{1/2} \qquad (51)$$

It is worth noting that Griffith (1963) also observed similar variation in V_{tT} with annuli diameters, although his data indicate a weaker dependence of this parameter with D_t/D_c. The rise velocity data of Filho (1984) were overestimated by 6.8 percent using the Sadatomi, Sato and Saruwatari (1982) correlation while Equation (48) under-estimates the same data by 2.09 percent.

Equations (48) and (51) were combined to account for the effects of both the inclination and the annulus diameter. It was noted, however, that the combination of the two expressions did not give the same accuracy as do

the individual expressions. Hence, the term $\sin^2 o$ was included to account for the discrepancies. The combined form of Equations (48) and (51) with the new term $\sin^2 o$ is shown in Equation (52).

$$VtT = [0.35 + 0.1(Dt/Dc)\sin^2\alpha][gD_c(d_1-d_g)/d_1]^{0.5}$$
$$[\sqrt{\sin\alpha}(1 + \cos\alpha)^{1.2}] \qquad (52)$$

Inserting the values for d_1, d_g, g and D_c for the system under consideration gives the following correlation:

$$VtT = [0.35 + 0.1(Dt/Dc)\sin^2\alpha](3.663)$$
$$[\sqrt{\sin\alpha}(1 + \cos\alpha)^{1.2}] \qquad (53)$$

" Taylor" bubble rise velocity data in annuli inclined at 58, 66, 74, 82, and 90 degrees to the horizontal are plotted against annulus diameter ratio in Figure 2. Figure 2 shows " Taylor" bubble rise velocity predictions of Equations (48) and (51) as solid lines. It is apparent from Figure 2, however, that when the channel is highly deviated from vertical, Equation (52) appears to overestimate the effect of the inclination. Because our system could not be deviated by more than 32 degrees from vertical, no attempt was made to further refine Equation (52) to account for this overestimation.

The predictions by our model of the data reported for vertical annular channels by Filho (1984), Sadatomi et al. (1982) and Griffith (1963) are shown in Figure 3. The agreement appears to be excellent.

It is noted from the values for velocity shown in Table 2 that the " Taylor" bubble rise velocity increases with
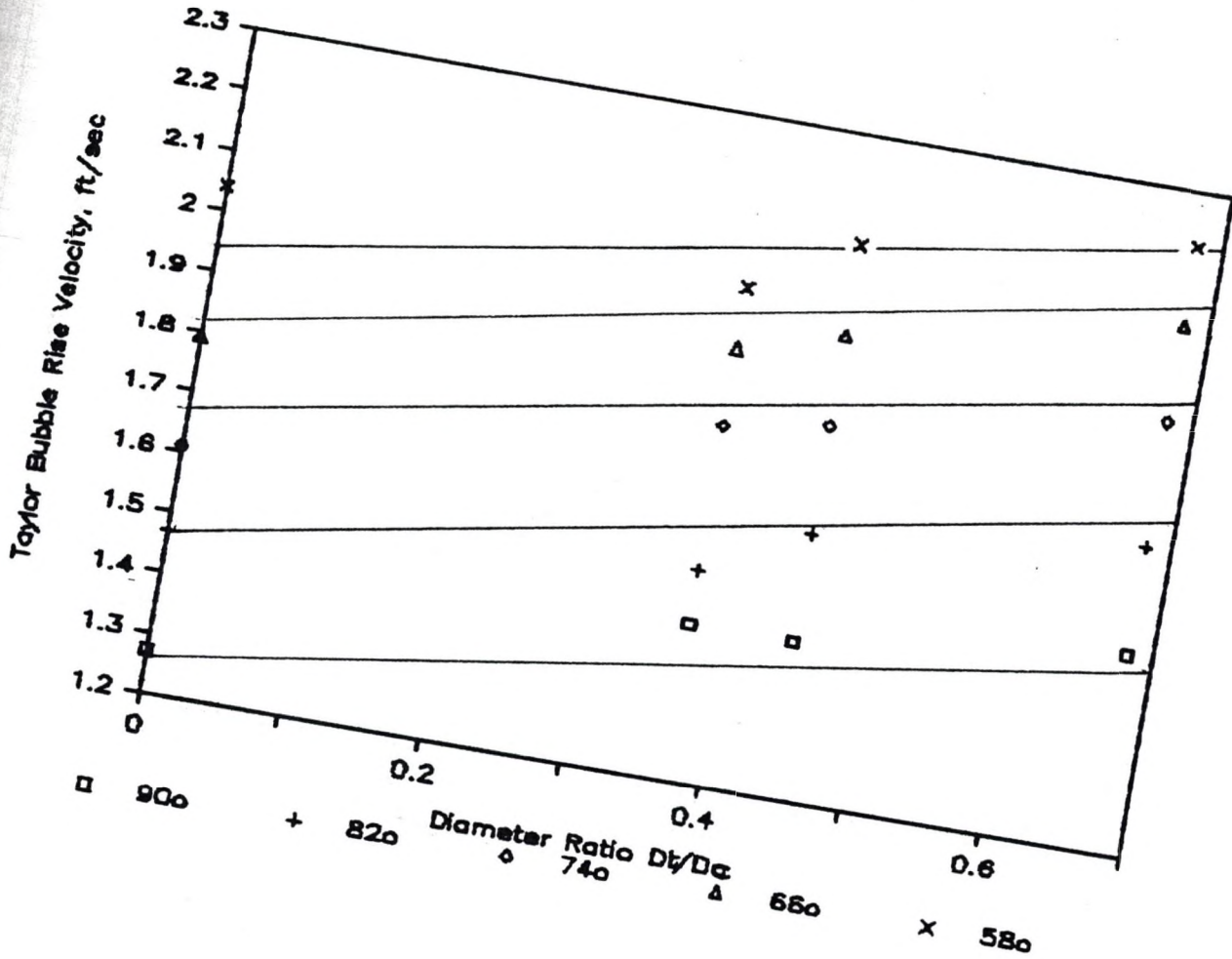
Figure 2: "Taylor" Bubble Rise Velocity Data in Annuli Inclined at 0, 8, 16, 24, and 32 degrees to the vertical.
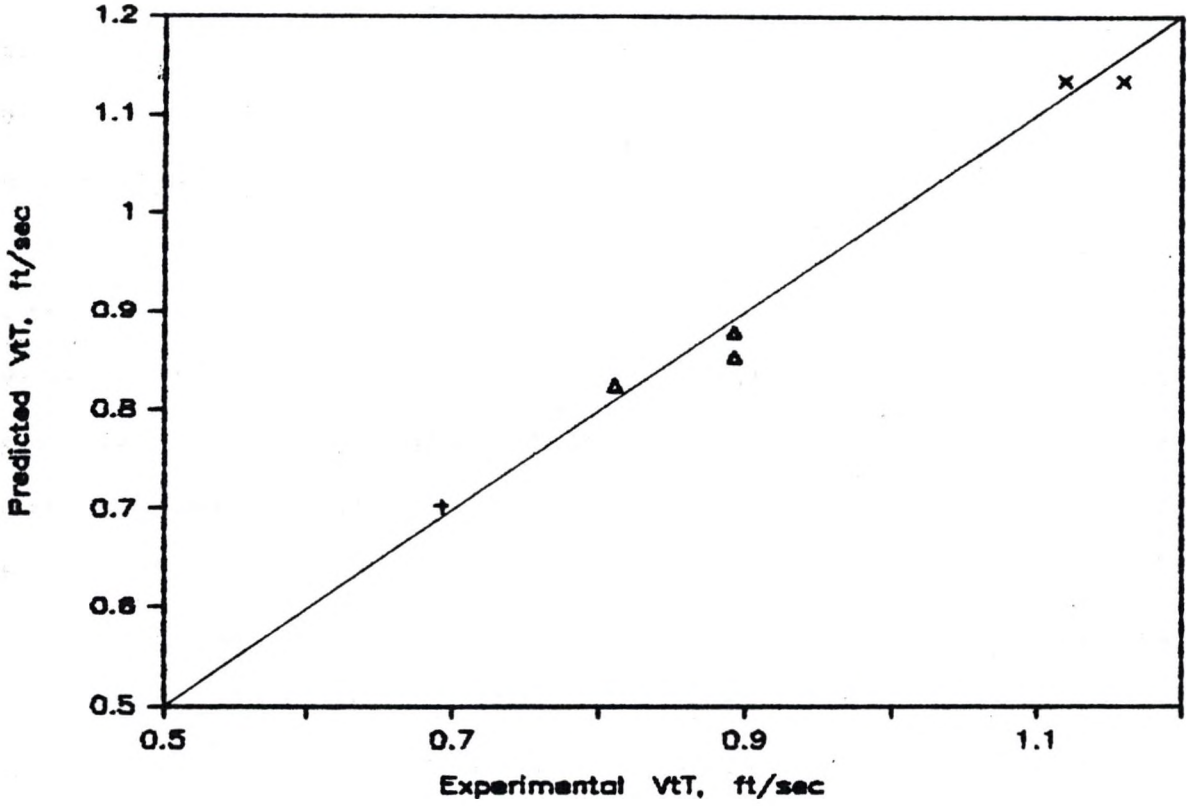
Figure 3: Comparison of "Taylor" Bubble Rise Velocity Data with that from Several Sources.

increase in the inner tube diameter. It is also noted that the " Taylor" bubble rise velocity is smaller than the predicted values, and it is fair to assume that the " Taylor" bubble rise velocity is affected by the containing walls.

6.3   VOID FRACTION DATA

6.3.1 Bubbly Flow

Void fraction data were gathered using the manometric method of void fraction measurement. Visual observation showed the existence of a bubbly flow pattern at low air flow rates while at higher flow rates, the lower part of the column showed bubbly flow while the upper section showed slug flow.

Experimental results obtained with the air-water system are shown in Figures 4 through 23. The figures are plots of the ratio of superficial gas velocity to void fraction, Vsg/Eg, versus the superficial gas velocity, Vsg. All plots yielded straight lines in two separate regions. The first region represents bubbly flow while the second represents slug flow. The scatter at lower values of superficial gas velocity, V_{sg}, reflects large errors in the calculation of Vsg/Eg caused by the sluggish response of the manometric fluid in response to changes in small pressure drops existing in the column.

Effect of Pipe Inclination

Figures 4, 8, 12, 16, and 20, which are plots for circular or open channels for different angles of

inclination, show that the pipe inclination apparently does not affect the void fraction in bubbly flow. It is also observed that the flow parameter C_o, for bubbly flow in circular channels does not depend on pipe inclination. This is consistent with the findings of Hasan and Kabir (1986) and Hasan (1986).

Effect of Annular Dimension

Figures 5, 7, 13, 17, and 21 are plots for an inner pipe of 1.87 inch diameter for different angles of inclination. The presence of an inner tube apparently does not affect the bubble concentration. For the large diameter system used in this study, C_o was found to be 2.0, which agrees with our circular channel data and that of Zahradnik and Kastanek (1979), Haug (1976) and Mashelkar (1970).

6.3.2 Bubbly-Slug Flow Transition

For circular channels, Hasan and Kabir (1988) and Griffith and Snyder (1964) have experimentally verified the contention of Radovcich and Moissis (1962) that the transition from bubbly to slug flow occurs at a void fraction of about 0.25. We found this transition to occur at the same void fraction in the annular geometry as well. Figures 4 through 23 support this conclusion. The transition from bubbly to slug flow is not seen to occur at a single value but rather over a wide range of values suggesting that the transition is gradual. In addition, the effect of pipe inclination on this transition is well represented by the angle factor, $\sin\alpha$, proposed by Hasan and

Figure 4: Ratio of Superficial Gas Velocity to Void Fraction as a Function of Gas Velocity - 0 degrees, Circular Channel.

Figure 5: Ratio of Superficial Gas Velocity to Void Fraction as a Function of Gas Velocity - 0 degrees, 1.87 inch inner pipe.

Figure 6: Ratio of Superficial Gas Velocity to Void Fraction as a Function of Gas Velocity - 0 degrees, 2.24 inch inner pipe.

Figure 7: Ratio of Superficial Gas Velocity to Void Fraction as a Function of Gas Velocity - 0 degrees, 3.409 inch inner pipe.
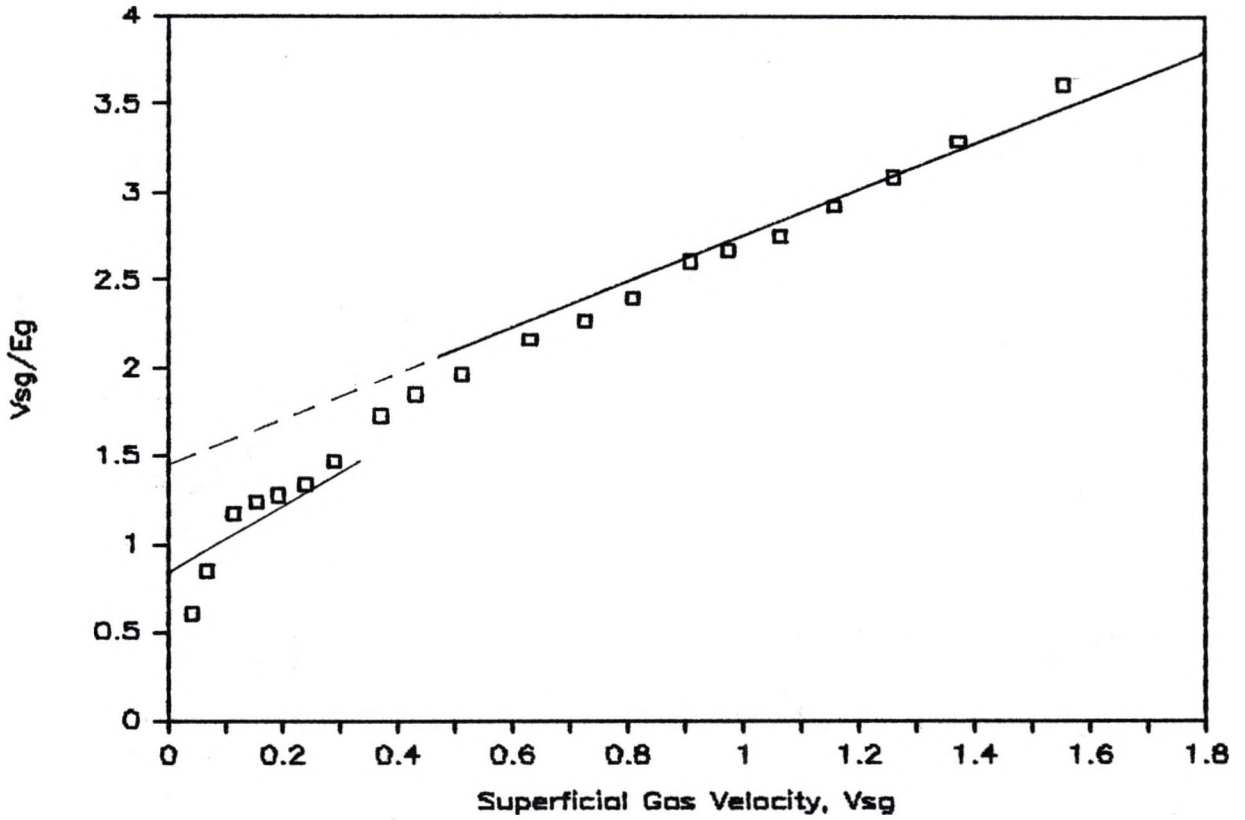
Figure 8: Ratio of Superficial Gas Velocity to Void Fraction as a Function of Gas Velocity - 8 degrees, Circular Channel.
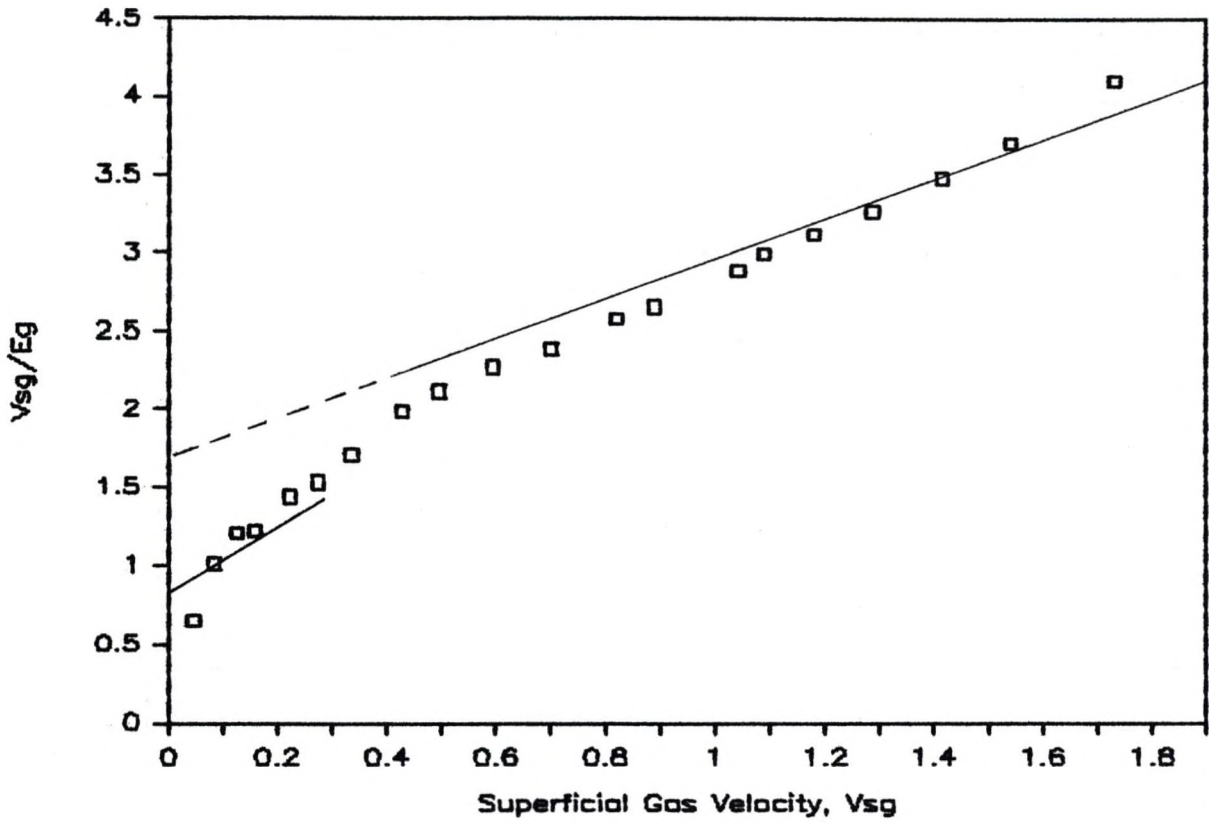
Figure 9: Ratio of Superficial Gas Velocity to Void
Fraction as a Function of Gas Velocity - 8
degrees, 1.87 inch inner pipe.
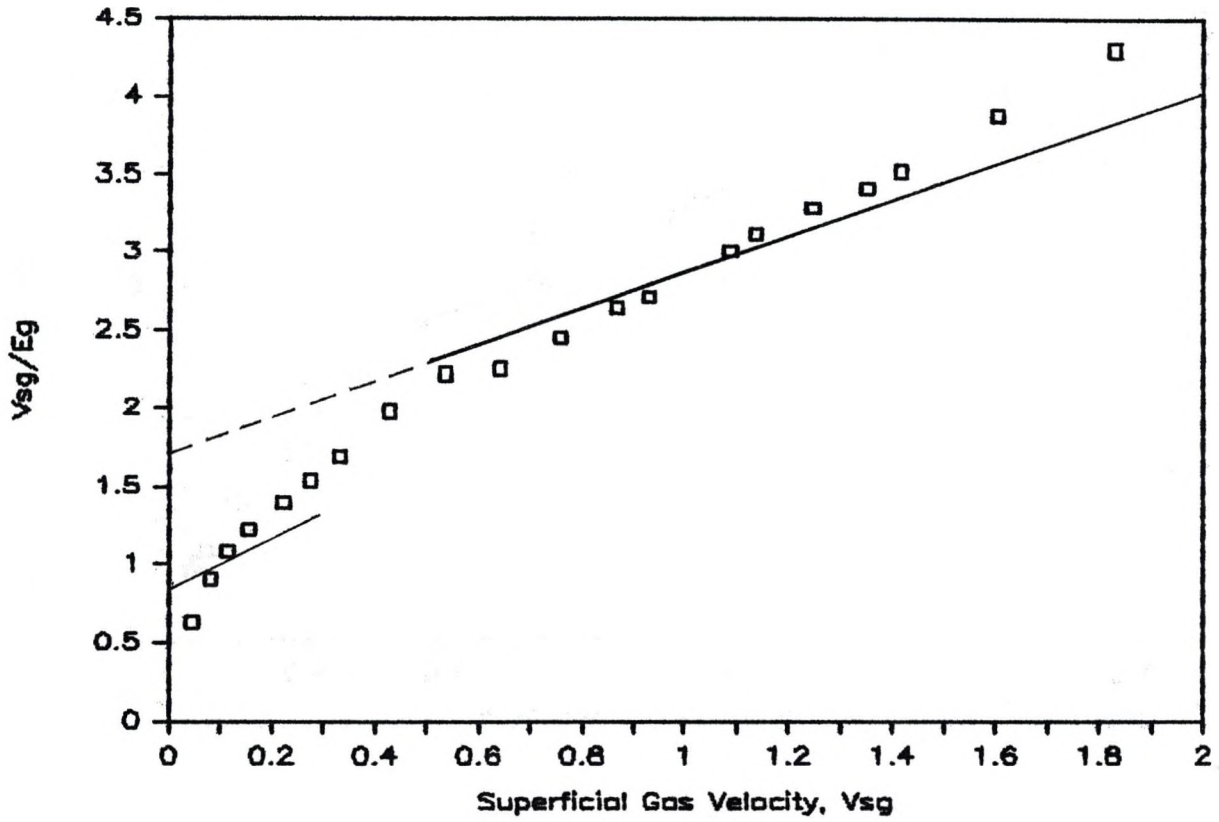
Figure 10: Ratio of Superficial Gas Velocity to Void Fraction as a Function of Gas Velocity - 8 degrees, 2.24 inch inner pipe.
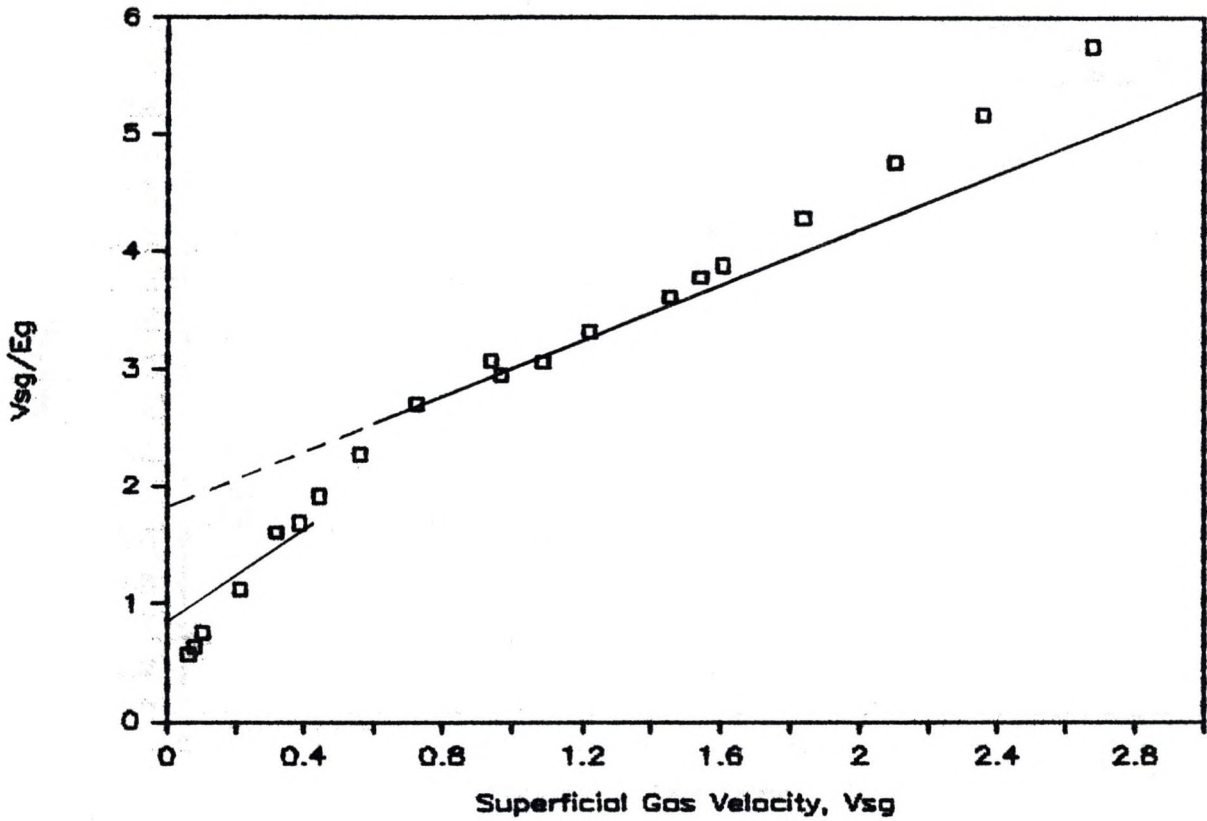
Figure 11: Ratio of Superficial Gas Velocity to Void
Fraction as a Function of Gas Velocity - 8
degrees, 3.409 inch inner pipe.
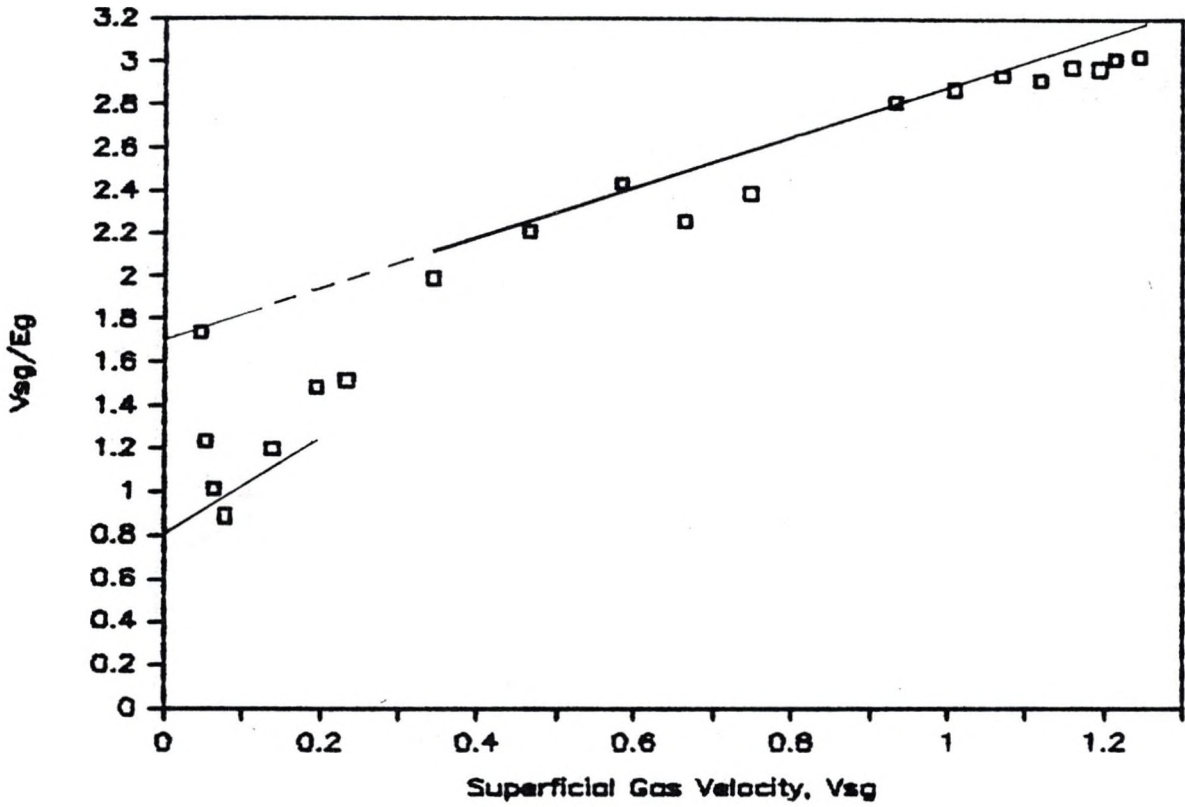
Figure 12: Ratio of Superficial Gas Velocity to Void
Fraction as a Function of Gas Velocity –
16 degrees, Circular Channel.
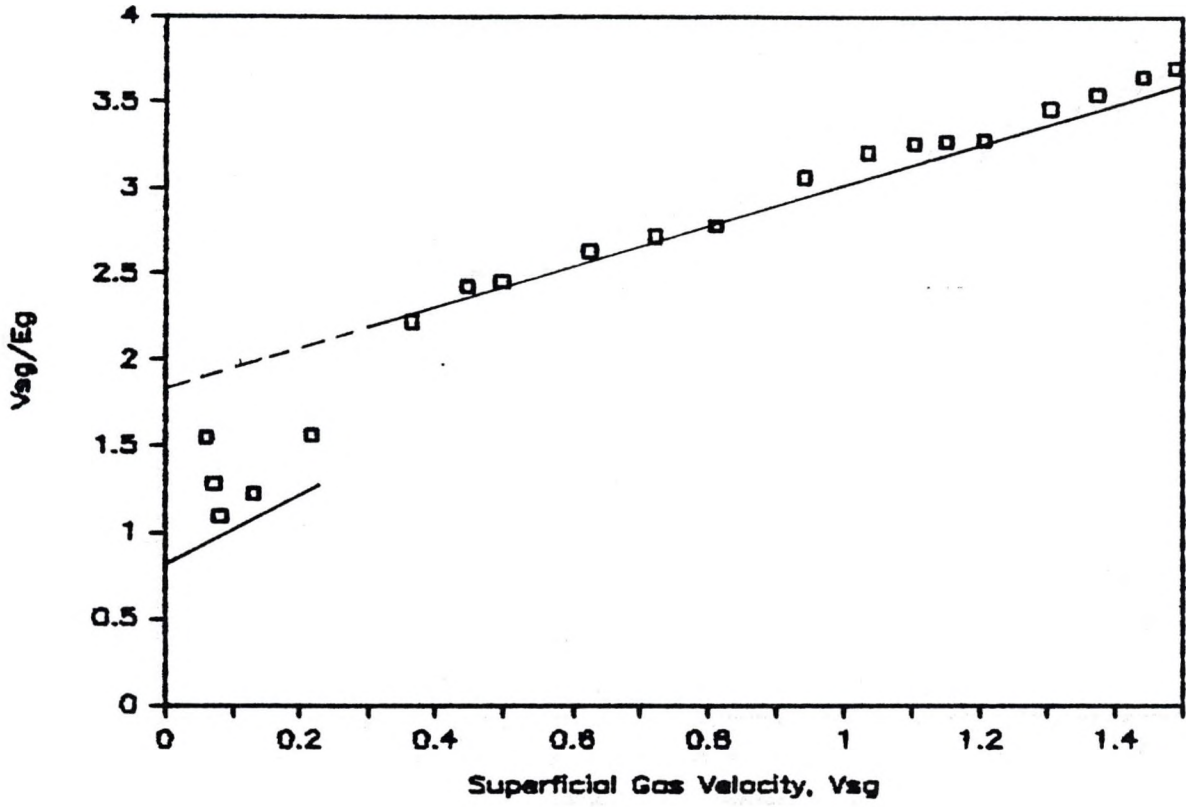
Figure 13: Ratio of Superficial Gas Velocity to Void
Fraction as a Function of Gas Velocity –
16 degrees, 1.87 inch inner pipe.
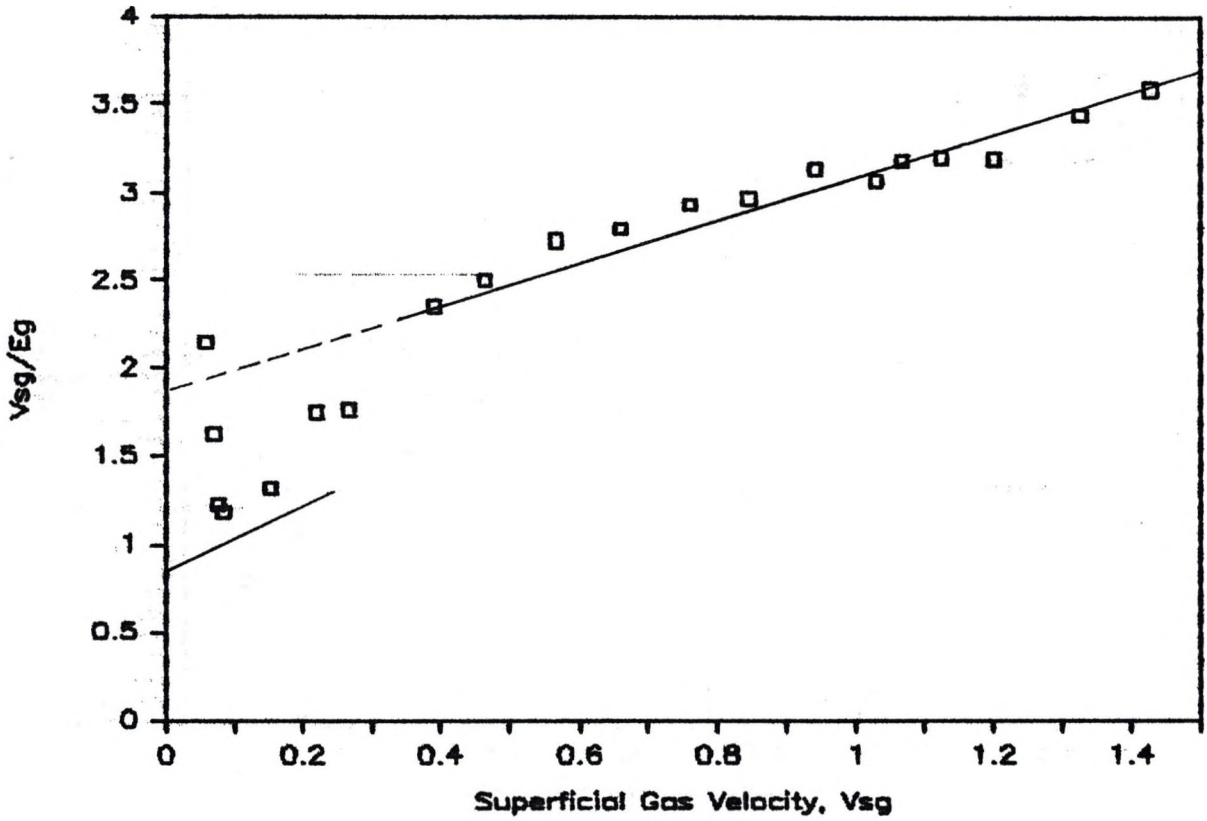
Figure 14: Ratio of Superficial Gas Velocity to Void
Fraction as a Function of Gas Velocity –
16 degrees, 2.24 inch inner pipe.
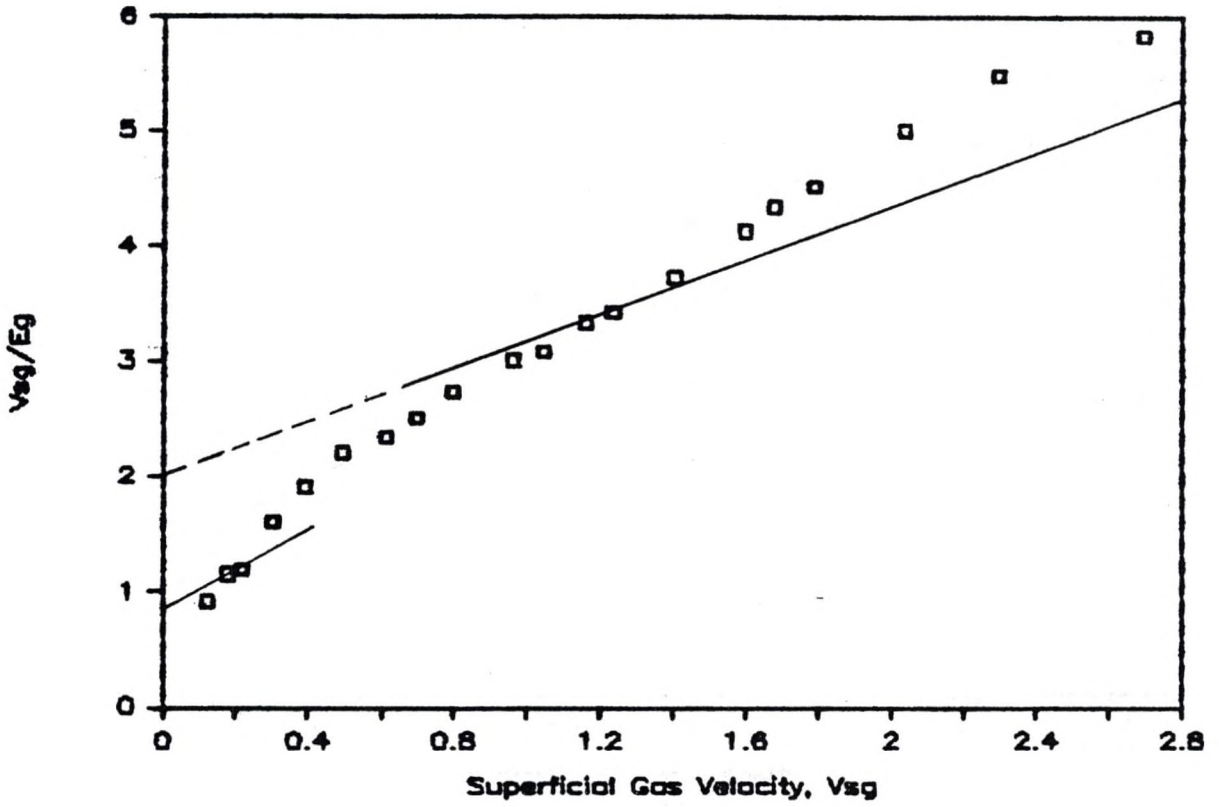
Figure 15: Ratio of Superficial Gas Velocity to Void
Fraction as a Function of Gas Velocity –
16 degrees, 3.409 inch inner pipe.

57
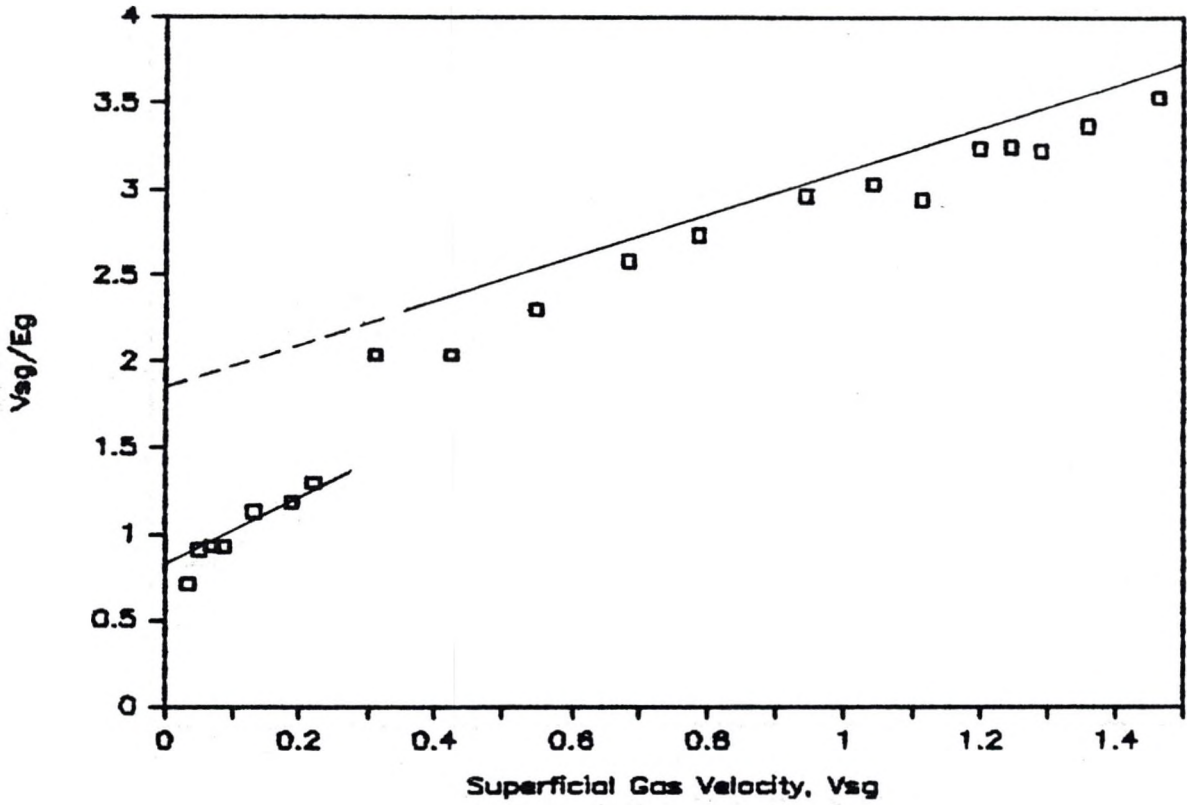
Figure 16: Ratio of Superficial Gas Velocity to Void
Fraction as a Function of Gas Velocity -
24 degrees, Circular Channel.
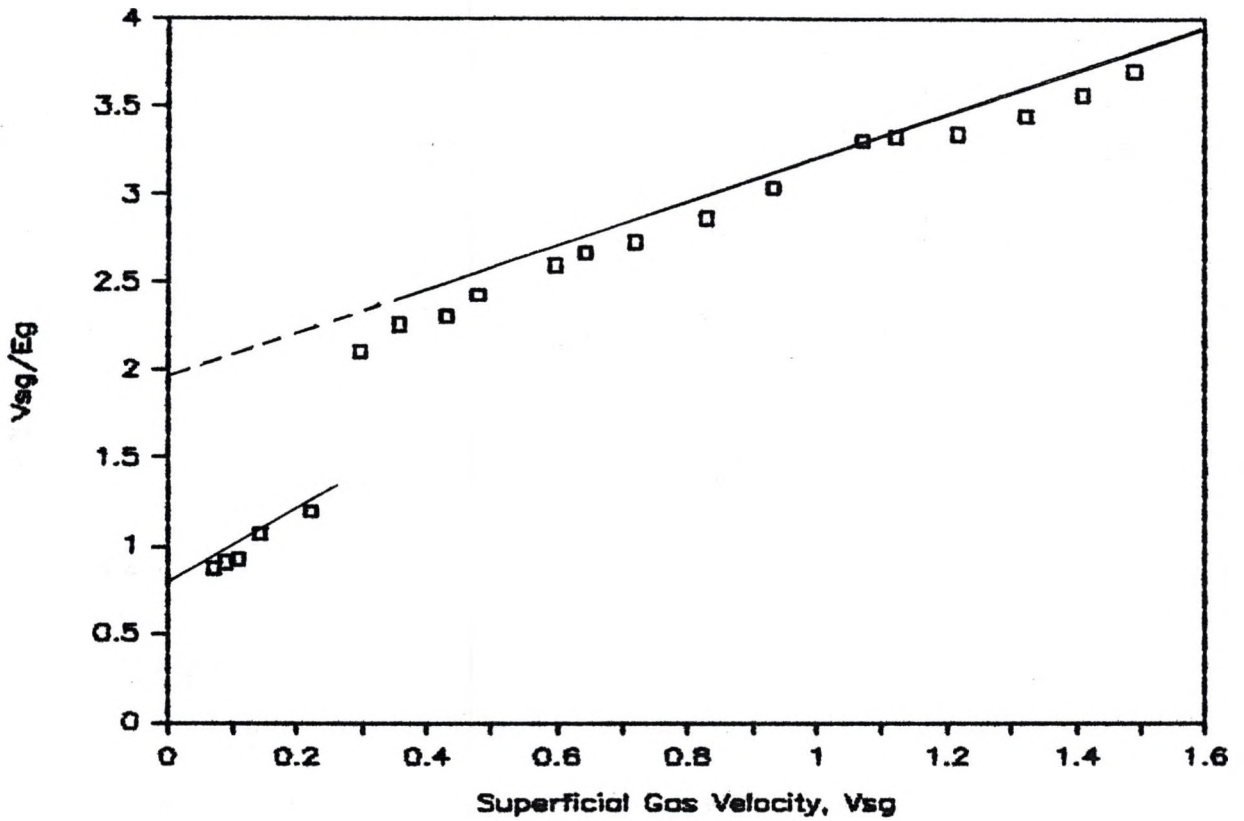
Figure 17: Ratio of Superficial Gas Velocity to Void
Fraction as a Function of Gas Velocity -
24 degrees, 1.87 inch inner pipe.
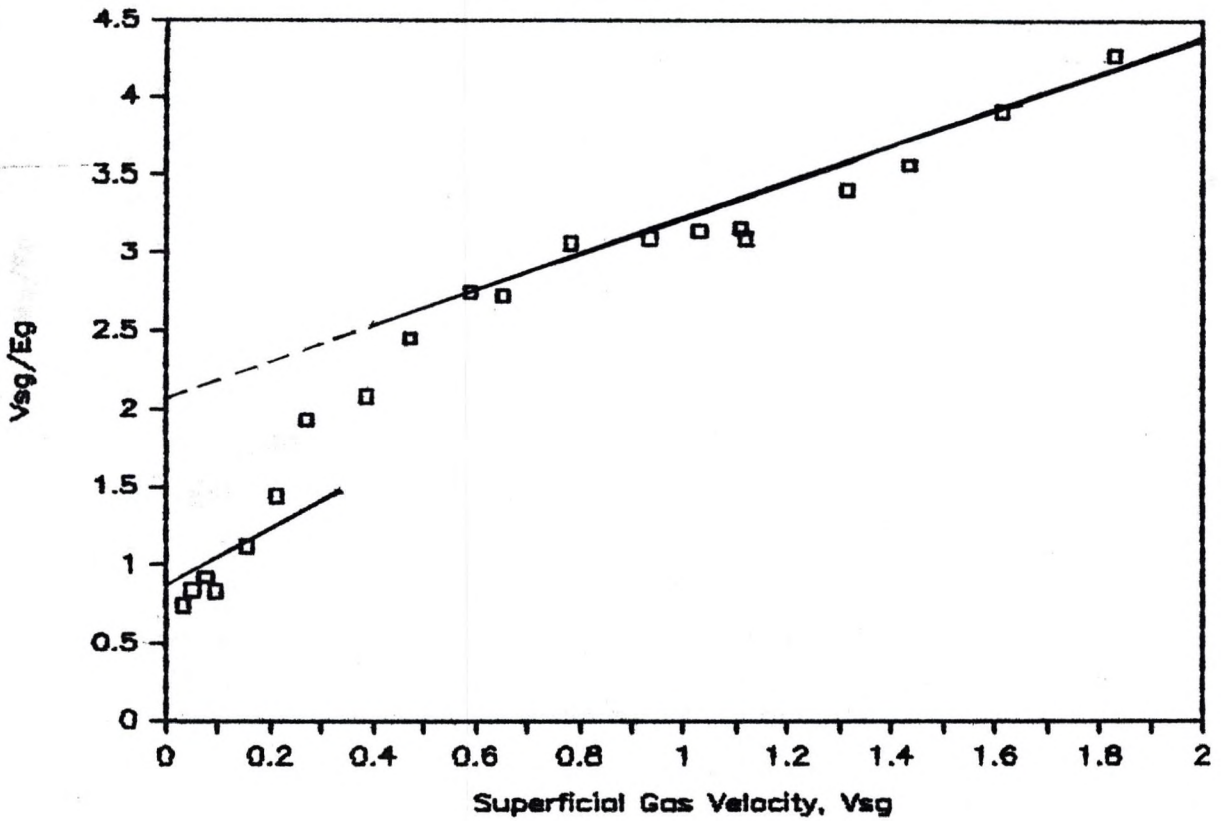
Figure 18: Ratio of Superficial Gas Velocity to Void
Fraction as a Function of Gas Velocity -
24 degrees, 2.24 inch inner pipe.
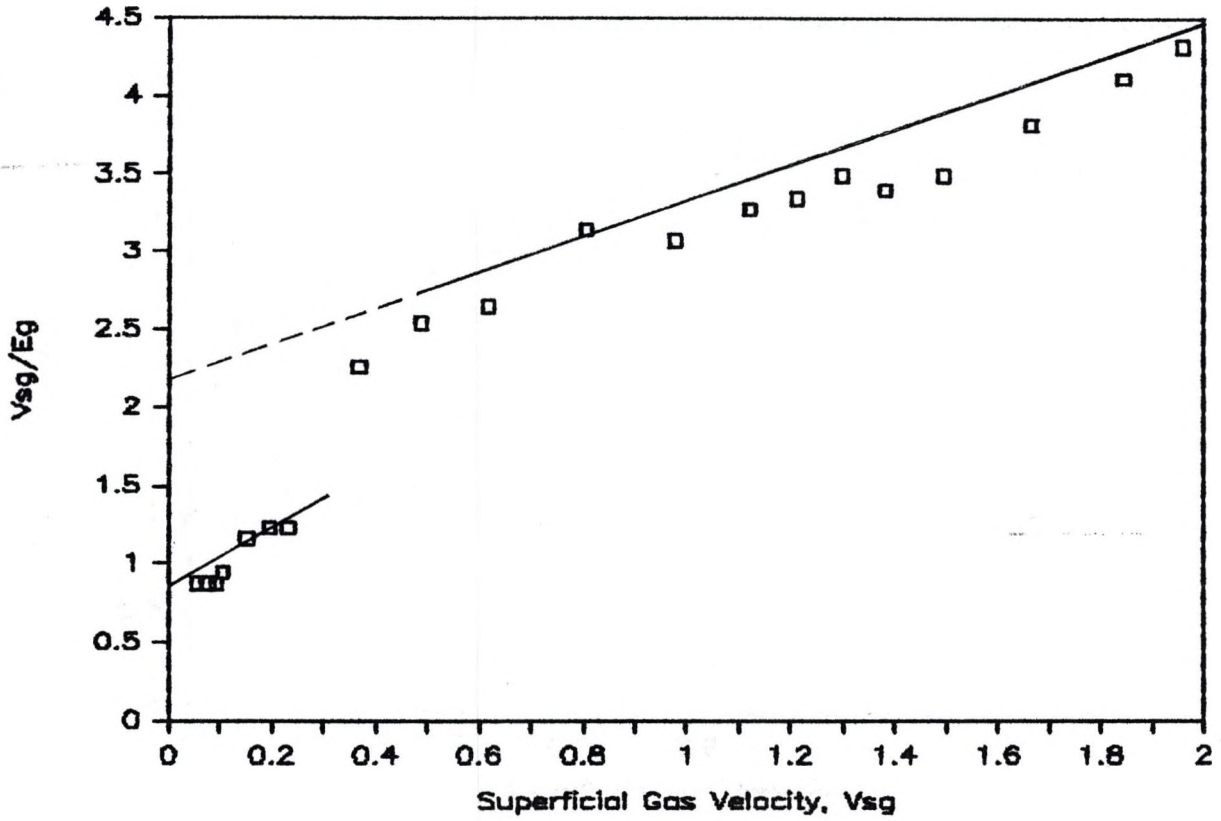
Figure 19: Ratio of Superficial Gas Velocity to Void
Fraction as a Function of Gas Velocity –
24 degrees, 3.409 inch inner pipe.
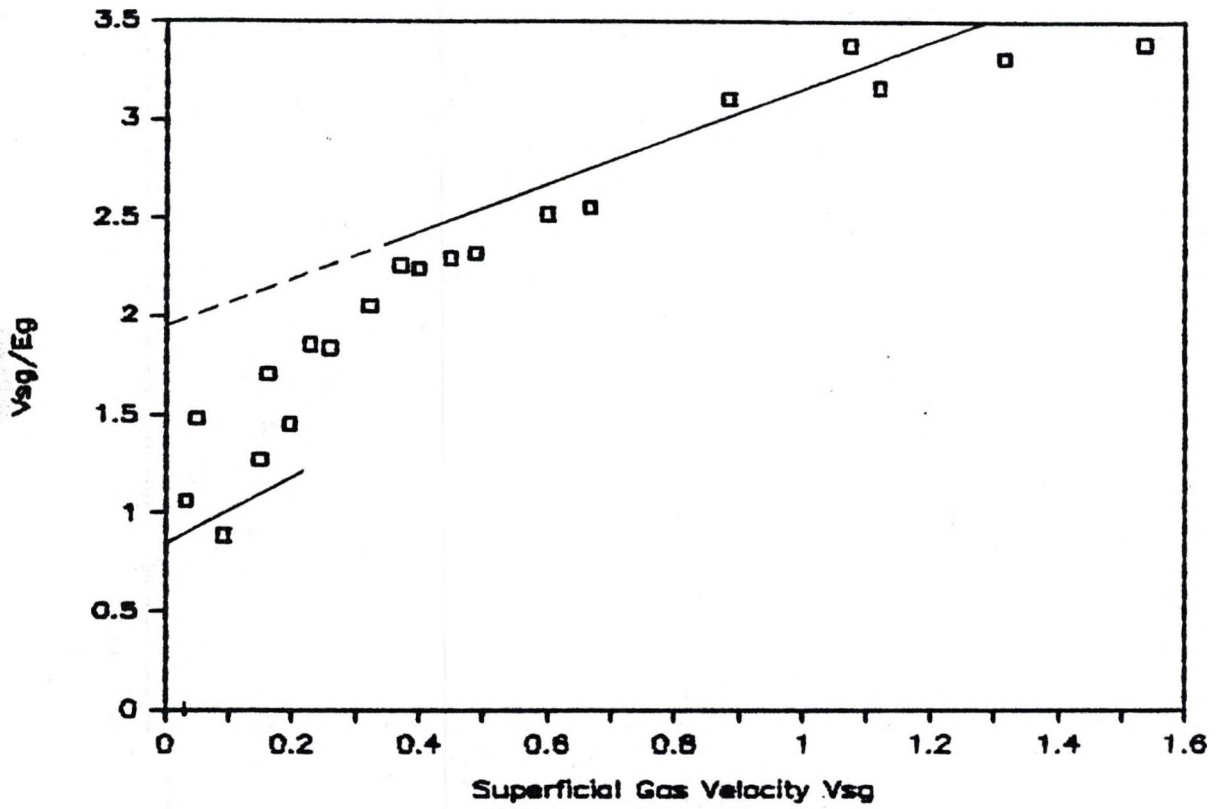
Figure 20: Ratio of Superficial Gas Velocity to Void
Fraction as a Function of Gas Velocity -
32 degrees, Circular Channel.
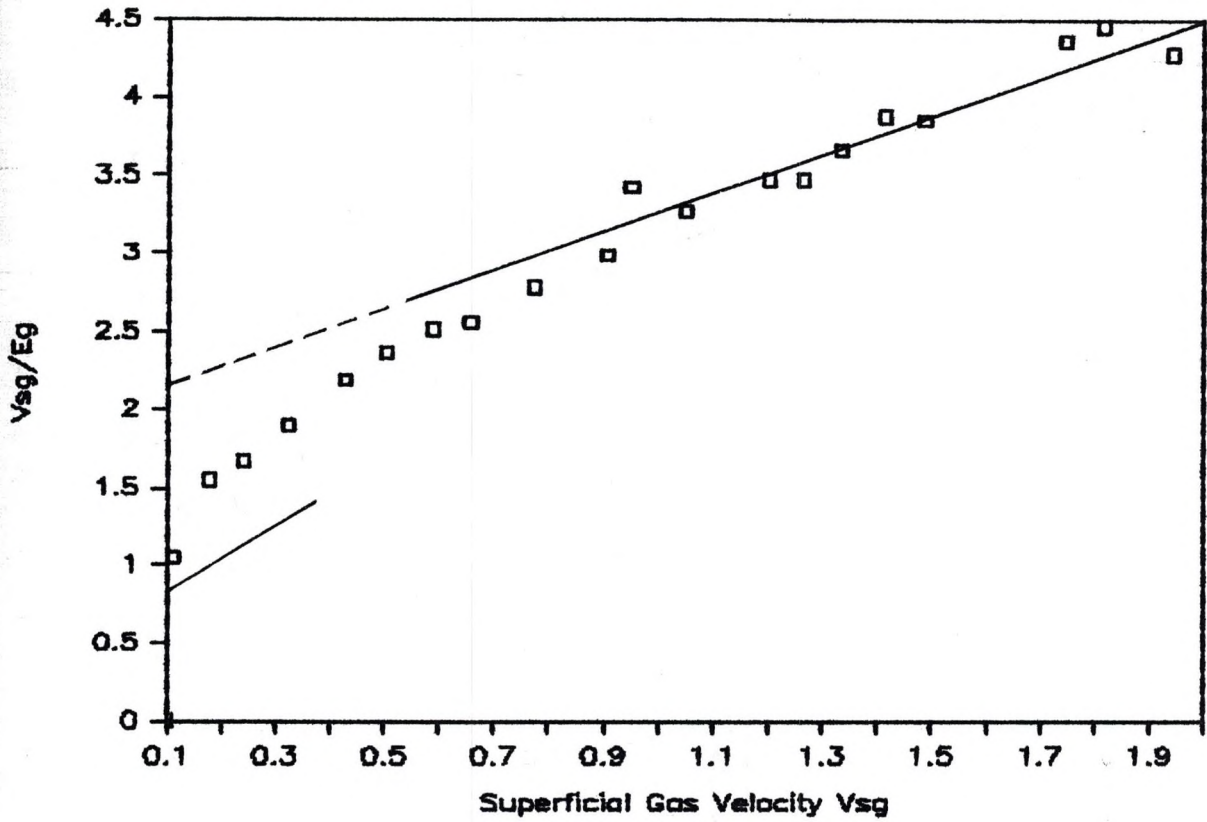
Figure 21: Ratio of Superficial Gas Velocity to Void
Fraction as a Function of Gas Velocity –
32 degrees, 1.87 inch inner pipe.
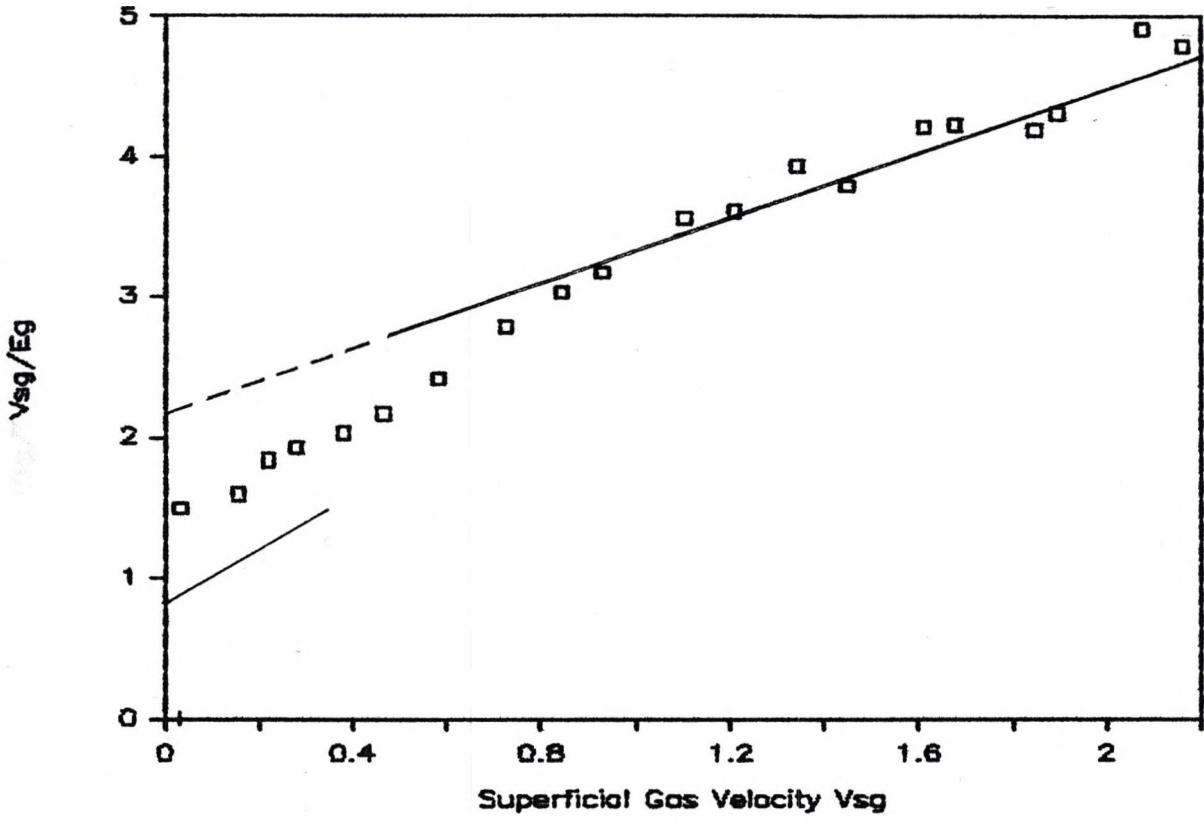
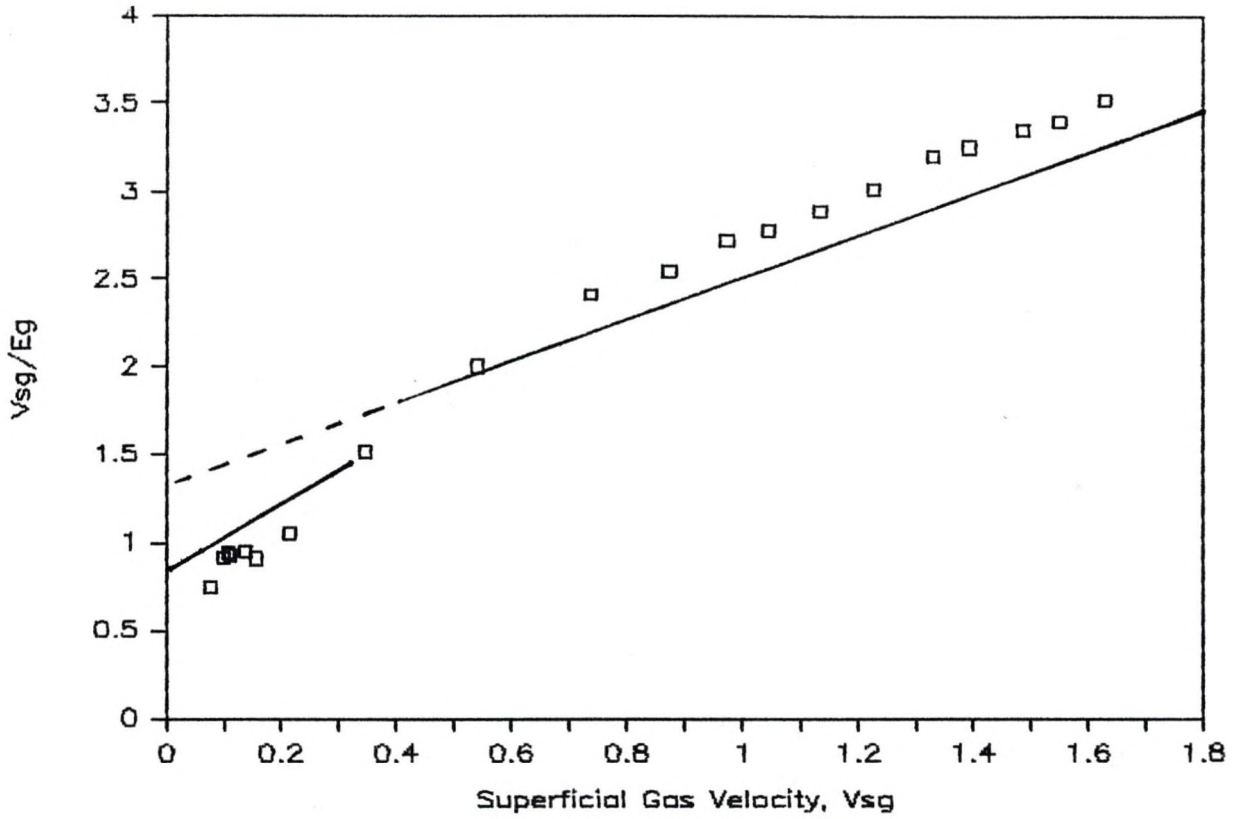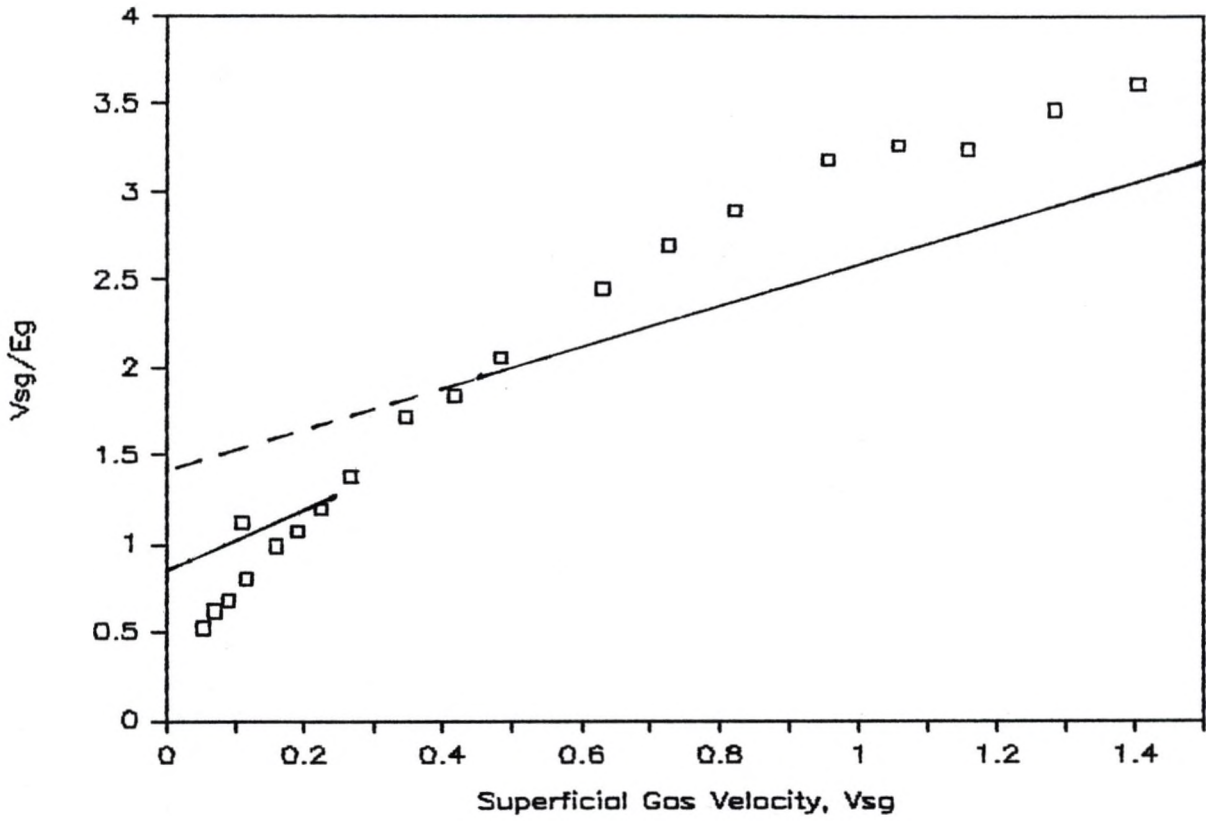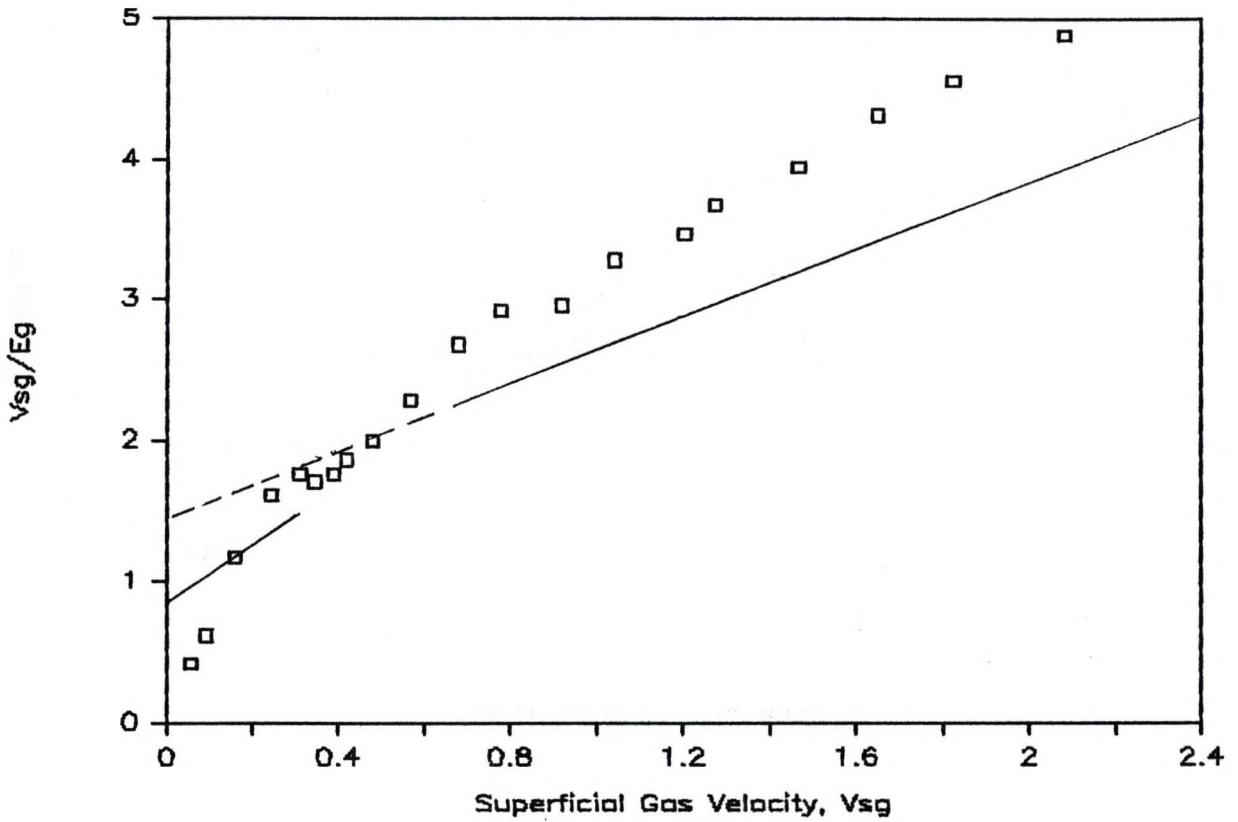Figure 22: Ratio of Superficial Gas Velocity to Void
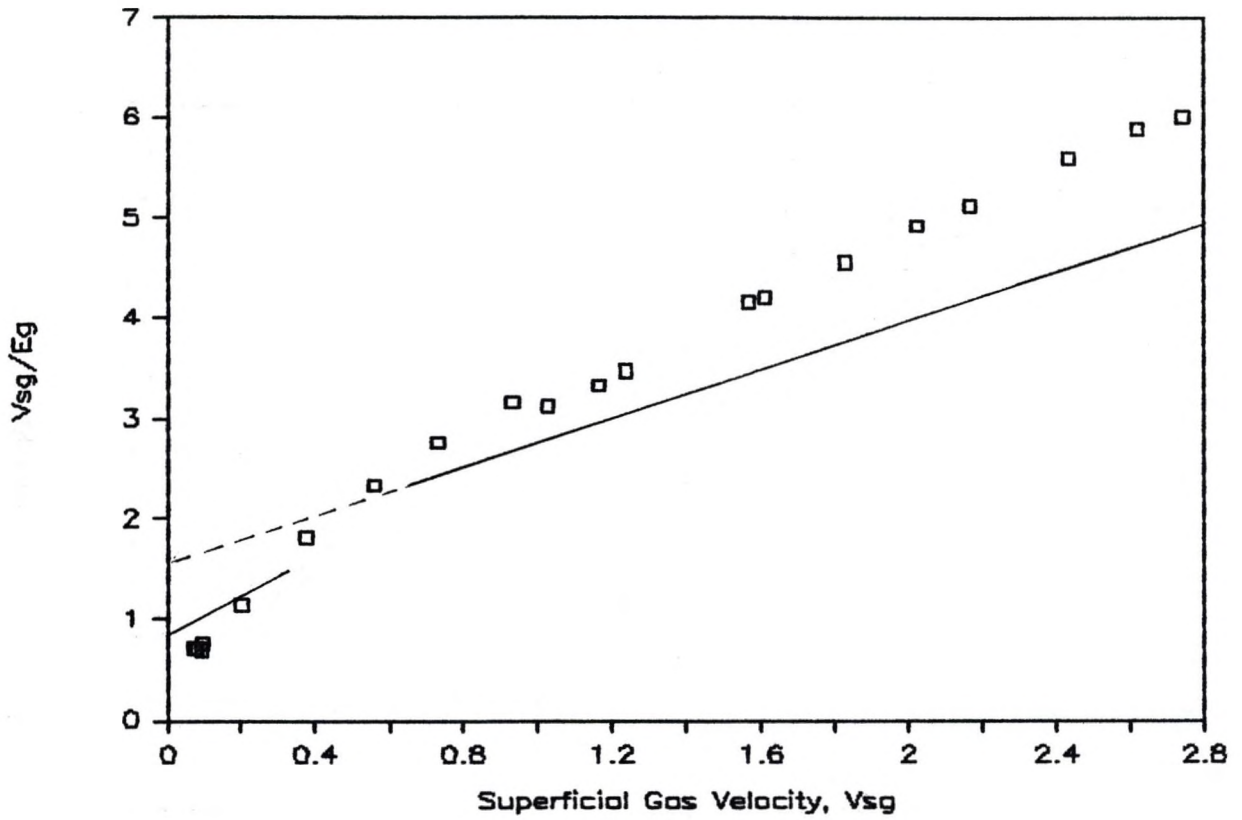Fraction as a Function of Gas Velocity –
32 degrees, 2.24 inch inner pipe.
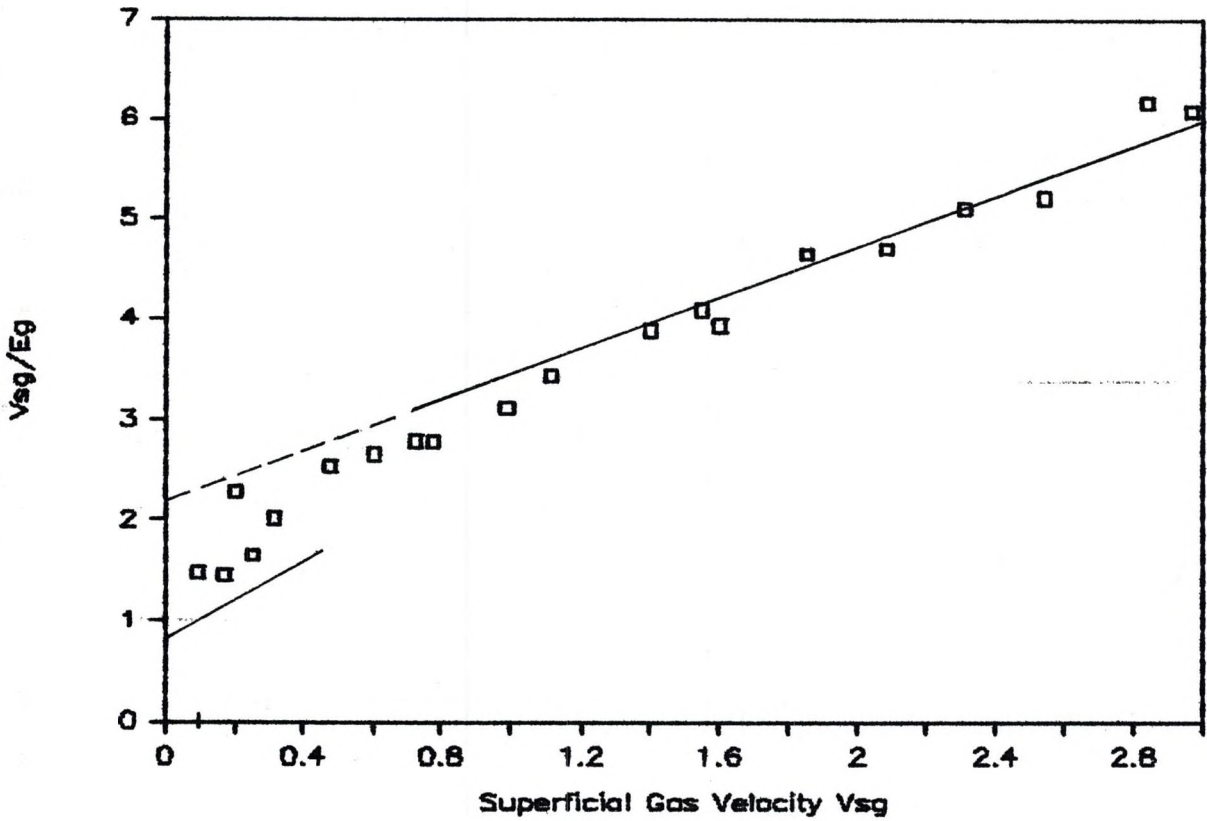
Figure 23: Ratio of Superficial Gas Velocity to Void
Fraction as a Function of Gas Velocity —
32 degrees, 3.409 inch inner pipe.

Kabir (1986) for inclined circular channels.

6.3.2 Dispersed Bubbly Flow

Dispersed bubbly flow was not observed during the experimental runs.

6.3.3 Slug Flow

The analysis for slug flow is similar to that for bubbly flow. Indeed, Equation (4) for void fraction in bubbly flow applies in slug flow as well, but with different constants (i.e. C_1 instead of C_o). The dark lines in Figures 4 through 23 are the predictions of the model. The lower dark line is the prediction for bubbly flow and has a slope of 2.0, i.e. $C_o = 2.0$. The upper dark line is the prediction for slug flow and it has a slope of 1.2, i.e. $C_1 = 1.2$. The value of C_1 was assumed to remain constant at 1.2 although Hasan and Kabir (1987) found C_1 to vary slightly with the inner to outer pipe diameter ratio.

Effect of Pipe Inclination

It is noted that the pipe inclination does affect the void fraction for slug flow. This effect appears to be well represented by Equation (53). Figures 4 through 23 show reasonably good agreement between the prediction (dark line) and the experimental data (symbols). However, these plots suggest that when the channel is highly deviated from the vertical, Equation (53) appears to overestimate the effect of inclination. Because our system could not be inclined more than 32 degrees from the vertical, no attempt was made to modify Equation (53) to account for this overestimation.

Effect of Annular Dimension

Equation (53) was used to estimate void fraction during slug flow in annuli. It shows that, as in the case of bubbly flow, the in-situ gas velocity in slug flow is linear with mixture velocity. The slope equals C_1 and the intercept is the terminal rise-velocity, V_{tTo}. As in bubbly flow, the flow parameter C_1 was not found to be significantly affected by the presence of an inner tube. To simplify analysis, C_1 was held at 1.2 and values of V_{tTo} were calculated for different angles of inclination and tubing diameters. The values are tabulated in Table 2. The numbers agree reasonably well with Equation (53). The solid lines in Figures 4 through 23 are representations of the model (i.e. with $C_1 = 1.2$ and V_{tTo} calculated from Equation (53)).

Figures 24 through 43 are plots of the observed void fraction against the predicted void fraction. The agreement appears to be good.

6.4   Comparison With Published Data

Published data for void fraction for two-phase flow through annular geometry is scarce. Filho (1984) gathered data for air-water and air-kerosene flow through an annulus. Predictions made using the proposed model are compared with this data set. Table 3 presents the average error and standard deviation in predicting each flow regime for the air-water system.

The air-water bubbly flow data gathered in this study were overestimated by 2.4 percent with a percent standard
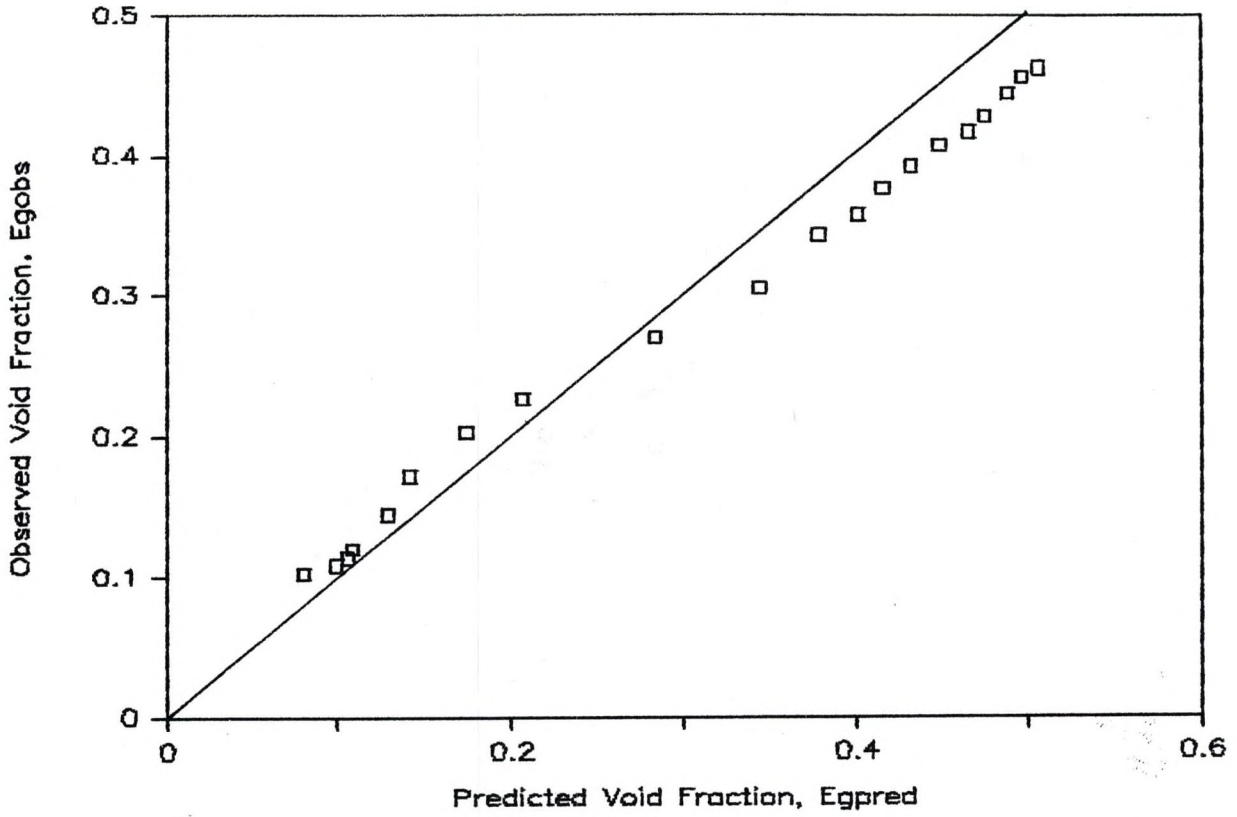
Figure 24: Comparison of the Experimental and the Predicted Void Fraction Values − 0 degrees, Circular Channel.
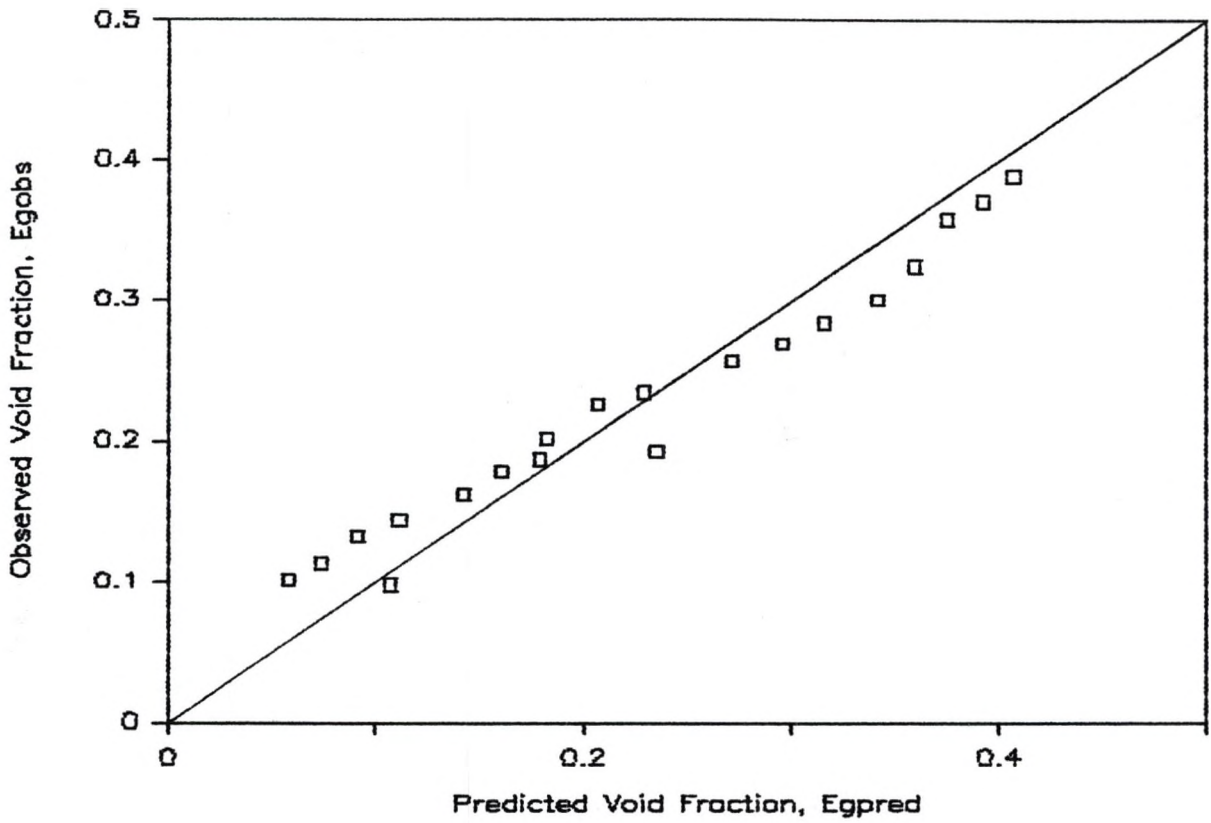
Figure 25: Comparison of the Experimental and the Predicted Void Fraction Values - 0 degrees, 1.87 inch inner pipe.
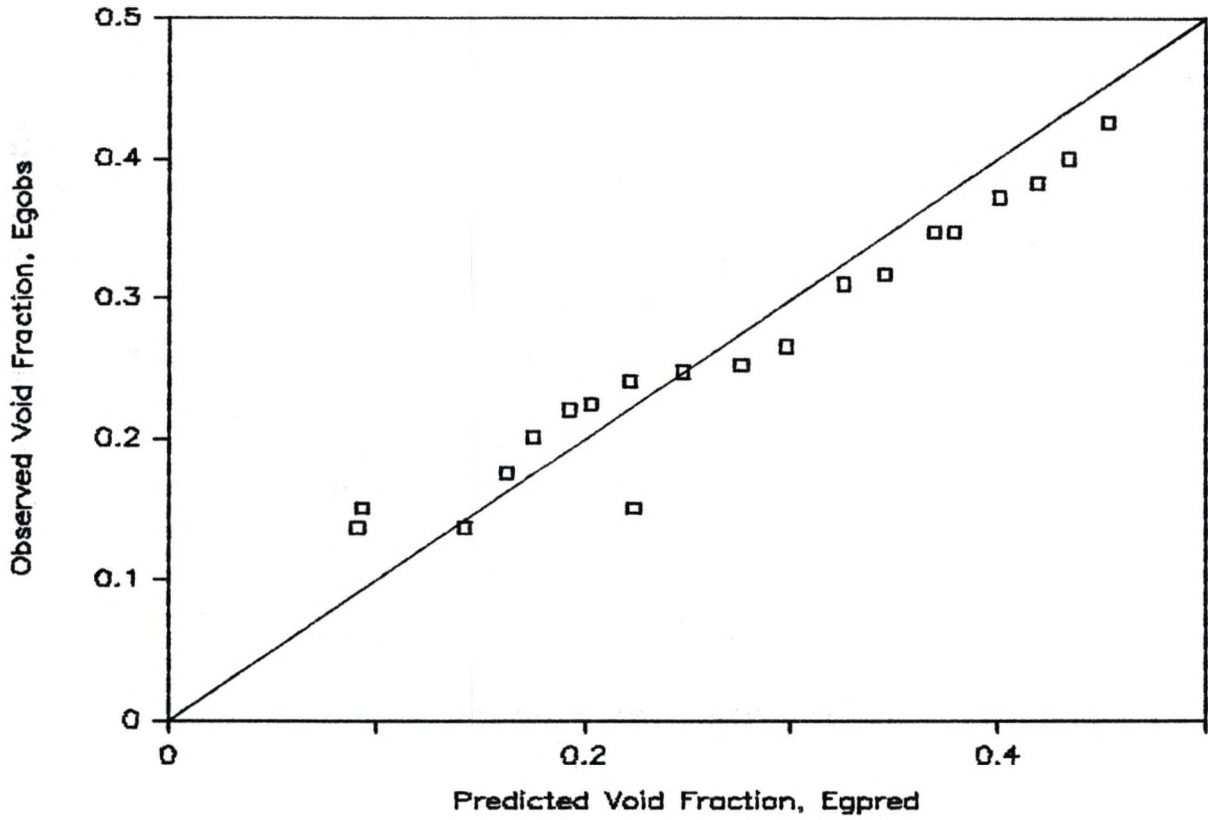
Figure 26: Comparison of the Experimental and the Predicted Void Fraction Values - 0 degrees, 2.24 inch inner pipe.
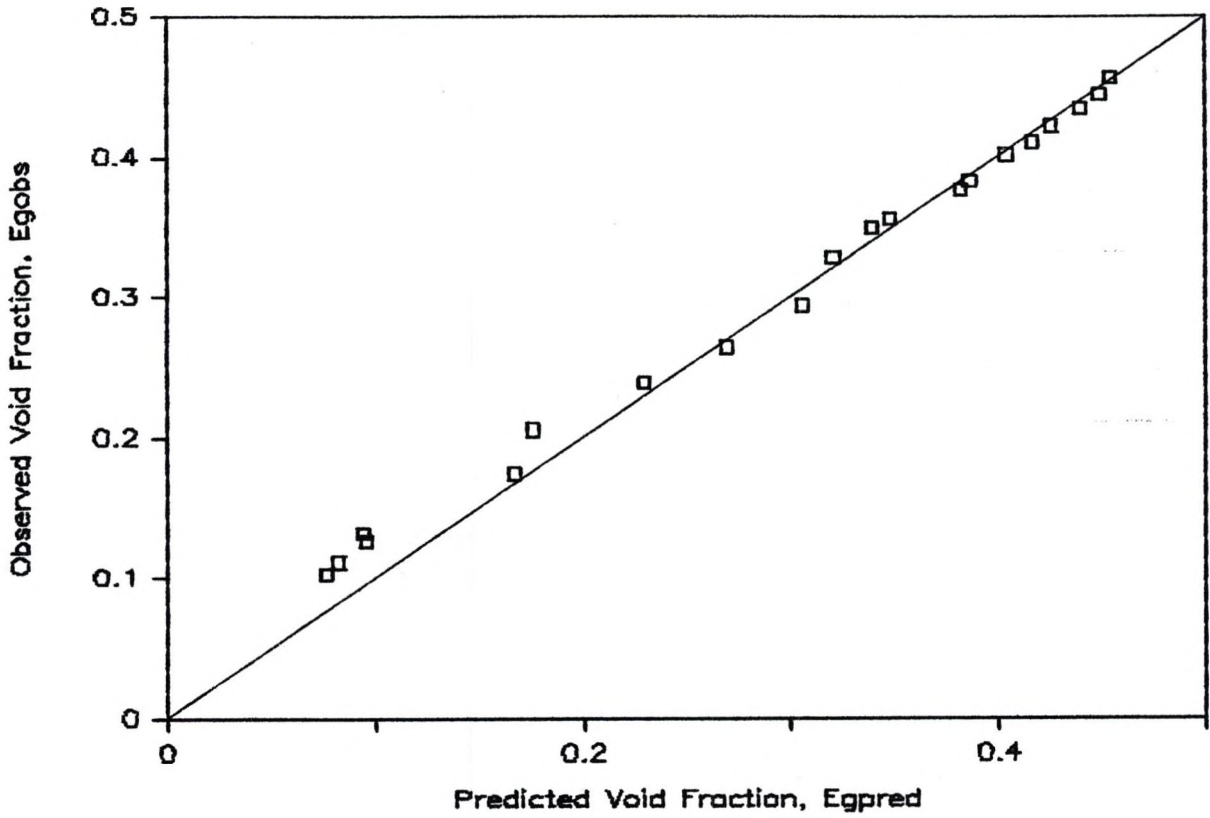
Figure 27: Comparison of the Experimental and the Predicted Void Fraction Values - 0 degrees, 3.409 inch inner pipe.
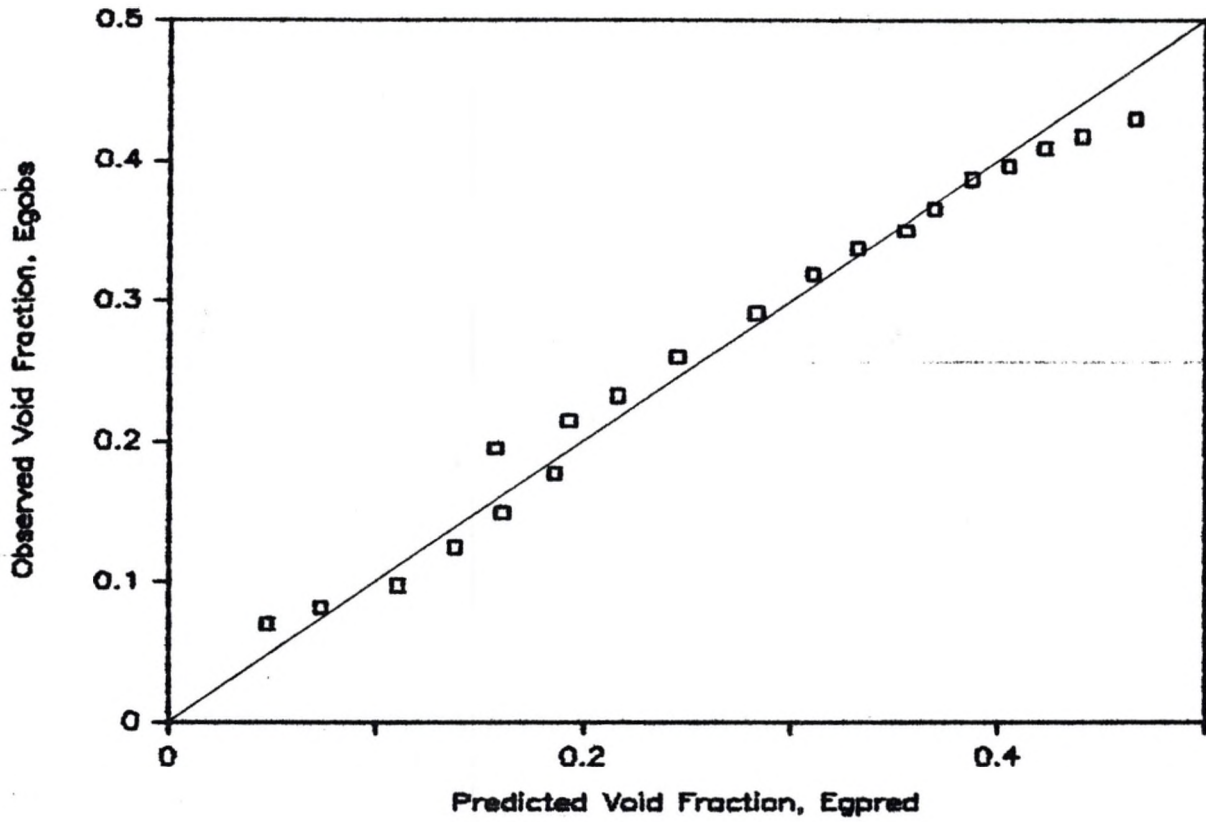
Figure 28: Comparison of the Experimental and the Predicted Void Fraction Values - 8 degrees, Circular Channel.
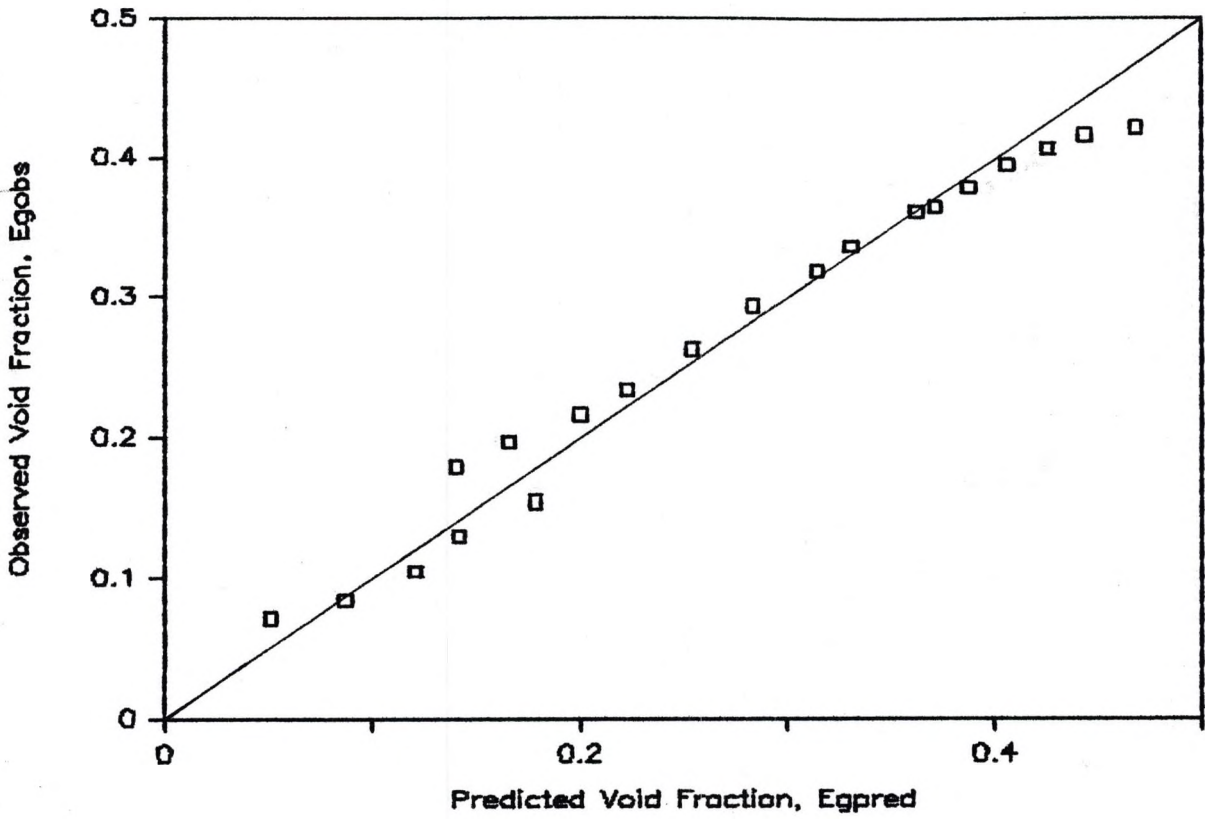
Figure 29: Comparison of the Experimental and the Predicted Void Fraction Values - 8 degrees, 1.87 inch inner pipe.
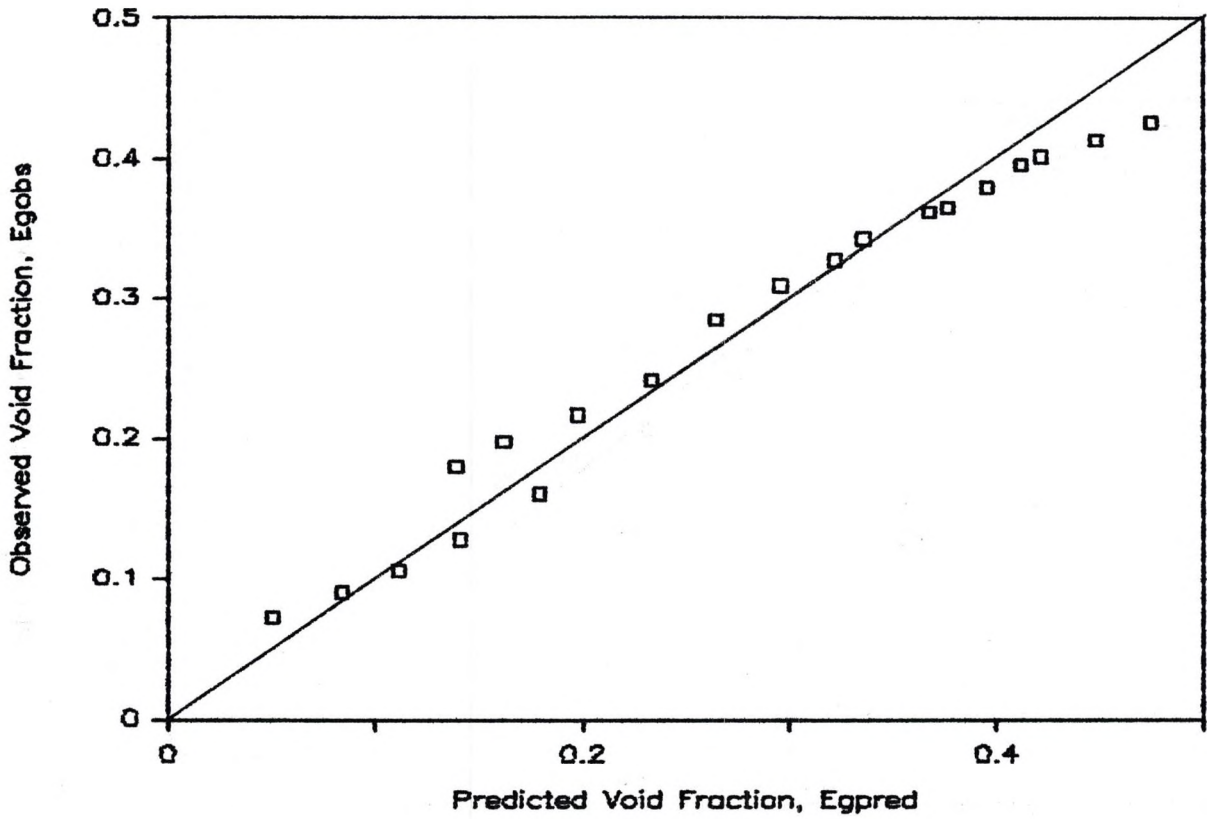
Figure 30: Comparison of the Experimental and the Predicted Void Fraction Values - 8 degrees, 2.24 inch inner pipe.
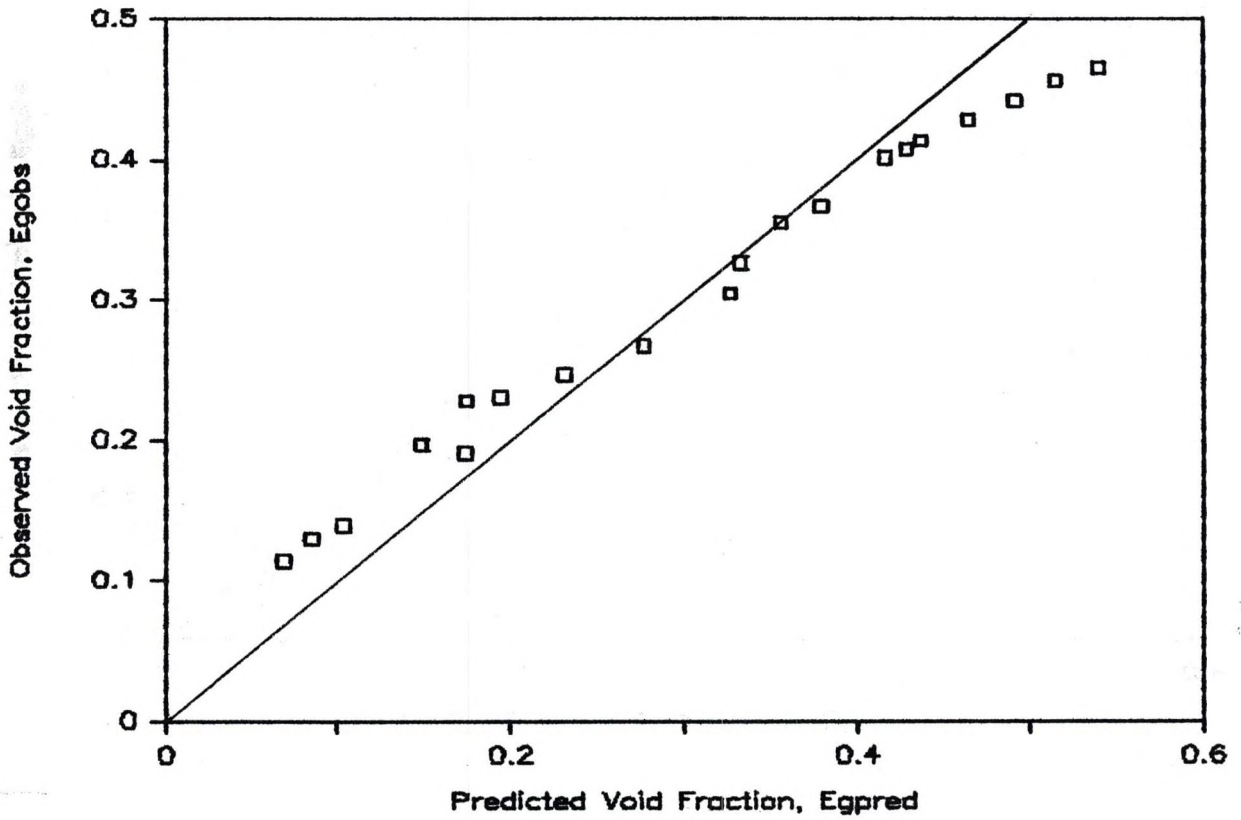
Figure 31: Comparison of the Experimental and the Predicted Void Fraction Values – 8 degrees, 3.409 inch inner pipe.
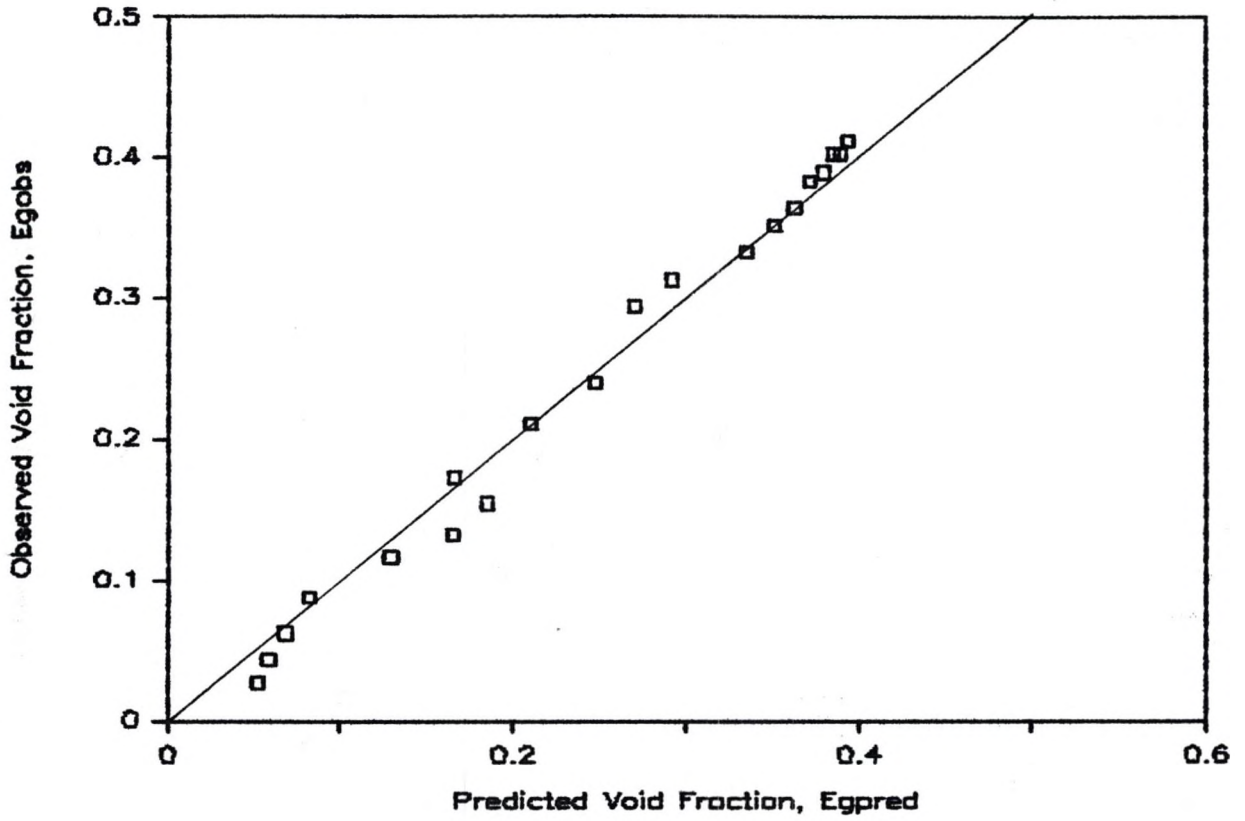
Figure 32: Comparison of the Experimental and the Predicted Void Fraction Values - 16 degrees, Circular Channel.
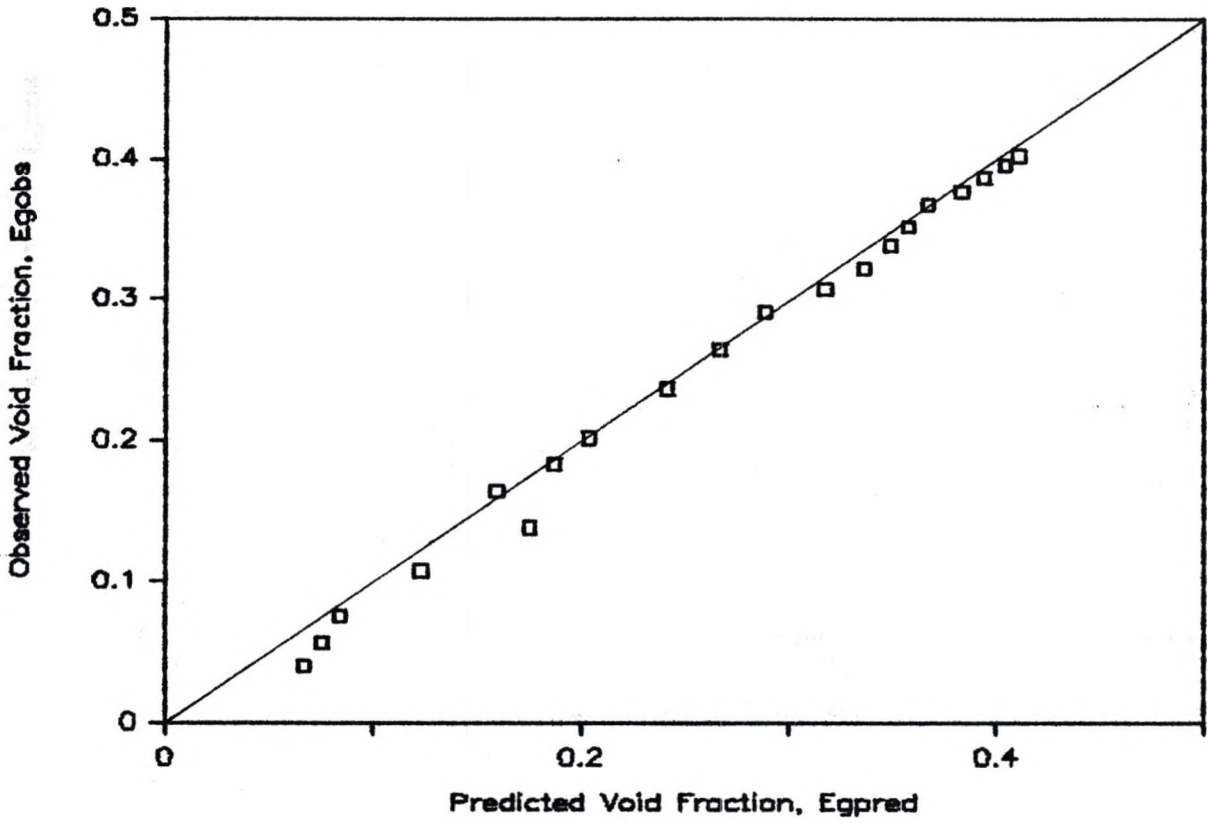
Figure 33: Comparison of the Experimental and the Predicted Void Fraction Values - 16 degrees, 1.87 inch inner pipe.
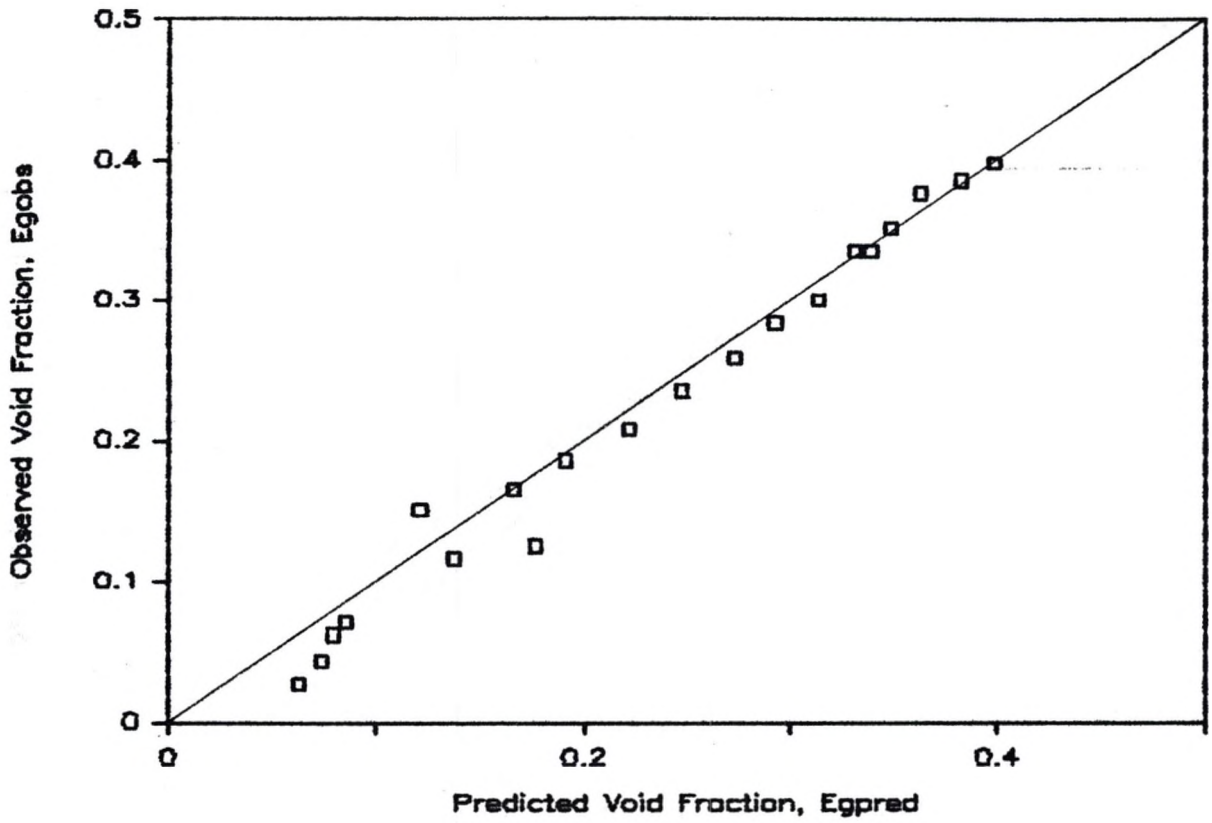
Figure 34: Comparison of the Experimental and the Predicted Void Fraction Values - 16 degrees, 2.24 inch inner pipe.
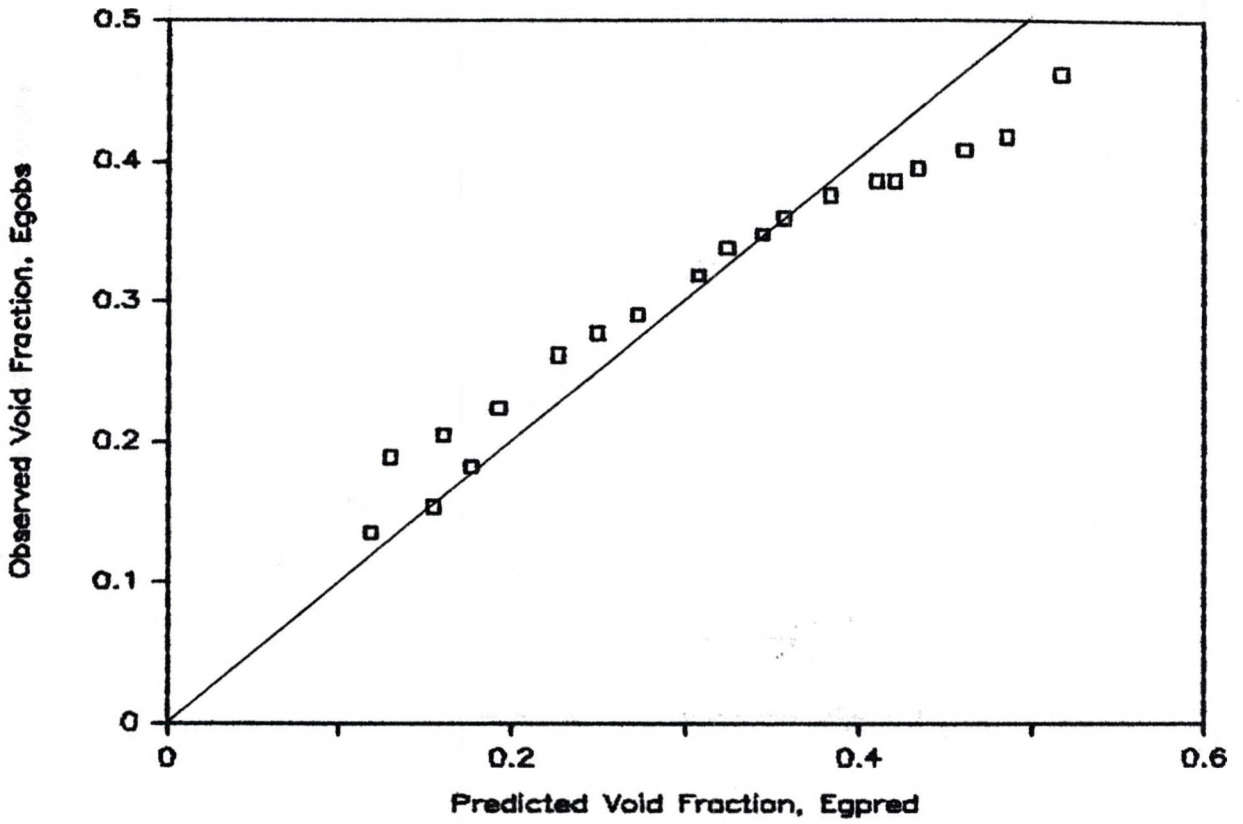
Figure 35: Comparison of the Experimental and the Predicted Void Fraction Values - 16 degrees, 3.409 inch inner pipe.
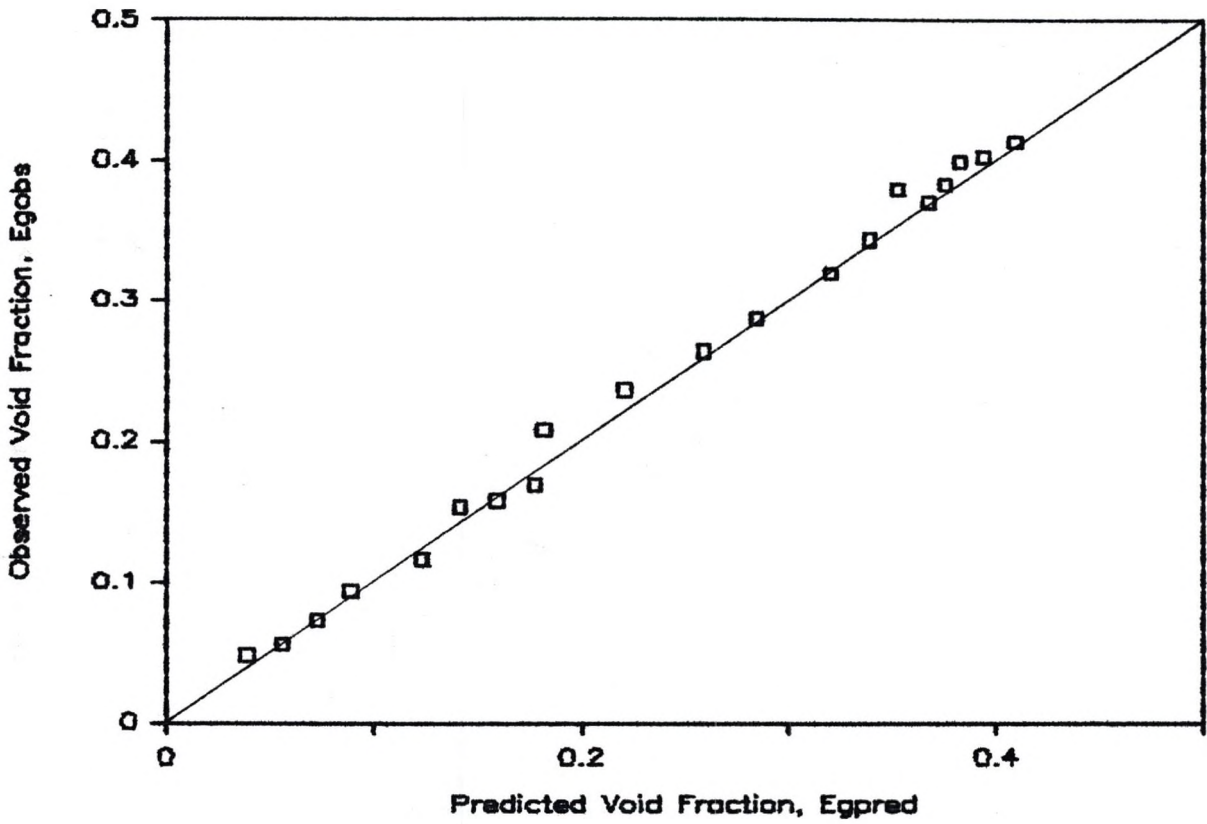
Figure 36: Comparison of the Experimental and the Predicted Void Fraction Values - 24 degrees, Circular Channel.
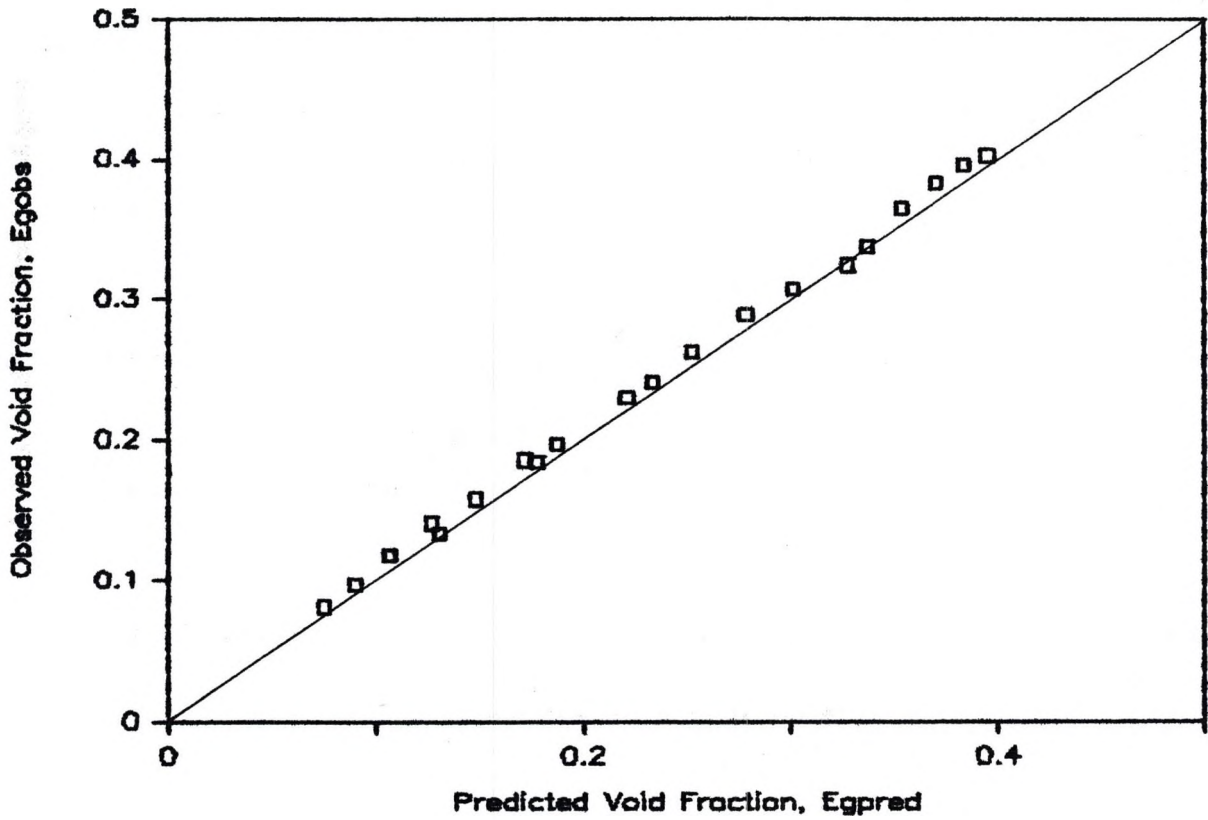
Figure 37: Comparison of the Experimental and the Predicted Void Fraction Values — 24 degrees, 1.87 inch inner pipe.
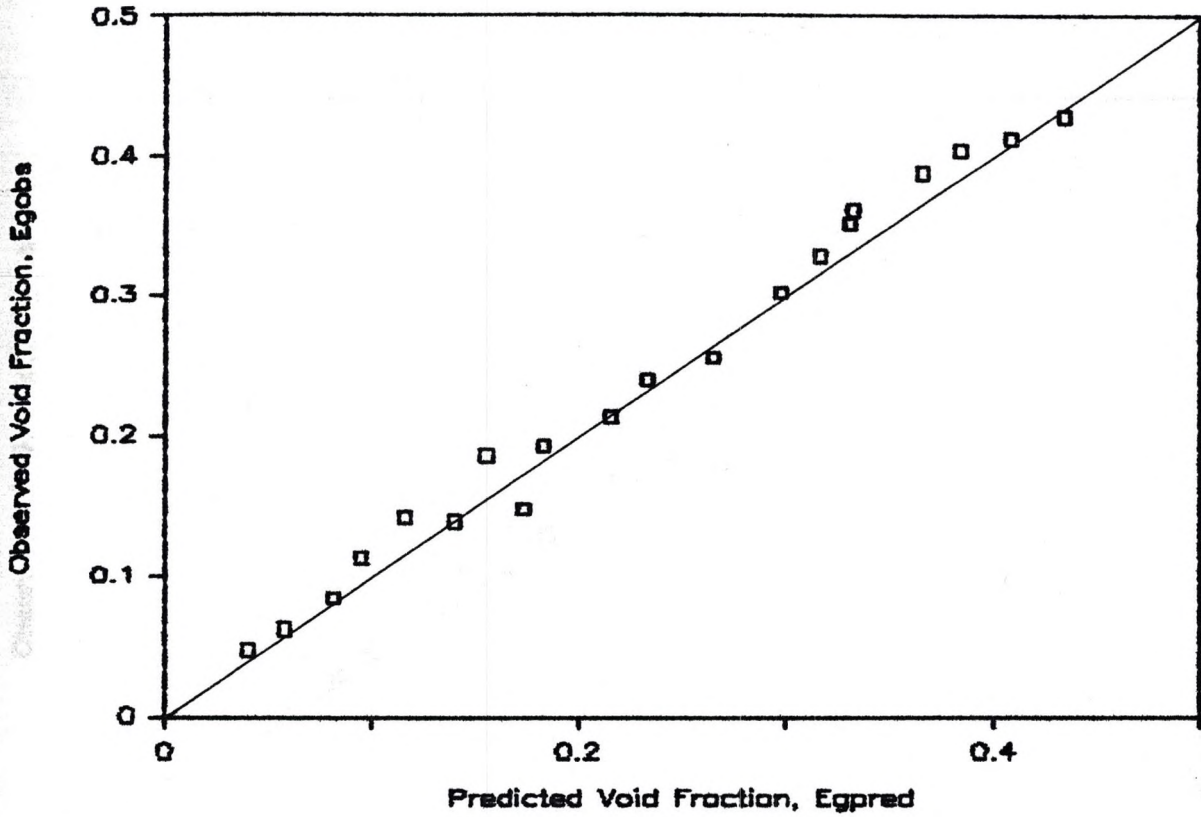
Figure 38: Comparison of the Experimental and the Predicted Void Fraction Values – 24 degrees, 2.24 inch inner pipe.
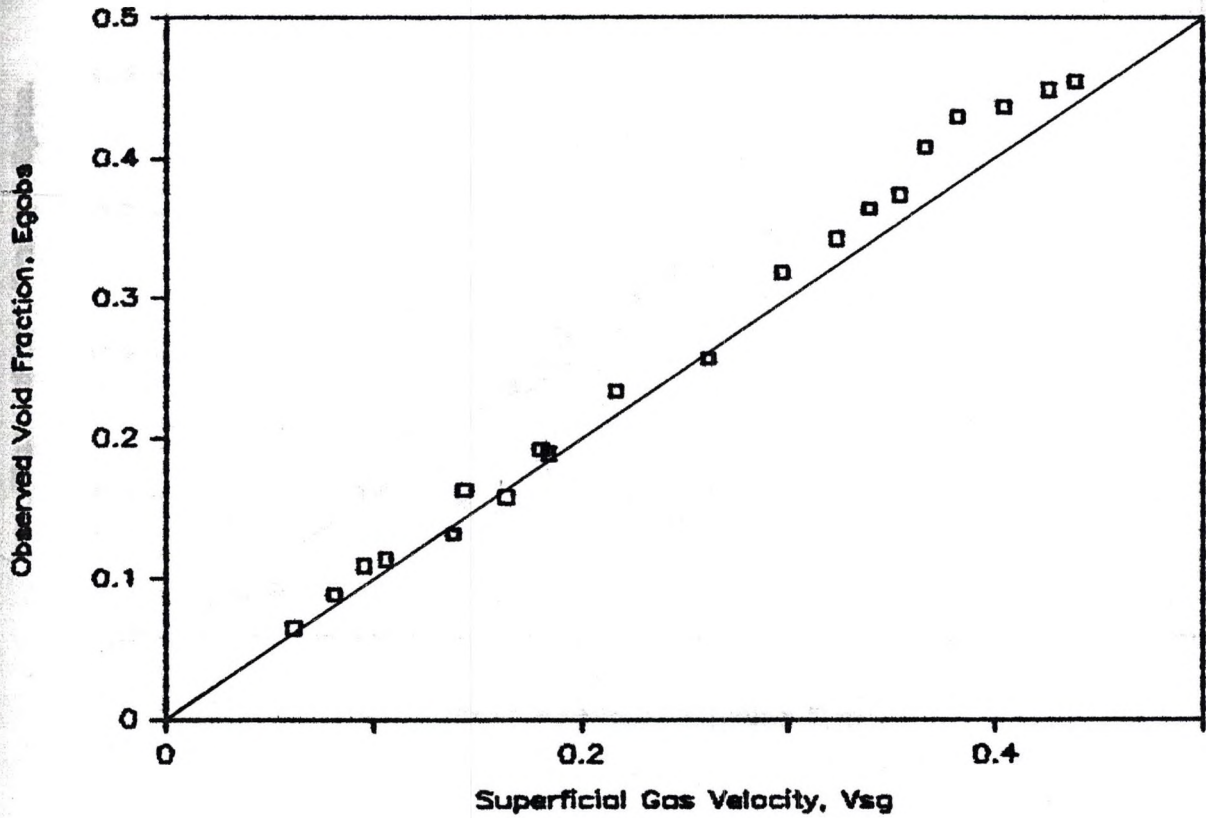
Figure 39: Comparison of the Experimental and the Predicted Void Fraction Values - 24 degrees, 3.409 inch inner pipe.
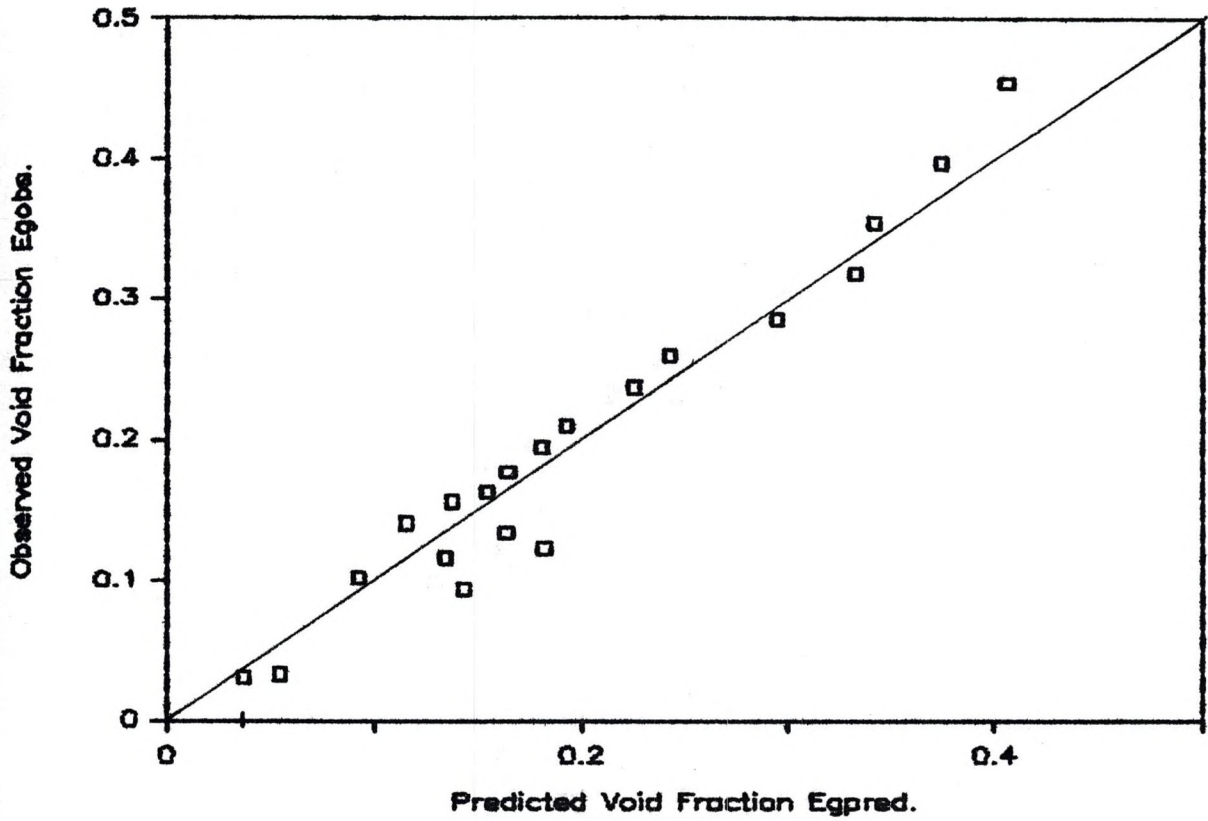
Figure 40: Comparison of the Experimental and the Predicted Void Fraction Values - 32 degrees, Circular Channel.
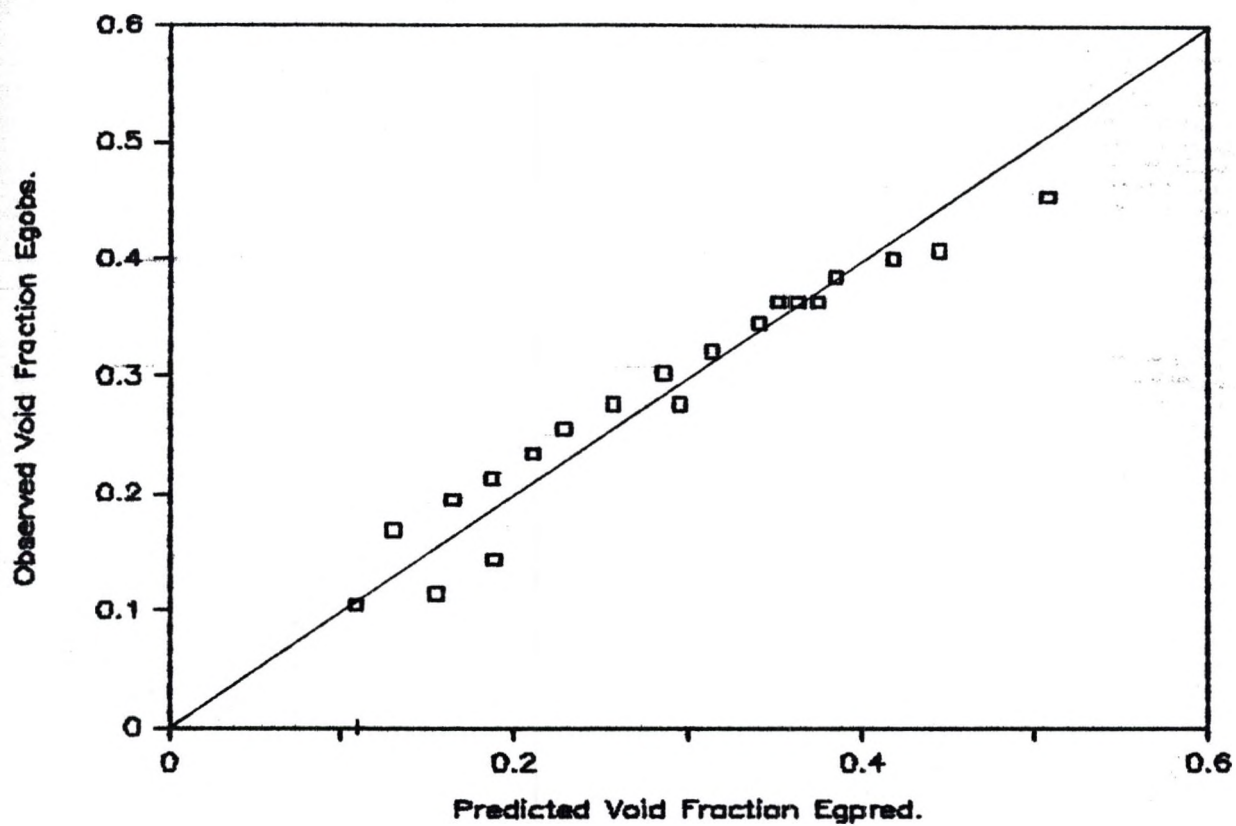
Figure 41: Comparison of the Experimental and the Predicted Void Fraction Values - 32 degrees, 1.87 inch inner pipe.
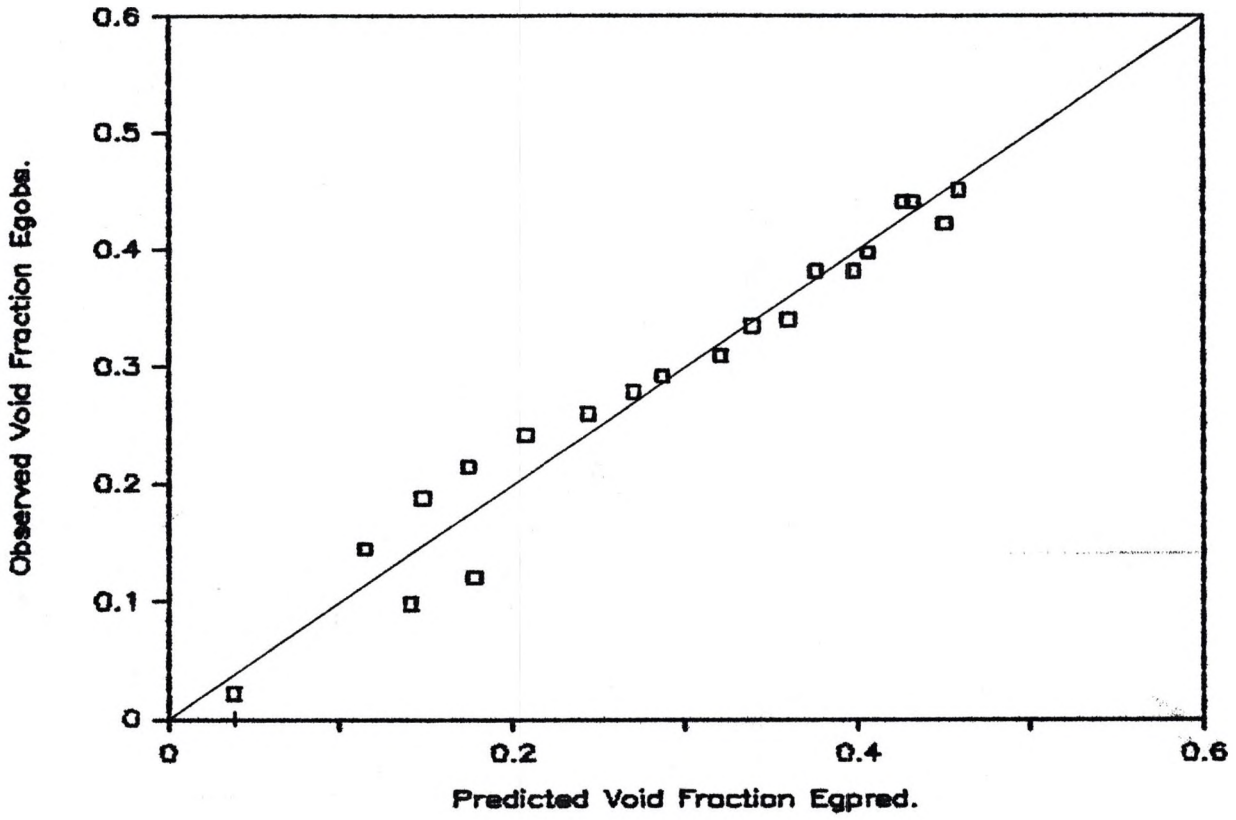
Figure 42: Comparison of the Experimental and the Predicted Void Fraction Values - 32 degrees, 2.24 inch inner pipe.
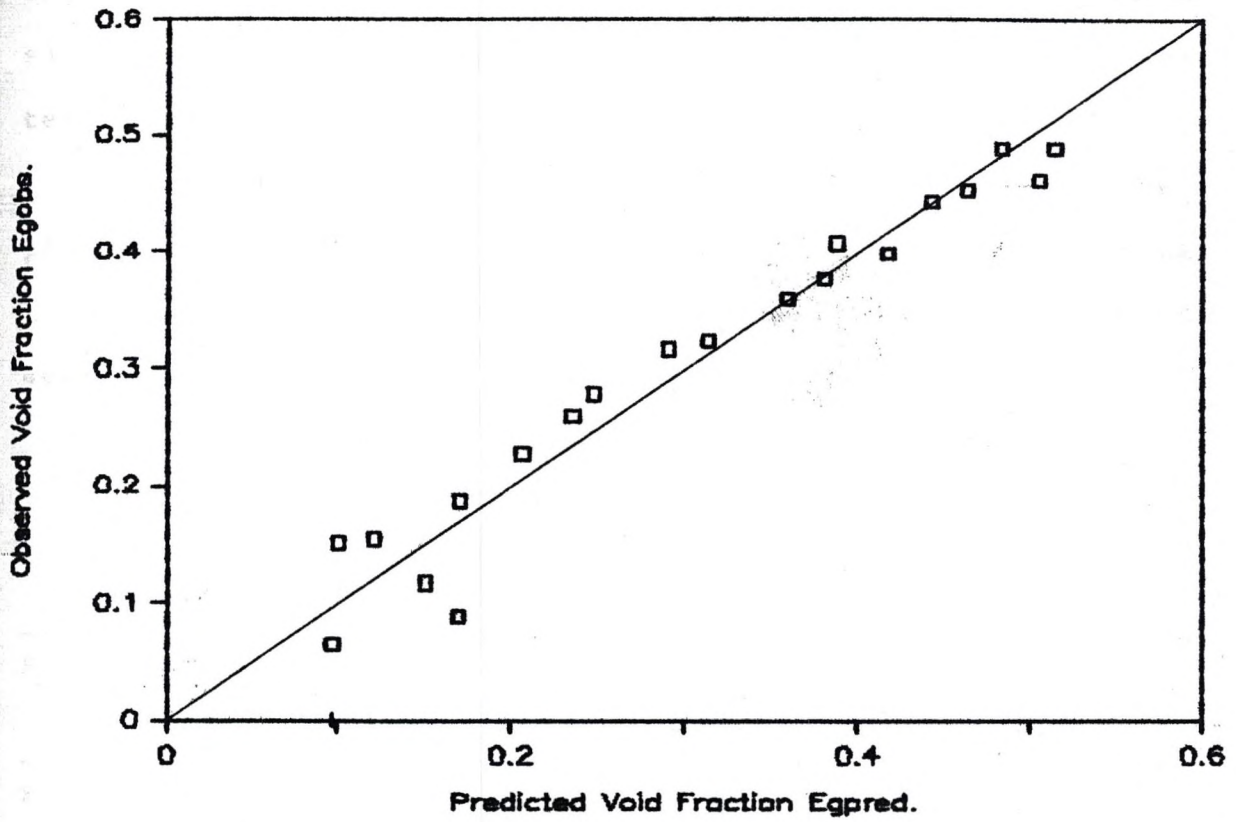
Figure 43: Comparison of the Experimental and the
Predicted Void Fraction Values - 32
degrees, 3.409 inch inner pipe.

deviation of 4.7 percent, compared to an underestimation of 4.36 percent and a percent standard deviation of 4.73 percent, respectively, for the model proposed by Filho (1984) that contains a parameter optimized using the data. The general overestimation by the model suggests either a slightly lower value of the flow parameter C_o or a lower terminal bubble rise velocity for annuli.

The slug flow data are also overestimated by the proposed model. The model overestimates the air-water slug flow data by 7.3 percent while the percent standard deviation is 10.5 percent.

Table 3

Statistical Comparison of the Predictions of the

Proposed Model with the Liquid Holdup Data of Filho

Flow Regime	Bubbly	Slug	Overall
	Air - Water Data		
Error	+0.022	+0.048	+0.021
Std. Deviation	0.040	0.066	0.049

This higher value of the percentage error reflects the generally lower value of liquid holdup, rather than a diminished accuracy in predicting the absolute values. The method proposed by Sadatomi et al. (1982), which utilizes Equation (39) with V_{tT} given by Equation (52), overestimates these data even more because of the higher estimated value of V_{tT}. For the air-water data, using the Sadatomi, Sato and Saruwatari (1982) correlation overestimates the data

with an error of 8.52 percent and a percent standard deviation of 11.06 percent. The proposed model predicted the gas void fraction in this data set with an average error of 0.0023 and a standard deviation of 0.0214.

The bubbly flow void fraction data are slightly underestimated (i.e. E_1 is overestimated), as in the case of the Filho (1984) data. A lower value of the terminal rise velocity (about 0.08 m/s, as opposed to 0.24 m/s used in this analysis) of small bubbles would make the predictions agree very well with the data. This would also be true of the Filho (1984) data. It is possible that for the small pipes used by Sadatomi et al. (1982), the terminal bubble rise velocity of small bubbles are actually lower, perhaps being affected by the pipe walls. However, Sadatomi et al. (1982) did not provide small bubble rise velocity data to verify this point. Filho (1984) did not provide small bubble rise velocity data either. Further data, with varying annuli dimensions, are needed to clarify this point.

Chapter VII

CONCLUSIONS and RECOMMENDATIONS

7.1 CONCLUSIONS

This thesis discusses flow pattern prediction criteria
and uses experimental data to examine a particular flow
pattern approach to predicting void fraction during two-
phase flow in annuli. The particular approach or model is
based on the relative motion between the liquid phases
caused by the density difference, and the tendency of the
gas phase to flow through the central portion of the
channel. The model accounts for the buoyancy effect using
the bubble rise velocity while the parameters C_o and C_1
account for the effect of the bubble concentration profile.
The following conclusions result from the study:

1)   The terminal rise velocity for bubbly flow appears to
be unaffected by annular geometry and is well represented by
the Harmathy (1960) equation. However, the Filho (1984) and
Sadatomi et al. (1982) void fraction data appear to suggest
a somewhat lower terminal rise velocity.

2)   The flow parameters in bubbly and slug flow appear to
be unaffected by annuli diameters. Values of C_o and C_1
appropriate for circular pipes are, therefore, recommended
for annuli.

3)   The transition from bubbly to slug flow was observed to
occur at a void fraction $E_g = 0.25$ for both annular and

89

cylindrical geometry.

4)   The equation used to estimate void fraction in inclined bubbly flow is exactly the same as that for vertical flow.

5)   The predictions of the model appear to be in good agreement with data from other sources.

7.2   RECOMMENDATIONS

It would be interesting to perform this experiment at higher column operating pressures so as to attain churn and, possibly, annular flow. It would be beneficial to perform a study of the effect of liquid properties (e.g. viscosity and surface tension) on the void fraction.

The experimental equipment needs to be improved. An integrator to accurately record manometer fluid fluctuations would minimize error.

APPENDICES

Appendix A

Computer Program to Convert Raw Data to Superficial

Gas Velocity and Void Fraction

PASCAL Program to Convert Raw Data

to Superficial Gas Velocity and Void Fraction.

```
10 PROGRAM CalcEasy (Input,Output);

20 CONST Length = 12.2;

30 VAR   H,Eg,Q,Qa,F,Vsg,P,Pa,L,A,K,L1,L2,L3,L4 : Real;
40        X,N,I1,I2,I3,I4                        : Integer;

50    (****************************************************)
60    (*                     Nomenclature:              *)
70    (*                                                *)
80    (* H  : The manometer pressure reading;           *)
90    (* Eg : Void fraction;                            *)
100   (* Q  : Measured gas flow rate;                   *)
110   (* Qa : Actual gas flow rate;                     *)
120   (* F  : Pressure correction;                      *)
130   (* Vsg: Superficial gas velocity;                 *)
140   (* P  : Measured pressure;                         *)
150   (* Pa : Actual pressure;                          *)
160   (* L  : Level of water in the column;             *)
170   (* A  : Flow cross-sectional area;                *)
180   (* K  : Ratio of Vsg to Eg;                       *)
190   (* L1,L2,L3,L4 : Height of water in column during *)
200   (*                  run;                          *)
210   (* X  : Angle of deviation from the vertical;     *)
220   (* N  : Loop counter;                             *)
230   (* I1,I2,I3,I4 :  Reading at which water was taken *)
240   (*               out of the column to enable incr- *)
250   (*               ease in the gas flow rate.       *)
260   (****************************************************)

270   BEGIN

280 I1 := _____ ;
290 I2 := _____ ;
300 I3 := _____ ;
310 I4 := _____ ;

320 N  := 0;

330 Writeln ("H","Q","Qa","P","Pa","F","Vsg","Eg","Vsg/Eg");
340 Readln(A,X);
350 Readln (L1,L2,L3,L4);

360 Repeat

370 N := N + 1;

380 If N = I1, then L := L1;
```

```
390 If N = I2, then L := L2;
400 If N = I3, then L := L3;
410 If N = I4, then L := L4;

420 Readln (H,Q,P);

430 Eg   := 0.305 * H/cos(X);
440 Pa   := 14.7 + 0.4336 * (L - (1-Eg) * Length);
450 F    := 0.00146 * (P + 14.7) + 0.8985;
460 Qa   := Q * F * ((P + 14.7)/Pa) * (530/520);
470 Vsg  := Qa/A;
480 K    := Vsg/Eg;

490 Write (H:8:3,Q:8:3,Qa:8:3,P:8:3,Pa:8:3,F:8:3,Vsg:8:3);
500 Writeln (Eg:8:3,K/60:8:3);

510 Until N = 20;

520 END.
```

Appendix B

Raw Data and Calculated Values of V_{sg} and E_g

Table 4

Void Fraction Data

Experimental Run: 1
Tubing Outside Diameter, Dt = 0 inches
Specific Gravity of Manometer Fluid = 1.6
Deviation from the vertical = 0 degrees

Manometer Reading	Measured Air Flow Rate	Superficial Gas Velocity	Observed Void Fraction	Predicted Void Fraction
H, cms	Q, cfm	Vsg, ft/s	Egobs	Egpred
10.2	0.444	0.076	0.102	0.080
10.8	0.579	0.099	0.108	0.099
11.4	0.625	0.107	0.114	0.106
11.9	0.649	0.111	0.120	0.109
14.5	0.806	0.138	0.145	0.128
17.2	0.917	0.157	0.172	0.141
20.3	1.245	0.213	0.203	0.174
22.7	2.016	0.345	0.227	0.206
26.9	3.161	0.541	0.270	0.283
30.6	3.552	0.738	0.306	0.343
34.3	4.201	0.873	0.343	0.378
35.8	4.683	0.973	0.358	0.400
37.6	5.024	1.044	0.376	0.415
39.2	5.453	1.133	0.392	0.432
40.7	5.572	1.226	0.407	0.448
41.6	5.723	1.329	0.416	0.465
42.8	5.998	1.393	0.428	0.475
44.4	6.083	1.487	0.444	0.488
45.6	6.345	1.551	0.456	0.496
46.2	6.660	1.628	0.462	0.506

Table 5

Void Fraction Data

Experimental Run: 2
Tubing Outside Diameter, Dt = 1.87 inches
Specific Gravity of Manometer Fluid = 1.6
Deviation from the vertical = 0 degrees

Manometer Reading	Measured Air Flow Rate	Superficial Gas Velocity	Observed Void Fraction	Predicted Void Fraction
H, cms	Q, cfm	Vsg, ft/s	Egobs	Egpred
10.1	0.266	0.053	0.101	0.058
11.3	0.352	0.070	0.113	0.074
13.2	0.452	0.090	0.132	0.092
9.8	0.553	0.110	0.098	0.108
14.4	0.583	0.116	0.144	0.112
16.2	0.804	0.160	0.162	0.143
17.8	0.955	0.190	0.178	0.161
18.7	1.126	0.224	0.187	0.179
19.3	1.342	0.267	0.193	0.235
20.2	1.749	0.348	0.202	0.182
22.6	2.091	0.416	0.226	0.207
23.5	2.433	0.484	0.235	0.230
25.7	3.167	0.630	0.257	0.271
26.9	3.649	0.726	0.269	0.295
28.4	4.132	0.822	0.284	0.316
29.9	4.795	0.954	0.300	0.341
32.4	5.313	1.057	0.324	0.359
35.7	5.820	1.158	0.357	0.375
36.9	6.019	1.283	0.370	0.392
38.8	6.587	1.404	0.388	0.407

Table 6

Void Fraction Data

Experimental Run: 3
Tubing Outside Diameter, Dt = 2.24 inches
Specific Gravity of Manometer Fluid = 1.6
Deviation from the vertical = 0 degrees

Manometer Reading	Measured Air Flow Rate	Superficial Gas Velocity	Observed Void Fraction	Predicted Void Fraction
H, cms	Q, cfm	Vsg, ft/s	Egobs	Egpred

H, cms	Q, cfm	Vsg, ft/s	Egobs	Egpred
13.7	0.262	0.056	0.137	0.092
15.1	0.430	0.092	0.151	0.093
13.7	0.747	0.160	0.137	0.143
15.1	1.140	0.244	0.151	0.224
17.6	1.448	0.310	0.176	0.163
20.1	1.607	0.344	0.201	0.176
22.1	1.817	0.389	0.221	0.193
22.5	1.957	0.419	0.225	0.203
24.1	2.242	0.480	0.241	0.222
24.8	2.648	0.567	0.248	0.248
25.3	2.771	0.678	0.253	0.276
26.6	3.172	0.776	0.266	0.298
30.9	3.756	0.919	0.310	0.325
31.7	3.997	1.039	0.317	0.346
34.7	4.624	1.202	0.347	0.369
34.7	4.628	1.274	0.347	0.379
37.2	5.322	1.465	0.372	0.401
38.3	5.994	1.650	0.383	0.419
39.9	6.274	1.823	0.400	0.434
42.6	6.477	2.080	0.426	0.453

Table 7

Void Fraction Data

Experimental Run: 4
Tubing Outside Diameter, Dt = 3.409 inches
Specific Gravity of Manometer Fluid = 1.6
Deviation from the vertical = 0 degrees

Manometer Reading	Measured Air Flow Rate	Superficial Gas Velocity	Observed Void Fraction	Predicted Void Fraction
H, cms	Q, cfm	Vsg, ft/s	Egobs	Egpred
10.2	0.228	0.073	0.102	0.077
11.1	0.247	0.079	0.111	0.082
13.2	0.291	0.093	0.132	0.094
12.6	0.297	0.095	0.126	0.096
17.5	0.629	0.201	0.175	0.167
20.6	1.173	0.375	0.206	0.176
23.9	1.748	0.559	0.239	0.229
26.4	2.286	0.731	0.264	0.269
29.4	2.915	0.932	0.294	0.305
32.8	3.212	1.027	0.328	0.320
34.9	3.397	1.164	0.349	0.339
35.5	3.605	1.235	0.355	0.348
37.6	4.565	1.564	0.376	0.382
38.3	4.699	1.610	0.383	0.386
40.1	4.708	1.828	0.401	0.404
40.9	5.207	2.022	0.410	0.417
42.2	5.264	2.164	0.422	0.426
43.4	5.913	2.431	0.434	0.440
44.4	6.368	2.618	0.444	0.449
45.6	6.667	2.741	0.456	0.454

Table 8

Void Fraction Data

Experimental Run: 5
Tubing Outside Diameter, Dt = 0 inches
Specific Gravity of Manometer Fluid = 1.6
Deviation from the vertical = 8 degrees

Manometer Reading	Measured Air Flow Rate	Superficial Gas Velocity	Observed Void Fraction	Predicted Void Fraction
H, cms	Q, cfm	Vsg, ft/s	Egobs	Egpred
6.9	0.228	0.042	0.069	0.048
8.1	0.375	0.069	0.081	0.074
9.6	0.619	0.114	0.097	0.111
12.3	0.836	0.154	0.124	0.139
14.8	1.037	0.191	0.149	0.162
17.6	1.292	0.238	0.177	0.187
19.3	1.558	0.287	0.195	0.158
21.2	2.009	0.370	0.214	0.193
22.9	2.334	0.430	0.232	0.217
25.8	2.780	0.512	0.260	0.246
28.8	2.993	0.630	0.291	0.283
31.6	3.449	0.726	0.319	0.310
33.4	3.843	0.809	0.337	0.331
34.6	4.323	0.910	0.349	0.355
36.2	4.627	0.974	0.365	0.369
38.2	5.050	1.063	0.386	0.387
39.2	5.496	1.157	0.396	0.405
40.4	5.985	1.260	0.408	0.423
41.3	6.139	1.373	0.417	0.440
42.5	6.217	1.554	0.429	0.466

Table 9

Void Fraction Data

Experimental Run: 6
Tubing Outside Diameter, Dt = 1.87 inches
Specific Gravity of Manometer Fluid = 1.6
Deviation from the vertical = 8 degrees

Manometer Reading	Measured Air Flow Rate	Superficial Gas Velocity	Observed Void Fraction	Predicted Void Fraction
H, cms	Q, cfm	Vsg, ft/s	Egobs	Egpred
7.0	0.212	0.046	0.071	0.052
8.3	0.392	0.085	0.084	0.088
10.4	0.586	0.127	0.105	0.120
12.9	0.733	0.159	0.130	0.142
15.2	1.024	0.222	0.154	0.178
17.7	1.264	0.274	0.179	0.140
19.5	1.550	0.336	0.197	0.166
21.4	1.978	0.429	0.216	0.200
23.2	2.283	0.495	0.234	0.223
25.9	2.744	0.595	0.262	0.254
28.9	3.009	0.699	0.293	0.284
31.5	3.529	0.820	0.318	0.314
33.3	3.835	0.891	0.336	0.331
35.7	4.485	1.042	0.361	0.362
36.0	4.687	1.089	0.364	0.371
37.5	5.079	1.180	0.379	0.388
39.1	5.539	1.287	0.395	0.406
40.3	5.706	1.414	0.407	0.426
41.2	5.852	1.541	0.416	0.443
41.8	6.394	1.733	0.422	0.468

Table 10

Void Fraction Data

Experimental Run: 7
Tubing Outside Diameter, Dt = 2.24 inches
Specific Gravity of Manometer Fluid = 1.6
Deviation from the vertical = 8 degrees

Manometer Reading	Measured Air Flow Rate	Superficial Gas Velocity	Observed Void Fraction	Predicted Void Fraction
H, cm	Q, cfm	Vsg, ft/s	Egobs	Egpred
7.1	0.192	0.045	0.072	0.051
8.9	0.349	0.082	0.091	0.085
10.5	0.489	0.115	0.106	0.112
12.6	0.668	0.157	0.128	0.141
15.9	0.953	0.224	0.161	0.179
17.8	1.179	0.277	0.180	0.139
19.6	1.422	0.334	0.198	0.162
21.5	1.826	0.429	0.217	0.198
23.9	2.281	0.536	0.242	0.233
28.2	2.732	0.642	0.285	0.264
30.6	3.230	0.759	0.309	0.296
32.4	3.690	0.867	0.328	0.321
33.9	3.958	0.930	0.343	0.335
35.8	4.631	1.088	0.362	0.367
36.1	4.839	1.137	0.365	0.376
37.6	5.303	1.246	0.380	0.395
39.2	5.750	1.351	0.396	0.412
39.8	5.815	1.415	0.402	0.422
40.9	5.974	1.604	0.414	0.448
42.1	6.231	1.830	0.426	0.475

Table 11

Void Fraction Data

Experimental Run: 8
Tubing Outside Diameter, Dt = 3.409 inches
Specific Gravity of Manometer Fluid = 1.6
Deviation from the vertical = 8 degrees

Manometer Reading	Measured Air Flow Rate	Superficial Gas Velocity	Observed Void Fraction	Predicted Void Fraction
H, cms	Q, cfm	Vsg, ft/s	Egobs	Egpred
11.3	0.174	0.064	0.114	0.069
12.9	0.222	0.082	0.130	0.085
13.8	0.282	0.104	0.139	0.103
18.9	0.578	0.213	0.191	0.174
19.5	0.863	0.318	0.197	0.149
22.6	1.047	0.386	0.228	0.174
22.9	1.202	0.443	0.231	0.194
24.4	1.522	0.561	0.247	0.231
26.5	1.967	0.725	0.268	0.276
30.2	2.547	0.939	0.305	0.326
32.4	2.620	0.966	0.327	0.332
35.1	2.949	1.087	0.355	0.355
36.3	3.304	1.218	0.367	0.379
39.7	3.936	1.451	0.401	0.415
40.3	4.177	1.540	0.407	0.427
40.9	4.354	1.605	0.413	0.436
42.4	4.980	1.836	0.428	0.464
43.6	5.694	2.099	0.441	0.491
45.1	5.965	2.356	0.456	0.514
46.0	6.351	2.676	0.465	0.539

Table 12

Void Fraction Data

Experimental Run: 9
Tubing Outside Diameter, Dt = 0 inches
Specific Gravity of Manometer Fluid = 1.6
Deviation from the vertical = 16 degrees

Manometer Reading	Measured Air Flow Rate	Superficial Gas Velocity	Observed Void Fraction	Predicted Void Fraction
H, cms	Q, cfm	Vsg, ft/s	Egobs	Egpred
2.6	0.275	0.047	0.027	0.053
4.1	0.310	0.053	0.043	0.058
5.9	0.368	0.063	0.062	0.068
8.5	0.456	0.078	0.088	0.082
11.1	0.812	0.139	0.116	0.129
12.7	1.145	0.196	0.132	0.164
14.8	1.367	0.234	0.154	0.185
16.6	2.016	0.345	0.173	0.166
20.3	2.729	0.467	0.211	0.210
23.1	3.413	0.584	0.240	0.247
28.2	3.622	0.664	0.294	0.269
30.1	4.080	0.748	0.313	0.292
31.9	5.089	0.933	0.332	0.335
33.7	5.503	1.009	0.351	0.350
34.9	5.836	1.070	0.364	0.362
36.8	6.098	1.118	0.383	0.371
37.4	6.117	1.159	0.389	0.379
38.6	6.302	1.194	0.402	0.385
39.5	6.571	1.245	0.411	0.394
38.6	6.402	1.213	0.402	0.388

Table 13

Void Fraction Data

Experimental Run: 10
Tubing Outside Diameter, Dt = 1.87 inches
Specific Gravity of Manometer Fluid = 1.6
Deviation from the vertical = 16 degrees

Manometer Reading	Measured Air Flow Rate	Superficial Gas Velocity	Observed Void Fraction	Predicted Void Fraction
H, cms	Q, cfm	Vsg, ft/s	Egobs	Egpred
3.8	0.312	0.062	0.040	0.067
5.4	0.362	0.072	0.056	0.076
7.2	0.412	0.082	0.075	0.085
10.3	0.658	0.131	0.107	0.123
13.3	1.086	0.216	0.138	0.175
15.8	1.830	0.364	0.164	0.160
17.6	2.237	0.445	0.183	0.188
19.4	2.493	0.496	0.202	0.204
22.8	3.141	0.625	0.237	0.241
25.5	3.629	0.722	0.265	0.267
27.9	3.795	0.809	0.291	0.288
29.5	4.139	0.941	0.307	0.317
30.9	4.543	1.033	0.322	0.336
32.5	4.847	1.102	0.338	0.349
33.7	5.062	1.151	0.351	0.357
35.3	5.300	1.205	0.367	0.367
36.1	5.398	1.304	0.376	0.383
37.1	5.683	1.373	0.386	0.394
37.9	5.969	1.442	0.395	0.404
38.6	6.163	1.489	0.402	0.411

Table 14

Void Fraction Data

Experimental Run: 11
Tubing Outside Diameter, Dt = 2.24 inches
Specific Gravity of Manometer Fluid = 1.6
Deviation from the vertical = 16 degrees

Manometer Reading	Measured Air Flow Rate	Superficial Gas Velocity	Observed Void Fraction	Predicted Void Fraction
H, cms	Q, cfm	Vsg, ft/s	Egobs	Egpred
2.6	0.253	0.058	0.027	0.063
4.1	0.305	0.070	0.043	0.074
5.9	0.331	0.076	0.062	0.080
6.8	0.366	0.084	0.071	0.087
11.1	0.667	0.153	0.116	0.138
12.0	0.955	0.219	0.125	0.177
14.5	1.164	0.267	0.151	0.122
15.9	1.705	0.391	0.166	0.167
17.9	2.027	0.465	0.186	0.191
19.9	2.472	0.567	0.208	0.222
22.7	2.877	0.660	0.236	0.248
24.9	3.313	0.760	0.259	0.273
27.3	3.679	0.844	0.284	0.293
28.8	4.102	0.941	0.300	0.313
32.2	4.482	1.028	0.335	0.331
32.2	4.652	1.067	0.335	0.338
33.7	4.896	1.123	0.351	0.349
36.1	5.236	1.201	0.376	0.362
36.9	5.776	1.325	0.385	0.383
38.2	6.225	1.428	0.398	0.398

Table 15

Void Fraction Data

Experimental Run: 12
Tubing Outside Diameter, Dt = 3.409 inches
Specific Gravity of Manometer Fluid = 1.6
Deviation from the vertical = 16 degrees

Manometer Reading	Measured Air Flow Rate	Superficial Gas Velocity	Observed Void Fraction	Predicted Void Fraction
H, cms	Q, cfm	Vsg, ft/s	Egobs	Egpred
12.9	0.337	0.123	0.135	0.118
14.8	0.487	0.178	0.154	0.154
17.6	0.597	0.218	0.183	0.176
18.1	0.829	0.303	0.189	0.129
19.7	1.070	0.391	0.205	0.160
21.5	1.349	0.493	0.224	0.192
25.1	1.677	0.613	0.262	0.226
26.7	1.907	0.697	0.278	0.248
27.9	2.178	0.796	0.291	0.271
30.6	2.627	0.960	0.319	0.307
32.4	2.859	1.045	0.338	0.323
33.4	3.174	1.160	0.348	0.344
34.6	3.374	1.233	0.360	0.356
36.1	3.836	1.402	0.376	0.383
37.1	4.364	1.595	0.386	0.410
37.1	4.586	1.676	0.386	0.420
37.9	4.884	1.785	0.395	0.433
39.2	5.577	2.038	0.408	0.461
40.2	5.908	2.294	0.418	0.485
44.4	6.212	2.696	0.462	0.517

Table 16

Void Fraction Data

Experimental Run: 13
Tubing Outside Diameter, Dt = 0 inches
Specific Gravity of Manometer Fluid = 1.6
Deviation from the vertical = 24 degrees

Manometer Reading	Measured Air Flow Rate	Superficial Gas Velocity	Observed Void Fraction	Predicted Void Fraction
H, cms	Q, cfm	Vsg, ft/s	Egobs	Egpred
4.4	0.179	0.034	0.048	0.039
5.1	0.269	0.051	0.056	0.057
6.7	0.359	0.068	0.073	0.073
8.6	0.459	0.087	0.094	0.089
10.6	0.697	0.132	0.116	0.124
14.4	0.992	0.188	0.158	0.160
15.4	1.161	0.220	0.169	0.177
13.9	1.647	0.312	0.153	0.142
18.9	2.238	0.424	0.208	0.182
21.6	2.887	0.547	0.237	0.221
24.1	3.605	0.683	0.264	0.259
26.2	4.149	0.786	0.287	0.284
29.1	4.983	0.944	0.319	0.320
31.3	5.489	1.040	0.343	0.339
34.5	5.686	1.112	0.378	0.353
33.7	5.765	1.198	0.369	0.368
34.9	5.811	1.243	0.382	0.375
36.4	6.026	1.289	0.399	0.383
36.7	6.168	1.357	0.402	0.394
37.7	6.300	1.463	0.413	0.409

Table 17

Void Fraction Data

Experimental Run: 14
Tubing Outside Diameter, Dt = 1.87 inches
Specific Gravity of Manometer Fluid = 1.6
Deviation from the vertical = 24 degrees

Manometer Reading	Measured Air Flow Rate	Superficial Gas Velocity	Observed Void Fraction	Predicted Void Fraction
H, cms	Q, cfm	Vsg, ft/s	Egobs	Egpred
7.4	0.357	0.071	0.081	0.075
8.9	0.442	0.088	0.097	0.090
10.8	0.548	0.109	0.118	0.107
12.1	0.714	0.142	0.133	0.131
16.8	1.111	0.221	0.184	0.178
12.9	1.493	0.297	0.141	0.127
14.4	1.799	0.358	0.158	0.148
16.9	2.151	0.428	0.185	0.171
17.9	2.408	0.479	0.197	0.187
20.9	3.001	0.597	0.230	0.221
22.0	3.232	0.643	0.241	0.233
24.0	3.609	0.718	0.263	0.252
26.4	4.167	0.829	0.289	0.278
28.0	4.377	0.933	0.307	0.301
29.6	5.020	1.070	0.324	0.327
30.8	5.254	1.120	0.337	0.337
33.2	5.709	1.217	0.364	0.353
34.9	5.810	1.321	0.383	0.370
36.1	5.836	1.410	0.395	0.384
36.7	6.168	1.490	0.402	0.395

Table 18

Void Fraction Data

Experimental Run: 15
Tubing Outside Diameter, Dt = 2.24 inches
Specific Gravity of Manometer Fluid = 1.6
Deviation from the vertical = 24 degrees

Manometer Reading	Measured Air Flow Rate	Superficial Gas Velocity	Observed Void Fraction	Predicted Void Fraction
H, cm	Q, cfm	Vsg, ft/s	Egobs	Egpred
4.3	0.163	0.035	0.047	0.040
5.7	0.245	0.052	0.062	0.058
7.7	0.364	0.078	0.084	0.082
10.3	0.439	0.094	0.113	0.095
12.7	0.729	0.156	0.139	0.140
13.5	0.995	0.213	0.148	0.174
12.9	1.280	0.274	0.142	0.117
16.9	1.808	0.387	0.186	0.156
17.6	2.209	0.473	0.193	0.183
19.5	2.751	0.589	0.214	0.216
21.9	2.673	0.654	0.240	0.233
23.4	3.204	0.784	0.256	0.265
27.6	3.821	0.935	0.302	0.298
29.9	4.210	1.030	0.328	0.317
32.0	4.524	1.107	0.351	0.331
32.9	4.569	1.118	0.361	0.333
35.3	5.374	1.315	0.387	0.366
36.8	5.869	1.436	0.403	0.384
37.6	6.024	1.612	0.412	0.408
39.1	6.298	1.830	0.428	0.434

Table 19

Void Fraction Data

Experimental Run: 16
Tubing Outside Diameter, Dt = 3.409 inches
Specific Gravity of Manometer Fluid = 1.6
Deviation from the vertical = 24 degrees

Manometer Reading	Measured Air Flow Rate	Superficial Gas Velocity	Observed Void Fraction	Predicted Void Fraction
H, cms	Q, cfm	Vsg, ft/s	Egobs	Egpred
5.9	0.179	0.057	0.065	0.062
8.1	0.244	0.078	0.089	0.082
9.9	0.297	0.095	0.109	0.096
10.4	0.338	0.108	0.114	0.106
12.1	0.482	0.154	0.132	0.139
14.4	0.610	0.195	0.158	0.164
17.3	0.729	0.233	0.189	0.184
14.9	1.154	0.369	0.163	0.144
17.5	1.529	0.489	0.192	0.181
21.4	1.939	0.620	0.234	0.216
23.5	2.521	0.806	0.257	0.261
29.0	3.055	0.977	0.318	0.297
31.2	3.503	1.120	0.342	0.323
33.1	3.793	1.213	0.363	0.339
34.1	4.062	1.299	0.373	0.353
37.2	4.322	1.382	0.407	0.366
39.2	4.678	1.496	0.429	0.382
39.8	5.204	1.664	0.436	0.404
40.9	5.764	1.843	0.448	0.425
41.4	6.129	1.960	0.454	0.438

Table 20

Void Fraction Data

Experimental Run: 17
Tubing Outside Diameter, Dt = 0 inches
Specific Gravity of Manometer Fluid = 1.6
Deviation from the vertical = 32 degrees

Manometer Reading	Measured Air Flow Rate	Superficial Gas Velocity	Observed Void Fraction	Predicted Void Fraction
H, cms	Q, cfm	Vsg, ft/s	Egobs	Egpred
2.5	0.187	0.032	0.030	0.037
2.8	0.286	0.049	0.033	0.055
8.6	0.532	0.091	0.102	0.093
9.8	0.865	0.148	0.116	0.135
7.9	0.941	0.161	0.094	0.143
11.4	1.140	0.195	0.134	0.164
10.4	1.338	0.229	0.123	0.182
11.9	1.519	0.260	0.141	0.116
13.2	1.545	0.321	0.156	0.138
13.8	1.776	0.369	0.163	0.155
15.0	1.915	0.398	0.177	0.165
16.5	2.161	0.449	0.195	0.181
17.8	2.344	0.487	0.210	0.193
20.2	2.887	0.600	0.238	0.226
22.0	3.200	0.665	0.260	0.243
24.2	3.909	0.884	0.285	0.295
26.9	4.754	1.075	0.318	0.333
30.0	4.953	1.120	0.354	0.341
33.6	5.815	1.315	0.397	0.374
38.5	6.793	1.536	0.454	0.406

Table 21

Void Fraction Data

Experimental Run: 18
Tubing Outside Diameter, Dt = 1.87 inches
Specific Gravity of Manometer Fluid = 1.6
Deviation from the vertical = 32 degrees

Manometer Reading	Measured Air Flow Rate	Superficial Gas Velocity	Observed Void Fraction	Predicted Void Fraction
H, cms	Q, cfm	Vsg, ft/s	Egobs	Egpred
8.9	0.558	0.111	0.105	0.109
9.8	0.900	0.179	0.115	0.155
12.2	1.211	0.241	0.144	0.188
14.3	1.618	0.322	0.169	0.130
16.5	2.151	0.428	0.195	0.164
18.1	2.533	0.504	0.213	0.187
19.8	2.961	0.589	0.234	0.211
21.7	3.297	0.656	0.256	0.228
23.5	3.885	0.773	0.277	0.256
25.7	3.985	0.906	0.303	0.285
23.5	4.174	0.949	0.277	0.294
27.2	4.350	1.051	0.321	0.314
29.3	4.975	1.202	0.346	0.340
30.9	5.232	1.264	0.364	0.350
30.9	5.522	1.334	0.364	0.361
30.9	5.849	1.413	0.364	0.373
32.6	6.151	1.486	0.385	0.384
33.9	6.304	1.747	0.400	0.417
34.5	6.553	1.816	0.407	0.444
38.5	6.840	1.944	0.454	0.507

Table 22

Void Fraction Data

Experimental Run: 19
Tubing Outside Diameter, Dt = 2.24 inches
Specific Gravity of Manometer Fluid = 1.6
Deviation from the vertical = 32 degrees

Manometer Reading	Measured Air Flow Rate	Superficial Gas Velocity	Observed Void Fraction	Predicted Void Fraction
H, cms	Q, cfm	Vsg, ft/s	Egobs	Egpred
1.9	0.154	0.033	0.022	0.038
8.3	0.733	0.157	0.098	0.141
10.2	1.028	0.220	0.120	0.177
12.3	1.308	0.280	0.145	0.114
15.9	1.784	0.382	0.188	0.148
18.2	2.177	0.466	0.215	0.174
20.5	2.728	0.584	0.242	0.207
22.0	3.386	0.725	0.260	0.242
23.6	3.938	0.843	0.278	0.269
24.7	4.330	0.927	0.292	0.287
26.3	4.504	1.102	0.310	0.320
28.4	4.941	1.209	0.335	0.339
28.9	5.011	1.341	0.341	0.360
32.4	5.260	1.448	0.382	0.375
32.4	5.396	1.609	0.382	0.397
33.6	5.624	1.677	0.397	0.406
37.3	6.190	1.846	0.440	0.426
37.3	6.355	1.895	0.440	0.431
35.8	6.458	2.074	0.422	0.450
38.2	6.473	2.158	0.451	0.458

Table 23

Void Fraction Data

Experimental Run: 20
Tubing Outside Diameter, Dt = 3.409 inches
Specific Gravity of Manometer Fluid = 1.6
Deviation from the vertical = 32 degrees

Manometer Reading	Measured Air Flow Rate	Superficial Gas Velocity	Observed Void Fraction	Predicted Void Fraction
H, cms	Q, cfm	Vsg, ft/s	Egobs	Egpred
5.5	0.300	0.096	0.065	0.097
9.9	0.538	0.172	0.118	0.150
7.6	0.641	0.205	0.090	0.169
12.9	0.785	0.251	0.152	0.100
13.1	0.982	0.314	0.155	0.121
15.9	1.489	0.476	0.188	0.171
19.3	1.895	0.606	0.228	0.206
22.0	2.261	0.723	0.260	0.235
23.6	2.424	0.775	0.279	0.246
26.8	3.090	0.988	0.317	0.291
27.4	3.481	1.113	0.324	0.314
30.5	3.603	1.399	0.360	0.359
32.0	3.982	1.546	0.378	0.380
34.5	4.126	1.602	0.407	0.387
33.8	4.385	1.853	0.399	0.418
37.5	4.922	2.080	0.443	0.442
38.4	5.464	2.309	0.453	0.463
41.4	6.021	2.544	0.489	0.483
39.0	6.217	2.840	0.461	0.505
41.4	6.499	2.969	0.489	0.514

Appendix C

NOMENCLATURE

C_o Parameter in Equation (4), dimensionless.

C_1 Terminal rise velocity $= 1.53(sg/d_1)^{1/4}$, ft/sec.

D Flow channel diameter, ft.

D_t Tubing outside diameter, ft.

D_c Casing inside diameter, ft.

D_e Equivalent diameter, $D_c - D_t$, ft.

d_b Bubble diameter, ft.

d_g Gas density, lbm/ft^3.

d_1 Liquid density, lbm/ft^3.

E_g Gas void fraction, dimensionless.

E_1 Liquid void fraction, dimensionless.

g Acceleration due to gravity, ft/sec^2.

j_{g1} Drift flux, ft/sec.

K Parameter in Equation (15), dimensionless.

n Exponent in Equation (28), dimensionless.

s Surface tension, dynes/cm.

V_g Actual gas velocity, ft/sec.

V_1 Actual liquid velocity, ft/sec.

V_m Total fluid velocity, ft/sec.

V_{sg} Superficial gas velocity (gas flow rate divided by the total flow cross-sectional area), ft/sec.

V_{s1} Superficial liquid velocity (liquid flow rate divided by the total flow cross-sectional area), ft/sec.

V_t Terminal rise velocity for a single bubble, ft/sec.

V_{tT} Terminal rise velocity for a 'Taylor' bubble, ft/sec.

Greek Letters

μ_1 Liquid viscosity, lbm/ft.sec.

Subscripts

b   Bubble.

g   Gas.

l   Liquid.

m   Mixture.

Appendix D

Error Analysis

Experimental Errors

In this study, pressure drop was measured using an U-tube manometer. This presents difficulties that need to be examined. The U-tube manometer was mounted vertically. This configuration allowed air to enter and accumulate in the manometer. Although bleeder valves on top of the manometer were used to rid the manometer system of air, it is possible that some amount of air did remain in the manometer. This air accumulation may cause an error in measuring the pressure drop of up to 0.5 cm. of manometric fluid height. Taking into consideration the range of pressure drop data taken during the experimental runs, (between 2.0 to 46.0 cms of manometric fluid), a maximum error of up to 25 percent in the calculated void fraction values is possible.

Another source of error is the fluctuation present in the manometric fluid at existing flow rates. At low flow rates, the fluctuations are small as the pressure drop is low. The error in reading the pressure drop may be 1 mm. (since the smallest pressure drop measurable on the manometer scale is 1 mm.) and as the lowest pressure drop measured is 2.0 cms., the maximum error possible is 5 percent. At high flow rates, the fluctuations tend to be high. The error in reading the pressure drop may be as much as 2 cms and since the highest manometric reading is 40 cms., the error is 5 percent.

BIBLIOGRAPHY

Asheim, H. MONA, An Accurate Two-Phase Well Flow Model Based on Phase Slippage. SPE Prod. Eng., **12**, 221-230 (1986).

Aziz, K., Govier, G.W. and Fogarasi, M. Pressure Drop in Wells Producing Oil and Gas. J. Can. Pet. Tech., **24**, 38-47 (1972).

Baker, O., Oil and Gas J., **55**, No. 45, 150 (1957).

Barnea, D., Shoham, O., Taitel, Y., and Dukler, A. E. Gas-Liquid Flow in Inclined Tubes: Flow Pattern Transition for Upward Flow. Chem. Eng. Sci., **40**, 131-136 (1985).

Beggs, H. D., and Brill, J. P. A Study of Two-Phase Flow Inclined Pipes. J. Pet. Tech., **25**, 607-617 (1973).

Birkoff, G. and Carter, D. Rising Plane Bubbles. J. Rational Mech and Anal., No. 6, 769-780 (1957).

Bonnecaze, R. H., Erskin, W., and Greskovich, E. J. Holdup and Pressure Drop for Two-Phase Slug Flow in Inclined Pipelines. AIChE J., **17**, 1109-1113 (1971).

Danesh, A. Discussion of Evaluation of Inclined Pipe Two-Phase Liquid Holdup and Pressure - Loss Correlations Using Experimental Data. J. Pet. Tech., **32**, 169-170 (1980).

Davis, R.M. and Taylor, G. I. Proc. of Royal Doc.(London) 200 series A, 375-390 (1950).

Dumitrescu, D.T. Stromung an einer Luftblase im senkrechten Rohr. agnew Math. Mech., **23**, 139 (1943).

Filho, E.C. Two-Phase Flow in a Vertical Annulus. TUFFP Report, University of Tulsa, OK. (1984).

Flanigan, O. Effect of Uphill Flow on Pressure Drop in Design of Two-Phase Gathering Systems. Oil and Gas J., **56**, No. 10, 132 (1958).

Gaylor, R., Roberts, N. W. and Patt, H. R. C. Liquid-Liquid Extraction IV. Further Study of Hold-up in Packed Columns. Trans Inst. of Chem. Engrs., **31**, 57-68 (1953).

Godbey, J.K. and Dimon, C. A. The Automatic Liquid Monitor for Pumping Wells. J. Pet. Tech., **29**, 79-83 (1977).

Govier, G.W. and Aziz, K. The Flow of Complex Mixtures in Pipes. Van Nostrand Reinhold Co., New York, 1972.

Griffith, P. The Prediction of Low Quality Boiling Voids. A.S.M.E. Paper No. 63-HT-20., Nat. Heat Transfer Confc., Boston, Mass., 1963.

Griffith, P. and Snyder, G.A. The Bubbly-Slug Transition in a High Velocity Two-Phase Flow. MIT Report 5003-29 (TID 20947), (1964).

Griffith, P. and Wallis, G. B. Two-phase Slug Flow. J. Heat Trans. ASME Series C, **83**, 7-21 (1961).

Guzhov, A. I., Mamayev, V. A., and Odishariya, G. E. Paper IGU/C19-67 presented at 10th International Gas Conf., Hamburg, Germany (1967).

Harmathy, T.Z. Velocity of Large drops and Bubbles in Media of Infinite or Restricted Extent. AIChE J., **6**, 281 (1960).

Hasan, A.R. Inclined Two-Phase Flow: Flow Pattern, Void Fraction and Pressure Drop in Bubbly, Slug and Churn Flow. Fourth Int. Symp. Multiphase Transport and Particulate Phenomena, Miami Beach, Dec 15-17, (1986). To be published by Elsivier.

Hasan, A.R. and Kabir, C.S. Predicting Multiphase Flow Behavior in a Deviated Well. Paper SPE 15449, Presented at the SPE Annual Meeting, New Orleans, LA. (1986).

Hasan, A. R. and Kabir, C. S. Oil/Water two-phase flow behavior in vertical wellbores. Report to Schlumberger Production Testing Center, Oct. 1987.

Hasan, A.R. and Kabir, C.S. Gas Void Fraction in Two-Phase Up-Flow in Vertical and Inclined Annuli. J. Multiphase Flow (1988) (In Press).

Hasan, A. R., Kabir, C. S. and Rahman, R. Predicting liquid gradient in pumping well annulus. SPE Prod. Eng., Feb. 1988.

Haug, H.F. Stability of Sieve Trays with High Overflow Weirs. Chem. Eng. Sci. **31**, 295 (1976).

Hewitt, G. F. and Hall-Taylor, N. Annular Two-Phase Flow. Pergammon Press, 1965.

Hewitt, G.F. and Roberts, D.N. Studies of Two-Phase Flow Patterns by Simultaneous X-ray and Flash Photography. AERE-M 2159. HMSO (1969).

Hubbard, M. G. and Dukler, A. E. Flow Model for Horizontal Gas- Liquid Slug Flow. Paper presented at the 65th National Meeting of A.I.Ch.E., Tampa, Fla., May 1968.

Hughmark, G.A. Hold Up and Pressure Drop with Gas-Liquid Flow in a Vertical Pipe. Ph.D. Dissertation, Louisiana State U., Baton Rouge, LA (1959).

Ishii, M. Thermofluid Dynamic Theory of Two-phase Flow. Scientific and Medical Publication of France. Eyrolles, Paris (1975).

Jones, O. C. and Zuber, N. Slug-Annular Transition with Particular Reference to Narrow Rectangular Ducts. International Seminar, Momentum, Heat and Mass Transfer in Two-Phase Energy and Chemical Systems, Dubrovnik, Yugoslavia, Sept. 1978.

Lawson, J.D. and Brill, J.P. A Statistical Evaluation of Methods Used to Predict Pressure Losses for Multiphase Flow in Vertical Oilwell Tubing. J. Pet. Tech., 26, 903-914 (1974).

Lockett, M.J. and Kirkpatrick, R. D. Ideal Bubbly Flow and Actual Flow in Bubble Columns. Trans. Inst. Chem. Engrs., 53, 267-273 (1976).

Mashelkar, R.A. Bubble Columns. Brit. Chem. Eng. 15, 1297-1304 (1970).

Mattar, L., and Gregory, G. A. Air-Oil Slug Flow in an Upward-Inclined Pipe-I: Slug Velocity, Holdup and Pressure Gradient. J. Can. Pet. Tech., 26, 69-76 (1974).

Miles, G.D., Shedlovsky, L. and Ross, J. Foam Drainage. J. Phys. Chem., 49, 93-107 (1943).

Mukherjee, H. and Brill, J.P. Liquid Holdup Correlations for Inclined Two-Phase Flow. J. Pet. Tech., 35, 1003-1008, (1983).

Nicklin, D.J., Wilkes, J. O. and Davidson, J. F. Two-phase Flow in Vertical Tubes. Trans. I. Che. Engrs., 40, 61-68 (1962).

Payne, G.A. et al. Evaluation of Inclined-Pipe Two-Phase Liquid Holdup and Pressure Loss Correlations Using Experimental Data. J. Pet. Tech., 31, 1198-1208 (1979).

Peebles, F.N. and Garber, H. J. Studies in the Motion of Gas Bubbles in the Liquids. Chem. Eng. Prog., 49, 88-97 (1953).

Porteous, A. Prediction of the upper limit of the slug flow regime. British Chemical Engineering, **14** (9), 117-119, Sept. 1969.

Radovcich, N.A. and Moissis, R. The Transition from Two Phase Bubble Flow to Slug Flow. Report No. 7-7673-22, Dept. of Mech. Eng., MIT, 1962.

Rahman, Rehana. Void Fraction During Gas Flow through a Stagnant Liquid Column in Annular Geometry. M.S. Thesis, University of North Dakota (1984).

Sadatomi, M., Sato, Y. and Saruwatari, S. Two-Phase Flow in Vertical Non-circular Channels. Int. J. Multiphase Flow, **8**, 641-655 (1982).

Shoham, O. Flow Pattern Transition and Characterization in Gas-Liquid Two-Phase Flow in Inclined Pipes. Ph. D. Thesis, Tel-Aviv University, Israel (1982).

Singh, G., and Griffith, P. Determination of Pressure Drop Optimum Pipe Size for a Two-Phase Slug Flow in an Inclined Pipe. J. Eng. for Ind. Trans. ASME, Ser. B, **92**, 717-726, (1970).

Taitel, Y. and Dukler, A. E. Flow Regime Transition for Vertical Upward Gas-Liquid Flow: A Prelimnary Approach through Physical Modeling. AIChE 70th Annual Meeting, New York (1977).

Taitel, Y., Bornea, D. and Dukler, A. E. Modeling Flow Pattern Transition for Steady Upward Gas-Liquid Flow in Vertical Tubes. AIChE J., **26**, 345-354 (1980).

Vermeulen, L. R., and Ryan, J. T. Can. Jour. Chem. Eng., **49**, 195-201, (1971).

Wallis, G.B. Some Hydrodynamic Aspects of Two-phase flow and Boiling. Paper No 38, 1st Heat Transfer Conf., ASME, Boulder, Co., 1961.

Wallis, G.B. General Correlations for the Terminal Rise Velocity of Cylindrical Bubbles in Vertical Tubes. Report No. 62G1130, General Engineering Laboratory, General Electric Company, Schenectady, N.Y., August 1962.

Wallis, G.B. One-dimensional Two-phase flow. McGraw Hill Book Co. Inc., New York, 1969, p 93,248,255.

Weisman, J. and Kang, S. Y. Flow Pattern transition in Vertical and Upwardly Inclined Lines. Int. J. Multiphase Flow, **7**, 271-291 (1981).

Whitaker, S. Introduction to Fluid Mechanics. Prentice-Hall Inc., New York, 189-192, 1968.

White, E.T. and Beardmore, R. H. Velocity of Rise of Single Cylindrical Air Bubbles Through Liquids Contained in Vertical Tubes. Eng. Sci., **7** 351-361 (1962).

Zahradnik, J. Intensification of Mass Transfer in Sieve Plate Bubble Columns. Coll. Czech. Chem. Commun. **44**, 348 (1979).

Zahradnik, J. and Kastanek, F. Gas Holdup in Uniformly Aerated Bubble Column Reactors. Chem. Eng. Commun., **3**, 413-429 (1979).

Zuber, N. Nucleate boiling - the region of isolated bubbles - similarity with natural convection. Int. J. Heat Mass Transfer, **6**, 53, 1965.

Zuber, N. and Findlay, J. A. Average Volumetric Concentration in Two-phase Flow System. Trans ASME J. Heat Transfer, **87**, 453, (1965a).

Zuber, N. and Findlay, J. A. J. Heat Trans., Trans. ASME Ser. C, **87**, 453 (1965b).

Zuber, H. and Hench, J. Steady State and Transient Void Fraction of Bubbling Systems and their Operating Limits. Report No 62 GL 100, General Electric Co., Schenectady, N.Y., 1962.

Zukoski, E. E., J. Fluid Mech., **25**, 821 (1966).